School of Nuclear Science and Engineering
Oregon State University

PhD Thesis Proposal

Global sensitivity analysis methods for Monte Carlo radiation transport solvers

Kayla Clements

Advisor: **Todd Palmer**

January, 2023

Contents

1 Introduction and Background

1.1 A brief overview

As computational modeling becomes more important to the scientific community, so does the necessity of quantifying and analyzing model reliability, accuracy, and robustness. As such, uncertainty quantification (UQ) and global sensitivity analysis (GSA) are important parts of the modeling workflow. Uncertainty quantification has been assigned a number of overlapping definitions - we refer to the mathematical characterization of how sources of input uncertainty affect model output. Global sensitivity analysis can be viewed as a broadening of uncertainty quantification: GSA aims to apportion, or divide and allocate, uncertainty in model output to different sources of uncertainty in the model input [1]. Another way to phrase this is that GSA aims to understand the relative importance of each of the uncertain inputs, as well as their interactions with one another, to the behavior of model output. To apportion model output uncertainty, one must first quantify the uncertainty effects of each input. In this way, UQ and GSA go hand-in-hand, with UQ typically acting as a step in GSA. There are a wide range of UQ and GSA methodologies which are applicable in different modeling scenarios. Typically, these methodologies assume that the computational model itself is deterministic, *i.e.* that given the same input, the model will produce the same output. This way, when analyzing the effects of uncertain input parameters, UQ and GSA methodologies can assume that any output variability is caused by input variability. If the model incorporates some non-deterministic, *i.e.* stochastic, behavior, that isn't necessarily the case. A stochastic model that nuclear engineers are likely familiar with is a Monte Carlo radiation transport solver, in which average particle behavior is modeled by sampling probability distributions that describe physical phenomena. In that case, the variance of the model's output is a function (amongst other things) of the number of particle histories used in the simulation. In the case of such a model, the typical UQ workflow which assumes that the output uncertainty can be analyzed as solely the function of uncertain input parameters is not applicable. This of course propagates through to GSA, absorbing the effects of the solver's stochastic behavior into the output uncertainty, apportioning it to the various UQ inputs, improperly analyzing the effects of the uncertain input sources.

Stochastic solvers are widely used and important for many applications in which physical systems are difficult or outright impossible to describe with deterministic models, and UQ and GSA are too important to forego simply because stochastic solvers make the process less straightforward. A brute-force method to address this complication is to over-resolve the stochastic solver, *e.g.*increase the number of particles in the

simulation to drive down the variance of the output, rendering it negligible compared to the effects of the uncertain input. Resolving stochastic models to this extent is already computationally expensive, and folding that into the UQ and GSA workflow which requires repeated evaluation of numerical codes increases the computational expense to the point of intractability. As problems become more complex, UQ and GSA become more important, while more and more histories are needed to use the brute-force method to over-resolve the radiation transport problem such that the solver variance can be assumed negligible, and the problem compounds.

The purpose of this proposal is to quantify and mitigate the effects of using a stochastic solver as part of UQ and GSA. This work continues ongoing efforts in this space, and the expected outcome is an in-depth discussion of how stochastic solvers can be incorporated into these methods, their performance, and their trade-offs over a collection of realistic scenarios. While these methods are developed with nuclear engineering applications in mind, the work and its results are applicable to a wide range of spaces which use stochastic modeling such as fluid flow, plasmas, etc. The remainder of this section provides background on uncertainty quantification, global sensitivity analysis, and Monte Carlo radiation transport. Section 2 is a detailed outline of the research objectives of this proposal. Section 3 provides the proposed methodology for accomplishing these objectives, as well as supporting theory. Section 4 contains results for work performed thus far and Section 5 includes a timeline for the remaining work that will form the basis of the PhD dissertation.

1.2 Background: Uncertainty quantification

Scientific progress involves comparing predictions from theory with experimental evidence, with updates to these two pillars happening in tandem to inform one another. Scientists observe and collect data about the physical world, use real-world data to validate or refine models and theories, use those models and theories to predict what other physical phenomena might be observed, compare the models to the data by observing the physical world, and so on and so forth. In [2], the authors describe uncertainty quantification as "the rational process by which proximity between predictions and observations is characterized." The process combines applied mathematics, computational science, statistics, and practical knowledge to characterize how well a computational model describes an existing system, or the reliability of the model in predicting new systems.

Computational models are widely useful across any discipline which hopes to take some real-world process – how the economy might perform under various circumstances, how radiation might move through a system, how disease might be transmitted through a population – and understand it without having to perform real-world experiments, or when real-world experimentation is not possible. Ideally, a computational model can be built and perfected with existing experimental data, and then used to predict how the system will behave when new conditions are introduced. A model's accuracy can be tested by comparing its prediction to how the system performs in the physical world.

There are a number of types of computational models. One such example is a

polynomial whose coefficients are computed using existing data – by plugging the existing data back into the model, one could ensure that they receive the correct known response back. Assuming the model were perfect, one could then plug new inputs into the model how the system would behave. In the nuclear engineering field, we may be more familiar with thinking of computational models as geometric descriptions of systems which incorporate material data to predict how radiation will be transported throughout the system. In this case as well, verification could be performed by comparing with existing analytic benchmarks and experimental data, and once the model has been verified, the model's behavior can be tested under new conditions.

The uncertainty which UQ hopes to quantify can come from a number of sources. Assuming the model is constructed and verified with perfectly accurate data, approximations used to build the model will introduce some discrepancy between the model output and the true real-world behavior. Unfortunately, we can assume that data is not perfectly accurate; even at the limit of perfectly collected data, there will be some unpredictable and unavoidable imperfection. The different types of uncertainty are sometimes broadly categorized as *epistemic* and *aleatoric* [3]. Epistemic uncertainty, *i.e.* systematic uncertainty, arises from the imperfect approximation of system conditions. Approximations may be used for any number of reasons, including assumption that the effects of approximation are negligible, hopes of avoiding computational complexity and expense, or simply the limit of current modeling capabilities. Aleatoric uncertainty, *i.e.* stochastic uncertainty, describes the impossibility of perfect data. There will be some random imperfections in the machinery, the experiment tools, the conditions of the experiment, etc. which will introduce some uncertainty to the problem. Mathematically, aleatoric uncertainty describes the case in which a system is described by a probability distribution, but the value of a drawn sample cannot be known a priori. Epistemic uncertainty describes the case in which the system can not be well-described by a probability distribution, or it's not known how well the distribution describes relevant behavior [4]. The methods used for UQ depend on the goal of the UQ. In inverse problems, experimental data are used to simultaneously characterize and solve for unknown model parameters [5]; for example, when new data are used to update and correct models [2, 6]. The Bayesian approach is a common UQ method for solving inverse problems [2, 5]. In forward problems, sources of uncertainty are propagated through a model, often with the aim of computing low order moments like mean and variance of the model output [2], with the intention of evaluating how the system will respond to uncertainty sources and how sensitive the model response is to various sources of uncertainty [7].

The focus of this dissertation proposal is on forward-propagation of aleatoric uncertainty, particularly using Monte Carlo sampling methods. In Monte Carlo UQ (MCUQ), input parameters are randomly sampled from known probability distributions and used to perform a simulation. This is repeated a number of times such that useful information can be gleaned from the series of outputs: sampling approximations for central moments like average response and variance, a sample-based probability distribution function and cumulative density function of system responses, and the envelope of possible system responses, for example [5]. Unlike polynomial model construction, the cost of MCUQ is independent of problem dimensionality, and converges reliably to a mean system response, albeit slowly, a s $\mathcal{O}(N^{-1/2}$ for N independent

simulations [8]. In multi-level and multi-fidelity methods, higher- and lower-fidelity models can be leveraged to allocate the number of samples used and take advantage of this convergence [5]. Workflows for MCUQ are well-established and continue to be optimized for various application spaces [9]. For complex systems, deterministic models are not always well-suited to capture system behavior. One such case is in the use of Monte Carlo radiation transport (MCRT) solvers, wherein the behavior of a fixed number of particles is simulated, and the model response is an average of the particle behavior. As with MCUQ, the model output of MCRT solvers converges $\mathcal{O}(N_p^{-1/2}$ for N_p independent particle histories [8]. If traditional MCUQ methods are applied to stochastic computational models, the subsequent UQ statistical analysis can be considered "polluted" by the variability introduced by the solver itself. When integrating MCRT codes into a UQ workflow, a brute-force method to "de-pollute" the UQ statistics is to drive down the MCRT solver variability by increasing the number of particle histories [10]. With this method, the variability contribution from the MCRT solver is assumed to be negligible compared to the variability one hopes to analyze, and the UQ workflow proceeds. However, as mentioned, the variability of the MCRT response is proportional to the inverse of the squared number of particle histories used, likely increasing the computational expense to the point of intractability when combined with the repeated runs necessary for MCUQ.

A recently derived alternative approach is *variance deconvolution* [11, 12], a framework which quantifies the variance contribution from a stochastic solver and effectively removes it from the total polluted variance, therefore calculating the desired UQ statistics. This is far more cost effective than the brute-force approach, and uses an unbiased estimator for the variance introduced by the solver and for the UQ variance (or parametric variance). We apply this variance deconvolution UQ workflow here to MCRT problems, but as we will show, the method is not specific to radiation transport and is widely applicable with solvers that use a Monte Carlo method.

1.3 Background: Global sensitivity analysis

Global sensitivity analysis is the study of the apportionment (division, or allocation) of model output uncertainty to various sources of uncertainty in the model input [1]. As with uncertainty quantification, global sensitivity analysis is extremely important in understanding model quality and reliability, and should be treated as an important step in the modeling and simulation workflow across all disciplines. There are a number of rationales for incorporating GSA into the computational modeling workflow [13]:

- Model reliability: Is the model overly-dependent on data which is very uncertain? Does model uncertainty seem independent of input uncertainty?
- Model improvement: Can the model be simplified by simplifying treatment of low-impact parameters? Are there any regions that could benefit from greater study or resolution?
- Data prioritization: Factor importance to model output variability correlates with the importance of factor analysis. Would improving the uncertainty of one

factor greatly improve output stability? Should the interactions between two inputs be further studied?

- Protection against erroneous assumptions: Studying sensitivity globally prevents drawing improper conclusions based on specific sampled input parameters.

One way GSA is performed is by computing an importance index for each of the uncertain input parameters [14]. Given some generic model $Y = f(X_1, X_2, \cdots, X_k)$ with k uncertain input parameters X, consider setting one of the factors X_i equal to a particular constant x_i. If we take the variance of Y over all of the non-i factors $X_{\sim i}$. With X_i frozen, $\mathbb{V}ar_{X_{\sim i}}[Y \mid X_i = x_i]$ is the variance of Y dependent on all factors *but* X_i. This is known as a conditional variance, because it is conditional on X_i being fixed to x_i. To ensure that this conditional variance is not dependent on a particular value of x_i, we can compute the average $\mathbb{V}ar_{X_{\sim i}}[Y \mid X_i = x_i]$ over all possible values of x_i, $\mathbb{E}_{X_i}\big[\mathbb{V}ar_{X_{\sim i}}[Y|X_i]\big]$. Using the law of total variance [7],

$$\mathbb{E}_{X_i}\big[\mathbb{V}ar_{X_{\sim i}}[Y|X_i]\big] + \mathbb{V}ar_{X_i}\big[\mathbb{E}_{X_{\sim i}}[Y|X_i]\big] = \mathbb{V}ar_{X_i}[Y]. \tag{1.1}$$

One can imagine that if $\mathbb{E}_{X_i}\big[\mathbb{V}ar_{X_{\sim i}}[Y|X_i]\big]$ is small, this indicates that all factors which are *not* X_i have a low impact on the output variance; a large $\mathbb{V}ar_{X_i}\big[\mathbb{E}_{X_{\sim i}}[Y|X_i]\big]$ indicates the same. The conditional variance $\mathbb{V}ar_{X_i}\big[\mathbb{E}_{X_{\sim i}}[Y|X_i]\big]$ is also known as the first-order effect of X_i on Y. The ratio of X_i's first-order effect on Y to the total variance of Y,

$$S_i = \frac{\mathbb{V}ar_{X_i}\big[\mathbb{E}_{X_{\sim i}}[Y|X_i]\big]}{\mathbb{V}ar[Y]}, \tag{1.2}$$

is known as the first-order sensitivity index (SI) of X_i on Y, a numerical measure of the importance of X_i on the variance of Y [7]. S_i can range between 0 and 1, where the importance of the variable increases as its S_i approaches 1. (Because these sensitivity indices were first introduced by Ilya Sobol' [14], they are also sometimes referred to as Sobol' indices.) We have also referenced the fact that two input parameters may interact in a way that also affects the variance. In terms of sensitivity indices, two factors are said to have an interaction effect when their combined effect on Y can not be fully described by the sum of their individual first order effects [7]. The interaction effect of the pair (X_i, X_j) is measured by removing their individual first-order effects from their combined effect. Introducing some shorthand notation,

$$\mathbb{V}_i = \mathbb{V}ar_{X_i}\big[\mathbb{E}_{X_{\sim i}}[Y|X_i]\big], \tag{1.3}$$

$$\mathbb{V}_{ij} = \mathbb{V}ar\big[\mathbb{E}[Y \mid X_i, X_j]\big] - \mathbb{V}_i - \mathbb{V}_j.$$

The term $\mathbb{V}_{ij}$ is the second-order effect, and this methodology can be extended for higher-order effects. From this, we can compute the *total effect* of X_i, which accounts for the individual effect of X_i plus all of its interaction effects. For a model with three uncertain input factors, $Y = f(X_1, X_2, X_3)$, the total effect of X_1 is the sum of all terms which include X_1:

$$S_{T1} = S_1 + S_{12} + S_{13} + S_{123}. \tag{1.4}$$

Though not all GSA methods are variance-based, variance- and variance-decomposition-based techniques are of particular interest in our application space. This is not only to take advantage of implementing the variance deconvolution technique introduced in Section 1.2, but also because of their applicability towards some important sensitivity tests. As outlined earlier, there are a number of questions one might hope to answer using these sensitivity indices; analogously, there are a number of sensitivity tests in GSA whose usefulness depends on the problem definition and type of uncertainty. Most relevant to this work are [7]:

- Factor Prioritization (FP). Used to identify the input or group of inputs whose variability accounts for most of the output variability. Once identified, focus can be shifted towards reducing the variability of these parameters.
- Factor Fixing (FF). Used to identify the input or group of inputs whose variability makes little to no contribution to the output variability. Once identified, these parameters can essentially be set at some arbitrary value within their probability distribution, because varying them does not largely affect the output.
- Variance Cutting (VC). Used to identify the smallest set of factors one could act upon in order to reduce the output variance below a given threshold. This ensures the most effective optimization for a given output uncertainty goal.

The Saltelli method [7] for computing sensitivity indices using Monte-Carlo based sampling is described below for a model with k uncertain inputs:

1. Generate two (N, k) matrices of random numbers, A and B. The base sample N is a number of independent re-samplings of input parameters that can range from a few hundreds to a few thousands.
2. Form the matrix C_i by replacing the i^{th} column of B with the i^{th} column of A.
3. Compute the model output as a function of input matrices A, B, and C_i to obtain $N \times 1$ vectors of model output $y_A = f(A)$, $y_B = f(B)$, and $y_{Ci} = f(C_i)$.
4. For all k columns of A, construct C_i and compute y_{Ci}.

First-order sensitivity indices can be estimated:

$$S_i = \frac{V[E(Y|X_i)]}{V(Y)} = \frac{y_a \cdot y_c - f_0^2}{y_a \cdot y_a - f_0^2} \tag{1.5}$$

where $\cdot$ indicates the dot product and

$$f_0^2 = \left(\frac{1}{N} \sum_j = 1^N y_A^{(j)} \right)^2 \; y_A \cdot y_A. \tag{1.6}$$

The total-effect index can be estimated:

$$S_{Ti} = 1 - \frac{V[E(Y|X_{\sim i})]}{V(Y)} = 1 - \frac{y_B \cdot y_C - f_0^2}{y_A \cdot y_A - f_0^2}. \tag{1.7}$$

Since the publication of Satelli's approach for computing first-order and total- effects, several algorithmic modifications have been introduced to improve the efficiency and accuracy and the main and total order effects [10, 15].

As was the case with MCUQ, the Saltelli approach uses MC to perform sensitivity analysis assuming a non-stochastic solver. While following this workflow with a stochastic solver is possible, the stochastic solver pollutes the results of the sensitivity analysis. With UQ, a fair assumption is that the stochastic solver increases the observed model output variance, possibly causing an analyst to over-estimate the model's response to an uncertain input. In the case of GSA, the effects of the stochastic solver may not be so straightforward; the additional solver variance can also have interaction effects with each of the individual uncertain input parameters. We can see by considering the matrix dimensions of the Saltelli approach that as the dimensionality of the UQ problem increases, over-resolving the stochastic solver to drive the solver variance down is once again extremely computationally expensive. The increased complexity and computational cost provide additional motivation to incorporate a variance deconvolution framework that quantifies and removes stochastic solver variance from Monte Carlo uncertainty quantification and the workflow of global sensitivity analysis.

1.4 Background: Monte Carlo radiation transport

While a brief discussion of general Monte Carlo sampling methods is included in the background for UQ and GSA, a detailed introduction to Monte Carlo radiation transport methods is also warranted. MC simulations for particle transport treat the physical system of interest as a statistical process, using nuclear data to construct probability distributions that describe the various ways particles can behave in the system. Individual particles are simulated and their behavior (*eg* collisions with other particles, exiting the system, detection at a point in space, etc.) is tallied based on user defined output quantities. The Central Limit Theorem [16] can then be applied to extrapolate the tallied behavior of the simulated particle as the average behavior of all particles in the system, with some associated uncertainty based on the number of particles simulated. In contrast, deterministic transport methods yield an approximation to the transport equation analytically or numerically for average particle behavior across an entire phase space [8].

Monte Carlo methods are useful depending on the information needed by the user, the problem space, or the complexity of the equations governing the system. For example, because Monte Carlo methods are event based rather than phase-space based, they can be used to handle time-dependent problems with complicated geometries more effectively than deterministic solvers because there is no need for an accurate discretization scheme, and are useful in cases where a deterministic solution may not be available or accurate [8].

The conceptual baseline of the Monte Carlo method would be to construct the probability distributions that govern the sampled behavior in the simulation directly from physical data, such that the history of each particle follows the exact physics of the problem. This is referred to as analog Monte Carlo, because it is directly analogous to the physical behavior of the particle in a real system [8]. Even for neutral particles,

this direct analog of transport can become restrictively computationally expensive as the physics of the system becomes more complicated. For example, if the tally of interest is geometrically located where few particles end up traveling, it can take a large number of histories to obtain a statistically significant result [8]. The physics that must be modeled to accurately simulate transport becomes more complicated when considering charged particle transport, and these simulations often incorporate non-analog methods. Non-analog methods, in general, forego the exact physics of a problem in order to reduce computation time or improve scaling with problem size.

As the systems modeled using MCRT become more complex, a single simulation of the model becomes more computationally expensive. In a UQMC or Saltelli method workflow, numerous simulations of the model must be evaluated to compute the UQ and GSA statistics of interest. By incorporating the proposed variance deconvolution method, we aim to make UQ and GSA more tractable for problems with real-world complexity, which would otherwise require very large numbers of particle histories to not just converge, but converge to the point that the MCRT variance can be assumed negligible.

2 Objectives

There are three main research objectives which will correlate with three journal article submissions.

2.1 Variance deconvolution for uncertainty quantification

Develop robust theory for an accurate, efficient, and broadly applicable variance deconvolution estimator for uncertainty quantification with stochastic solvers. Demonstrate the estimator's practical use over a number of relevant radiation transport test cases.

- ☑ Develop a theoretical framework for forward uncertainty propagation which accounts for the additional variability introduced by the stochastic solver. Build on previous work by Aaron Olson [17], which uses a version of this variance deconvolution estimator that slightly inaccurately estimated the total and solver variance.
- ☑ Verify accuracy of estimator by with a test problem. The validation problem will consider transmittance through a 1D slab with different material sections. In the case of attenuation-only physics, the problem has an analytic solution to compare how MCUQ with an analytic solver compares to numerical results from MCUQ with MCRT.
- ☑ Develop an optimization method such that given a fixed total computational cost, a user could determine an ideal ratio of MCUQ samples to MCRT histories. This optimum configuration would be such that the estimate of UQ statistics like mean and variance have the highest possible accuracy given the cost constraint.

A subset of the above work has been presented at ANS 2022 Annual Meeting, the transactions publication of which is in the Appendix. Full paper submission is intended for the Journal of Quantitative Spectroscopy and Radiative Transfer. A draft version of the full paper is also available in the Appendix.

2.2 Global sensitivity analysis for stochastic solvers

Understand how use of a stochastic solver affects both sampling-based and PCE surrogate-based GSA. Develop methodologies to use stochastic solvers in GSA by explicitly accounting for the variability they introduce.

- ☐ Compare standard MC-Saltelli approach with a stochastic solver to MC-Saltelli approach with a deterministic solver to understand what variability is introduced.
- ☐ Compare surrogate-based GSA with a stochastic solver to surrogate-based GSA with a deterministic solver to understand what variability is introduced.
- ☐ Explore what other approaches exist to account for stochastic solvers in GSA.
- ☐ Apply the developed variance deconvolution method to the standard MC-Saltelli approach, standard PCE approach, and other popular existing approaches. How does the computational cost compare? How does the accuracy compare? In what situations is it worth applying variance deconvolution?

We submitted an extended abstract for consideration for ANS M&C 2023, included in Appendix. If accepted, develop into full summary, then into full paper for submission to special issue of *Nuclear Science and Engineering*. (From the M&C2023 website, `https://mc2023.com/`: Authors of M&C 2023 are invited to submit their work for consideration in a special issue of the Nuclear Science and Engineering (NSE) journal. Details of the submission process will be posted closer to the Conference date.)

2.3 Challenge problem

Demonstrate larger applicability of the methods developed for UQ and GSA with stochastic solvers by applying the methods to radiation transport problems with more complex and realistic physics, particularly physics relevant to CEMeNT's PSAAP challenge problem, using CEMeNT's MC/DC codebase. Understand how the cost of the approaches change with tally mesh resolution.

- ☐ Integrate MCUQ variance deconvolution framework into existing MC/DC codebase. Test against results from paper 1.
- ☐ Develop more complex cost model such that estimator is tuneable for different configurations. Current estimator assumes linear cost model, *i.e.* that one UQ re-sample and one RT re-sample cost the same; incorporate possibility that this is not the case.
- ☐ Create library that functions as wrapper around MC/DC such that a user can create an MC/DC input, specify uncertainty parameters, and perform a GSA study similar to the capabilities of the Dakota (Sandia) UQ software..
- ☐ Test library with complex radiation transport physics, complex quantities of interest, and realistically large numbers of tallies.
- ☐ Publication of this work.

2.4 Possible difficulties and contingencies

As work for the second paper is ongoing, unforeseen complications that need to be explored could arise with both the sampling-based GSA and PCE/surrogate-based GSA. If the scope of the work becomes too large, such that there is too much to include both forms of GSA in the paper, shift focus away from PCE and stick to sampling-based GSA analysis.

The cost of the MCUQ estimator is not expected to will scale with the number of tallies any differently than the cost of MCRT, but if it is significantly slower with larger numbers of tallies, additional methods may need to be developed to reduce cost.

3 Proposed method

3.1 Variance deconvolution for uncertainty quantification

This section outlines the methodology for developing a robust theory for an accurate, efficient, and broadly applicable variance deconvolution estimator for uncertainty quantification with stochastic solvers. It also outlines plans for demonstrating the estimator's practical use.

3.1.1 Building the estimator

We start building the variance deconvolution estimator by considering a generic scalar QoI Q which is a function of a vector of uncertain input parameters $\xi \in \Xi \subseteq \mathbb{R}^d$, where $d \in \mathbb{N}_0$ is the number of uncertain parameters that Q depends on. As is typical for UQ, we consider the uncertain parameters to be described by a joint probability density function (PDF) $p(\xi)$ such that $\int_\Xi p(\xi) d\xi = 1$.

For UQ, we are interested in computing (central) moments of Q, such as

$$\begin{aligned} \mathbb{E}[Q] &= \int_\Xi Q(\xi)\, p(\xi)\, \mathrm{d}\xi \quad \text{and} \\ \mathbb{V}ar[Q] &= \int_\Xi \left(Q(\xi) - \mathbb{E}[Q]\right)^2 p(\xi)\, \mathrm{d}\xi, \end{aligned} \tag{3.1}$$

with $\mathbb{E}[Q]$ and $\mathbb{V}ar[Q]$ denoting the mean and the variance of Q, respectively. These central moments can be approximated with Monte Carlo (MC) by drawing N_ξ samples for the QoI, each of them corresponding to an independent sample of ξ from its PDF and subsequent application of a possibly expensive computational code, as

$$\begin{aligned} \mathbb{E}[Q] &\approx \frac{1}{N_\xi} \sum_{i=1}^{N_\xi} Q(\xi^{(i)}) \\ \mathbb{V}ar[Q] &\approx \frac{1}{N_\xi - 1} \sum_{i=1}^{N_\xi} \left(Q(\xi^{(i)}) - \frac{1}{N_\xi} \sum_{k=1}^{N_\xi} Q(\xi^{(k)}) \right)^2 . \end{aligned} \tag{3.2}$$

Both estimators in Eq. (3.2) are unbiased, meaning that if we take the expectation of the MC estimators, they are exactly equal to the integral moments in Eq. (3.1)[1].

[1] For more details, the interested reader can refer to [18].

In the case of a non-deterministic solver, our QoI is obtained as statistics of elementary and observable events. We consider observing a single elementary realization $f(\xi, \eta)$. We have introduced the random variable η, possibly a random vector, to notionally represent the code's stochastic behavior; unlike with ξ, knowledge of η is neither implied nor required. In the case of a Monte Carlo radiation transport (MCRT) solver, η describes the inaccessible vector of random variables used by the solver to generate the particle's random walk, and $f(\xi, \eta)$ is the result of a single particle history. One realization of the QoI $Q(\xi)$ is obtained as an expected value of elementary events f over multiple realizations of η,

$$Q(\xi) = \mathbb{E}\left[f(\xi, \eta) \mid \xi\right] \triangleq \mathbb{E}_\eta\left[f(\xi, \eta)\right]; \tag{3.3}$$

we have defined the shorthand notation $\mathbb{E}_X[\cdot]$ to indicate the expected value over realizations drawn with respect to the variable X, *i.e.* with all non-X variables fixed. In practice, the elementary event will have a finite number of realizations, so $Q(\xi)$ is approximated using a finite number of particles N_η,

$$Q(\xi^{(i)}) \approx \frac{1}{N_\eta} \sum_{j=1}^{N_\eta} f(\xi^{(i)}, \eta^{(j)}) \triangleq \tilde{Q}\left(\xi^{(i)}\right). \tag{3.4}$$

Combining Eqs. (3.2) and (3.4) provides approximations for the expected value of the QoI,

$$\mathbb{E}[Q] \approx \frac{1}{N_\xi} \sum_{i=1}^{N_\xi} \tilde{Q}(\xi^{(i)}) = \frac{1}{N_\xi} \sum_{i=1}^{N_\xi} \left(\frac{1}{N_\eta} \sum_{j=1}^{N_\eta} f(\xi^{(i)}, \eta^{(j)}) \right) \triangleq \hat{Q}, \tag{3.5}$$

nesting the MC approximation for $Q(\xi)$ inside the MC approximations for the UQ statistics of interest. We can understand how the use of a stochastic solver impacts forward uncertainty propagation by evaluating features of this nested MC-MC UQ estimator.

3.1.2 Statistical properties of the MC-MC estimator

The following evaluates statistical properties of the MC-MC estimator under the assumption that the number of histories N_η is constant for each UQ sample[2], such that the total estimator cost is $\mathcal{C} = N_\xi \times N_\eta$. We first consider the effects of the nested sampling estimator by studying its bias, taking the expected value of the estimator

[2]This assumption is not strictly required, but simplifies derivations.

over both spaces,

$$\begin{aligned}
\mathbb{E}\left[\hat{Q}\right] &= \mathbb{E}\left[\frac{1}{N_\xi}\sum_{i=1}^{N_\xi}\left(\frac{1}{N_\eta}\sum_{j=1}^{N_\eta} f(\xi^{(i)},\eta^{(j)})\right)\right] \\
&= \frac{1}{N_\xi}\sum_{i=1}^{N_\xi}\left(\frac{1}{N_\eta}\sum_{j=1}^{N_\eta}\mathbb{E}_\xi\left[\mathbb{E}_\eta\left[f(\xi^{(i)},\eta^{(j)})\right]\right]\right) \\
&= \frac{1}{N_\xi}\sum_{i=1}^{N_\xi}\left(\frac{1}{N_\eta}\sum_{j=1}^{N_\eta}\mathbb{E}_\xi\left[Q(\xi^{(i)})\right]\right) \\
&= \frac{1}{N_\xi}\sum_{i=1}^{N_\xi}\mathbb{E}_\xi\left[Q(\xi^{(i)})\right] = \mathbb{E}_\xi\left[Q(\xi)\right].
\end{aligned} \tag{3.6}$$

By taking advantage of the linearity of the expected value operator, *i.e.* $\mathbb{E}\left[X_1 + X_2 + \cdots + X_j\right] = \mathbb{E}\left[X_1\right] + \mathbb{E}\left[X_2\right] + \cdots + \mathbb{E}\left[X_j\right]$ [16], we see that the nested MC-MC sampling estimator for $\mathbb{E}\left[Q\right]$ is unbiased. We next consider the variance of nested sampling estimator, using the known property of the variance of a linear combination [16],

$$\begin{aligned}
\mathbb{V}ar\left[\hat{Q}\right] &= \mathbb{V}ar\left[\frac{1}{N_\xi}\sum_{i=1}^{N_\xi}\left(\frac{1}{N_\eta}\sum_{j=1}^{N_\eta} f(\xi^{(i)},\eta^{(j)})\right)\right] \\
&= \mathbb{V}ar\left[\frac{1}{N_\xi}\sum_{i=1}^{N_\xi}\tilde{Q}(\xi^{(i)})\right] \\
&= \frac{1}{{N_\xi}^2}\sum_{i=1}^{N_\xi}\mathbb{V}ar\left[\tilde{Q}(\xi^{(i)})\right] \\
&= \frac{1}{N_\xi}\mathbb{V}ar\left[\tilde{Q}(\xi)\right].
\end{aligned} \tag{3.7}$$

Because $\tilde{Q}(\xi)$ is the average of elementary observable events which depend on η, we can apply the law of total variance [19] to $\tilde{Q}(\xi)$ to evaluate further:

$$\begin{aligned}
\mathbb{V}ar\left[Y\right] &= \mathbb{E}\left[\mathbb{V}ar\left[Y|X\right]\right] + \mathbb{V}ar\left[\mathbb{E}\left[Y|X\right]\right] \\
\rightarrow \mathbb{V}ar\left[\tilde{Q}(\xi)\right] &= \mathbb{E}_\xi\left[\mathbb{V}ar_\eta\left[\tilde{Q}(\xi)\right]\right] + \mathbb{V}ar_\xi\left[\mathbb{E}_\eta\left[\tilde{Q}(\xi)\right]\right] \\
&= \mathbb{E}_\xi\left[\mathbb{V}ar_\eta\left[\frac{1}{N_\eta}\sum_{j=1}^{N_\eta} f(\eta^{(j)},\xi)\right]\right] + \mathbb{V}ar_\xi\left[Q(\xi)\right] \\
&= \mathbb{E}_\xi\left[\frac{1}{{N_\eta}^2}\sum_{j=1}^{N_\eta}\mathbb{V}ar_\eta\left[f(\eta^{(j)},\xi)\right]\right] + \mathbb{V}ar_\xi\left[Q(\xi)\right] \\
&= \mathbb{E}_\xi\left[\frac{1}{N_\eta}\mathbb{V}ar_\eta\left[f(\xi,\eta)\right]\right] + \mathbb{V}ar_\xi\left[Q(\xi)\right].
\end{aligned} \tag{3.8}$$

Combining Eqs. (3.7) and (3.8), the variance of the MC-MC estimator is

$$\mathbb{V}ar\left[\hat{Q}\right] = \frac{\mathbb{E}_\xi\left[\mathbb{V}ar_\eta\left[f\right]\right] + N_\eta \mathbb{V}ar_\xi\left[Q\right]}{N_\xi} \tag{3.9}$$

These evaluations allow us to better understand the effects of the nested MC-MC estimator on UQ statistics. It is known that given population mean μ, population variance σ^2, and sample mean $\bar{X}$ over sample size n, $\mathbb{E}\left[\bar{X}\right] = \mu$ and $\mathbb{V}ar\left[\bar{X}\right] = \sigma^2/n$. If we think of the nested MC-MC estimator for $\mathbb{E}\left[Q\right]$ as a nested sample mean with nested sample sizes N_ξ and N_η, it follows that $\mathbb{E}\left[\hat{Q}\right] = \mathbb{E}\left[Q\right]$. Similarly, it follows that $\mathbb{V}ar\left[\hat{Q}\right] = \mathbb{V}ar\left[\tilde{Q}\right]/N_\xi$. Perhaps the less intuitive result is that the variance of $\tilde{Q}$, also a sample estimator, decomposes into two distinct contributions: $\mathbb{V}ar_\xi\left[Q(\xi)\right]$, which we may think of as the parametric (traditional UQ) variance of the QoI; and $\mathbb{E}_\xi\left[\frac{1}{N_\eta}\mathbb{V}ar_\eta\left[f(\xi,\eta)\right]\right]$, which we may think of as the variance contribution from the stochastic solver.

3.1.3 Variance deconvolution and practical implementation

The typical sampling-based UQ workflow is to collect evaluations of the QoI over the UQ space $Q(\xi)$, then approximate $\mathbb{E}\left[Q\right]$ and $\mathbb{V}ar\left[Q\right]$ with MC estimators (Eq. (3.2)). When a stochastic solver is introduced, $Q(\xi)$ becomes inaccessible and may only be approximated by $\tilde{Q}(\xi)$. This does not present a problem in computing $\mathbb{E}\left[Q\right]$, because as we've shown, $\mathbb{E}\left[\hat{Q}\right]$ provides an unbiased estimate for $\mathbb{E}\left[Q\right]$. For $\mathbb{V}ar\left[Q\right]$, this is not the case – Eq. (3.8) shows that the stochastic solver introduces a bias, $\mathbb{E}_\xi\left[\mathbb{V}ar_\eta\left[f(\xi,\eta)\right]\right]/N_\eta$. Existing methods [10] have used a brute-force approach to this issue, increasing the number of elementary event realizations N_η such that the noise contribution from the stochastic solver can be assumed to be negligible, approximating $\lim_{N_\eta\to\infty}\mathbb{V}ar_\eta\left[f(\xi,\eta)\right] = 0$. In many application spaces, increasing N_η enough that this assumption holds can increase computational cost to the point of intractability. In that sense, perhaps the most important result of Eq. (3.8) is a practical path to a fully unbiased estimate of $\mathbb{V}ar\left[Q\right]$. Given that $\tilde{Q}$ is an accessible quantity, $\mathbb{V}ar\left[\tilde{Q}\right]$ is calculable by taking the variance of several evaluations of $\tilde{Q}(\xi)$. Similarly, $\mathbb{V}ar_\eta\left[f(\xi,\eta)\right]$ is calculable given N_η realizations of $f(\xi,\eta)$ per UQ sample, making $\mathbb{E}_\xi\left[\mathbb{V}ar_\eta\left[f(\xi,\eta)\right]\right]$ calculable by averaging $\mathbb{V}ar_\eta\left[f(\xi,\eta)\right]$ over the number of UQ samples. Re-arranging Eq. (3.8), an unbiased estimate of $\mathbb{V}ar\left[Q\right]$ can be estimated by removing the stochastic solver noise from the total polluted variance,

$$\mathbb{V}ar\left[Q\right] = \mathbb{V}ar_\xi\left[Q\right] = \mathbb{V}ar\left[\tilde{Q}\right] - \frac{\mathbb{E}_\xi\left[\sigma_\eta^2\right]}{N_\eta}, \tag{3.10}$$

where σ_η^2 is defined as the variance of the histories for one fixed UQ parameter, *i.e.* $\sigma_\eta^2 \triangleq \mathbb{V}ar_\eta\left[f(\xi,\eta)\right]$. To practically implement this method for computing $\mathbb{V}ar\left[Q\right]$, we

will use several sample-estimator counterparts,

$$\begin{aligned}
\mathbb{V}ar\left[\tilde{Q}\right] &\approx \frac{1}{N_\xi - 1}\sum_{i=1}^{N_\xi}\left(\tilde{Q}(\xi^{(i)}) - \hat{Q}\right)^2 \triangleq \tilde{S}^2 \\
\sigma_\eta^2(\xi^{(i)}) &\approx \frac{1}{N_\xi - 1}\sum_{j=1}^{N_\eta}\left(f(\xi^{(i)},\eta^{(j)}) - \tilde{Q}(\xi^{(i)})\right)^2 \triangleq \hat{\sigma}_\eta^2(\xi^{(i)}) \\
\frac{\mathbb{E}_\xi\left[\sigma_\eta^2\right]}{N_\eta} &\approx \frac{1}{N_\eta}\frac{1}{N_\xi}\sum_{i=1}^{N_\xi}\hat{\sigma}_\eta^2(\xi^{(i)}) \triangleq \hat{\mu}_{\sigma^2_{RT,N_\eta}}.
\end{aligned} \tag{3.11}$$

The sample estimator counterpart of Eq. (3.10) is then

$$\mathbb{V}ar\left[Q\right] \approx S^2 = \tilde{S}^2 - \hat{\mu}_{\sigma^2_{RT,N_\eta}}. \tag{3.12}$$

3.1.4 Prescribing a computational budget

The goal of a precise estimator is to obtain statistics with the lowest possible variance for a prescribed computational budget. In the case of this MC-MC estimator, assuming a linear cost model with a constant N_η for all N_ξ UQ runs, the total computational budget is $\mathcal{C} = N_\xi \times N_\eta$. Eq. (3.7) suggests that the variance of the estimator, $\mathbb{V}ar\left[\hat{Q}\right]$, is minimized when $\mathbb{V}ar\left[\tilde{Q}\right]$ is; the most effective computational budget for $\hat{Q}$ is that which minimizes $\mathbb{V}ar\left[\tilde{Q}\right]$. In practical implementation, the most effective computational budget for $\hat{Q}$ is that which minimizes the variance of $\tilde{Q}$'s sample estimator, $\tilde{S}^2$.
Before presenting the derivation for minimizing $\mathbb{V}ar\left[\tilde{S}^2\right]$, we introduce some notation:

$$\begin{aligned}
\mu\left[X\right] &\triangleq \mathbb{E}\left[X\right] \\
\mu_k\left[X\right] &\triangleq \mathbb{E}\left[(X-\mu)^k\right] \\
\mu_{\eta,k}\left[X\right] &\triangleq \mathbb{E}_\eta\left[(X-\mu_\eta)^k\right] \\
\sigma^2\left[X\right] &= \mu_2\left[X\right].
\end{aligned} \tag{3.13}$$

Given that $\tilde{S}^2$ is a sample variance, its variance is [20]:

$$\mathbb{V}ar\left[\tilde{S}^2\right] = \frac{\mu_4\left[\tilde{Q}\right]}{N_\xi} - \frac{\sigma^4\left[\tilde{Q}\right](N_\xi - 3)}{N_\xi(N_\xi - 1)}. \tag{3.14}$$

Introducing the shorthand notation $\tilde{\mu}_k \triangleq \mu_k\left[\tilde{Q}\right]$,

$$\mathbb{V}ar\left[\tilde{S}^2\right] = \frac{\tilde{\mu}_4}{N_\xi} - \frac{\tilde{\sigma}^4(N_\xi - 3)}{N_\xi(N_\xi - 1)}. \tag{3.15}$$

Our objective is to study Eq. (3.15) as a function of N_η to understand, given a fixed total estimator cost, much we need to resolve each stochastic code simulation to

minimize $\mathbb{V}ar\left[\tilde{S}^2\right]$, and therefore $\mathbb{V}ar\left[\hat{Q}\right]$. We start by considering a simple linear cost model in which the start-up time is negligible, *i.e.* $\mathcal{C} = N_\xi \times N_\eta$ and we re-write Eq. (3.15) as a function of N_η (while $\mathcal{C}$ is kept constant)

$$\mathbb{V}ar\left[\tilde{S}^2\right] = N_\eta \frac{\tilde{\mu}_4}{\mathcal{C}} - \frac{\tilde{\sigma}^4 N_\eta \left(\mathcal{C} - 3N_\eta\right)}{\mathcal{C}\left(\mathcal{C} - N_\eta\right)}. \tag{3.16}$$

We want to solve $\partial \mathbb{V}ar\left[\tilde{S}^2\right]/\partial N_\eta = 0$, which is

$$\frac{\partial \mathbb{V}ar\left[\tilde{S}^2\right]}{\partial N_\eta} = \frac{\tilde{\mu}_4}{\mathcal{C}} + \frac{N_\eta}{\mathcal{C}}\frac{\partial \tilde{\mu}_4}{\partial N_\eta} - \frac{\partial \tilde{\sigma}^4}{\partial N_\eta}\frac{N_\eta\left(\mathcal{C} - 3N_\eta\right)}{\mathcal{C}\left(\mathcal{C} - N_\eta\right)} - \tilde{\sigma}^4 \frac{\partial N_\eta\left(\mathcal{C} - 3N_\eta\right)}{\partial \mathcal{C}\left(\mathcal{C} - N_\eta\right)}, \tag{3.17}$$

where the statistics of interest are

$$\begin{aligned}
\tilde{\mu}_4 &= \mathbb{E}\left[\tilde{Q}^4\right] - 4\mathbb{E}\left[\tilde{Q}^3\right]\mathbb{E}\left[Q\right] + 6\mathbb{E}\left[\tilde{Q}^2\right]\mathbb{E}\left[Q\right]^2 - 3\mathbb{E}\left[Q\right]^4 \\
\mathbb{E}\left[\tilde{Q}^4\right] &= \mathbb{E}\left[Q^4\right] + \frac{1}{{N_\eta}^4}\left[6{N_\eta}^3\mathbb{E}_\xi\left[Q^2\sigma_\eta^2\right] + 4{N_\eta}^2\mathbb{E}_\xi\left[Q\mu_{\eta,3}[f]\right] + N_\eta\mathbb{E}_\xi\left[\mu_{\eta,4}[f] + 3\left(N_\eta - 1\right)\left(\sigma_\eta^2\right)^2\right]\right] \\
\mathbb{E}\left[\tilde{Q}^3\right] &= \mathbb{E}\left[Q^3\right] + \frac{3}{N_\eta}\mathbb{E}_\xi\left[Q\sigma_\eta^2\right] + \frac{1}{{N_\eta}^2}\mathbb{E}_\xi\left[\mu_{\eta,3}\right] \\
\mathbb{E}\left[\tilde{Q}^2\right] &= \mathbb{V}ar\left[\tilde{Q}\right] + \mathbb{E}_\xi\left[Q\right]^2 = \mathbb{V}ar_\xi\left[Q\right] + \frac{\mathbb{E}_\xi\left[\sigma_\eta^2\right]}{N_\eta} + \mathbb{E}_\xi\left[Q\right]^2 = \mathbb{E}_\xi\left[Q^2\right] + \frac{1}{N_\eta}\mathbb{E}_\xi\left[\sigma_\eta^2\right] \\
\tilde{\sigma}^4 &= \mathbb{V}ar_\xi\left[Q\right]^2 + 2\mathbb{V}ar_\xi\left[Q\right]\mathbb{E}_\xi\left[\sigma^2_{RT,N_\eta}\right] + \mathbb{E}_\xi\left[\sigma^2_{RT,N_\eta}\right]^2 = \left(\mathbb{V}ar\left[\tilde{Q}\right]\right)^2
\end{aligned} \tag{3.18}$$

and the derivatives are

$$\begin{aligned}
\frac{\partial \tilde{\mu}_4}{\partial N_\eta} &= \frac{\partial \mathbb{E}\left[\tilde{Q}^4\right]}{\partial N_\eta} - 4\mathbb{E}\left[Q\right]\frac{\partial \mathbb{E}\left[\tilde{Q}^3\right]}{\partial N_\eta} + 6\mathbb{E}\left[Q\right]^2\frac{\partial \mathbb{E}\left[\tilde{Q}^2\right]}{\partial N_\eta} \\
\frac{\partial \mathbb{E}\left[\tilde{Q}_4\right]}{\partial N_\eta} &= -\frac{6}{{N_\eta}^2}\mathbb{E}_\xi\left[Q^2\sigma_\eta^2\right] - \frac{8}{{N_\eta}^3}\mathbb{E}_\xi\left[Q\mu_{\eta,3}\right] - \frac{3}{{N_\eta}^4}\mathbb{E}_\xi\left[\mu_{\eta,4}\right] - \frac{3}{{N_\eta}^3}\left(2 - \frac{3}{N_\eta}\right)\mathbb{E}_\xi\left[\left(\sigma_\eta^2\right)^2\right] \\
\frac{\partial \mathbb{E}\left[\tilde{Q}^3\right]}{\partial N_\eta} &= -\frac{3}{{N_\eta}^2}\mathbb{E}_\xi\left[Q\sigma_\eta^2\right] - \frac{2}{{N_\eta}^3}\mathbb{E}_\xi\left[\mu_{\eta,3}\right] \\
\frac{\partial \mathbb{E}\left[\tilde{Q}^2\right]}{\partial N_\eta} &= -\frac{1}{{N_\eta}^2}\mathbb{E}_\xi\left[\sigma_\eta^2\right] \\
\frac{\partial \tilde{\sigma}^4}{\partial N_\eta} &= -\frac{2}{{N_\eta}^2}\mathbb{V}ar_\xi\left[Q\right]\mathbb{E}_\xi\left[\sigma_\eta^2\right] - \frac{2}{{N_\eta}^3}\left(\mathbb{E}_\xi\left[\sigma_\eta^2\right]\right)^2 = -\frac{2}{{N_\eta}^2}\left(\mathbb{V}ar_\xi\left[Q\right] + \frac{\mathbb{E}_\xi\left[\sigma_\eta^2\right]}{N_\eta}\right) \\
\frac{\partial\left(N_\eta\left(\mathcal{C} - 3N_\eta\right)\right)}{\partial\left(\mathcal{C}\left(\mathcal{C} - N_\eta\right)\right)} &= \frac{\mathcal{C}^2 - 6\mathcal{C}N_\eta + 3{N_\eta}^2}{\mathcal{C}\left(\mathcal{C} - N_\eta\right)^2}.
\end{aligned} \tag{3.19}$$

The previous expressions suggest which statistics are needed to compute in order to solve the resource allocation problem.

Unbiased estimators for analytical terms

In practical application, a pilot study is needed to compute the necessary terms to find the optimal cost configuration for a subsequent UQ study. After developing the analytic expressions (Eq. (3.17), (3.18), and (3.19)) we need to find unbiased estimators to compute these analytic terms from available tallies. We introduce some notation for a (biased) sample central moment:

$$m_k[X] = \frac{1}{N}\sum_{i=1}^{N}(x_i - m)^k \tag{3.20}$$

where m is the (unbiased) sample central mean. We use the notation $\hat{\cdot}$ to indicate a sample estimator. The unbiased central moments over N_η are[3]:

$$\begin{aligned}
\hat{\sigma}_\eta^2 &= \frac{N_\eta}{N_\eta - 1} m_{\eta,2} \\
\hat{\mu}_{\eta,3} &= \frac{{N_\eta}^2}{(N_\eta - 1)(N_\eta - 2)} \\
\hat{\mu}_{\eta,4} &= \frac{N_\eta\left[\left({N_\eta}^2 - 2N_\eta + 3\right) m_{\eta,4} - 3\left(2N_\eta - 3\right) m_{\eta,2}^2\right]}{(N_\eta - 1)(N_\eta - 2)(N_\eta - 3)} \\
\hat{\sigma}_\eta^4 &= \frac{N_\eta\left[\left({N_\eta}^2 - 3N_\eta + 3\right) m_{\eta,2}^2 - \left(N_\eta - 1\right) m_{\eta,4}\right]}{(N_\eta - 1)(N_\eta - 2)(N_\eta - 3)}
\end{aligned} \tag{3.21}$$

such that

$$\begin{aligned}
\mathbb{E}\left[\hat{\sigma}_\eta^2\right] &= \mathbb{E}_\xi\left[\sigma_\eta^2\right], \\
\mathbb{E}\left[\hat{\mu}_{\eta,3}\right] &= \mathbb{E}_\xi\left[\mu_{\eta,3}\right], \\
\mathbb{E}\left[\hat{\mu}_{\eta,4}\right] &= \mathbb{E}_\xi\left[\mu_{\eta,4}\right], \text{and} \\
\mathbb{E}\left[\hat{\sigma}_\eta^4\right] &= \mathbb{E}_\xi\left[\sigma_\eta^4\right].
\end{aligned} \tag{3.22}$$

Equations (3.18) give us unbiased estimators for $\mathbb{E}\left[Q^2\right]$, $\mathbb{E}\left[Q^3\right]$, and $\mathbb{E}\left[Q^4\right]$, leaving us needing to compute estimators for $\mathbb{E}\left[Q\sigma_\eta^2\right]$, $\mathbb{E}\left[Q\mu_{\eta,3}\right]$, and $\mathbb{E}\left[Q^2\sigma_\eta^2\right]$ from the available $\tilde{Q}\hat{\sigma}_\eta^2$, $\tilde{Q}\hat{\mu}_{\eta,3}$, and $\tilde{Q}^2\hat{\sigma}_\eta^2$.

$$\begin{aligned}
m_{\eta,2} &= \frac{1}{N_\eta}\sum_{j=1}^{N_\eta}\left(f - \tilde{Q}\right)^2 = \frac{1}{N_\eta}\left(\sum_{j=1}^{N_\eta} f^2 - N_\eta\tilde{Q}^2\right) \\
\hat{\sigma}_\eta^2 &= \frac{1}{N_\eta - 1}\left(\sum_{j=1}^{N_\eta} f^2 - N_\eta\tilde{Q}^2\right) \\
\mathbb{E}_\eta\left[\tilde{Q}\hat{\sigma}_\eta^2\right] &= \frac{1}{N_\eta - 1}\left(\mathbb{E}_\eta\left[\tilde{Q}\sum_{j=1}^{N_\eta} f^2\right] - N_\eta\mathbb{E}_\eta\left[\tilde{Q}^3\right]\right) \\
&= \ldots = Q\sigma_\eta^2 + \frac{1}{N_\eta}\mu_{\eta,3} \\
\mathbb{E}_\xi\left[Q\sigma_\eta^2\right] &= \mathbb{E}\left[\tilde{Q}\hat{\sigma}_\eta^2\right] - \frac{1}{N_\eta}\mathbb{E}\left[\hat{\mu}_{\eta,3}\right]
\end{aligned} \tag{3.23}$$

[3]See appendix for full derivations of unbiased central moments.

$$
\begin{aligned}
m_{\eta,3} &= \frac{1}{N_\eta}\sum_{j=1}^{N_\eta}\left(f-\tilde{Q}\right)^3 = \frac{1}{N_\eta}\left(\sum_{j=1}^{N_\eta} f^3 - 3\tilde{Q}\sum_{j=1}^{N_\eta} f^2 + 2N_\eta\tilde{Q}^3\right)\\
\hat{\mu}_{\eta,3} &= \frac{N_\eta}{(N_\eta-1)(N_\eta-2)}\left(\sum_{j=1}^{N_\eta} f^3 - 3\tilde{Q}\sum_{j=1}^{N_\eta} f^2 + 2N_\eta\tilde{Q}^3\right)\\
\mathbb{E}_\eta\left[\tilde{Q}\hat{\mu}_{\eta,3}\right] &= \frac{N_\eta}{(N_\eta-1)(N_\eta-2)}\left(\mathbb{E}_\eta\left[\tilde{Q}\sum_{j=1}^{N_\eta} f^3\right] - 3\mathbb{E}_\eta\left[\tilde{Q}^2\sum_{j=1}^{N_\eta} f^2\right] + 2N_\eta\mathbb{E}_\eta\left[\tilde{Q}^4\right]\right)\\
&= \ldots = Q\mu_{\eta,3} + \frac{1}{N_\eta}\mu_{\eta,4} + \frac{2-3N_\eta}{N_\eta(N_\eta-2)}(\sigma_\eta^2)^2\\
\mathbb{E}_\xi\left[Q\mu_{\eta,3}\right] &= \mathbb{E}\left[\tilde{Q}\hat{\mu}_{\eta,3}\right] - \frac{1}{N_\eta}\mathbb{E}\left[\hat{\mu}_{\eta,4}\right] - \frac{2-3N_\eta}{N_\eta(N_\eta-2)}\mathbb{E}_\xi\left[(\hat{\sigma}_\eta^2)^2\right]
\end{aligned}
\tag{3.24}
$$

$$
\begin{aligned}
m_{\eta,2} &= \frac{1}{N_\eta}\sum_{j=1}^{N_\eta}\left(f-\tilde{Q}\right)^2 = \frac{1}{N_\eta}\left(\sum_{j=1}^{N_\eta} f^2 - N_\eta\tilde{Q}^2\right)\\
\hat{\sigma}_\eta^2 &= \frac{1}{N_\eta-1}\left(\sum_{j=1}^{N_\eta} f^2 - N_\eta\tilde{Q}^2\right)\\
\mathbb{E}_\eta\left[\tilde{Q}^2\hat{\sigma}_\eta^2\right] &= \frac{1}{N_\eta-1}\left(\mathbb{E}_\eta\left[\tilde{Q}^2\sum_{j=1}^{N_\eta} f^2\right] - N_\eta\mathbb{E}_\eta\left[\tilde{Q}^4\right]\right)\\
&= \ldots = Q^2\sigma_\eta^2 + \frac{2}{N_\eta}Q\mu_{\eta,3} + \frac{1}{{N_\eta}^2}\mu_{\eta,4} + \frac{N_\eta-3}{{N_\eta}^2}(\sigma_\eta^2)^2\\
\mathbb{E}_\xi\left[Q^2\sigma_\eta^2\right] &= \mathbb{E}\left[\tilde{Q}^2\hat{\sigma}_\eta^2\right] - \frac{2}{N_\eta}\mathbb{E}\left[\tilde{Q}\hat{\mu}_{\eta,3}\right] + \frac{1}{{N_\eta}^2}\mathbb{E}\left[\hat{\mu}_{\eta,4}\right] - \frac{(N_\eta+1)^2}{{N_\eta}^2(N_\eta-2)}\mathbb{E}\left[(\hat{\sigma}_\eta^2)^2\right]
\end{aligned}
\tag{3.25}
$$

To conduct a pilot study:

1. For a single $\xi^{(i)}$, complete a MCRT calculation with N_η histories.
2. Compute $\hat{\mu}_{\eta,3,i}$, $\hat{\mu}_{\eta,4,i}$, and $\hat{\sigma}^4_{\eta,i}$ using the equations above, in addition to $\hat{\sigma}^2_{\eta,i}$ and $\tilde{Q}_i$.
3. After all N_ξ have run, average $\hat{\mu}_{\eta,3,i}$, $\hat{\mu}_{\eta,4,i}$, $\hat{\sigma}^4_{\eta,i}$, $\hat{\sigma}^2_{\eta,i}$, and $\tilde{Q}_i$ over N_ξ for unbiased estimates of $\mathbb{E}_\xi\left[\sigma_\eta^2\right]$, $\mathbb{E}_\xi\left[\mu_{\eta,3}\right]$, $\mathbb{E}_\xi\left[\mu_{\eta,4}\right]$, $\mathbb{E}_\xi\left[(\sigma_\eta^2)^2\right]$, and $\mathbb{E}\left[Q\right]$.
4. Use the equations above to compute unbiased estimates of $\mathbb{E}\left[Q^2\right]$, $\mathbb{E}\left[Q^3\right]$, $\mathbb{E}\left[Q^4\right]$, $\mathbb{E}\left[Q\sigma_\eta^2\right]$, $\mathbb{E}\left[Q\mu_{\eta,3}\right]$, and $\mathbb{E}\left[Q^2\sigma_\eta^2\right]$.
5. Pass these terms to a function that will compute $\tilde{\mu}_4$, $\frac{\partial\tilde{\mu}_4}{\partial N_\eta}$, $\tilde{\sigma}^4$, and $\frac{\partial\tilde{\sigma}^4}{\partial N_\eta}$ to optimize $\frac{\partial\mathbb{V}ar\left[\tilde{S}^2\right]}{\partial N_\eta}$ as a function of N_η.

This would ideally compute the optimum N_η at which to run a full UQ study, and assign the number of UQ samples in accordance with the prescribed total estimator cost.

3.2 Global sensitivity analysis for stochastic solvers

This section outlines the methodology for understanding how use of stochastic solvers affects both sampling-based and PCE surrogate-based GSA.

3.2.1 Global sensitivity analysis - sampling approach

The novel contribution of the proposed work starts with understanding what variability is introduced by stochastic solvers to sensitivity index analysis. To get a sense of this, we can perform numerical studies with and without stochastic solvers. Dakota is a software developed by Sandia National Laboratories with a broad range of capabilities in uncertainty quantification, sensitivity analysis, optimization, and calibration designed to be coupled with existing simulation codes [21]. We plan to use Dakota coupled with a deterministic radiation transport solver to develop baseline values for global sensitivity indices, then couple Dakota with a MCRT solver to scope how the additional uncertainty introduced by the solver is handled by a production-level software.

Outside of Dakota, we can turn to the equations of the Saltelli method, Eq. (1.2) and (1.4) to analyze any biases introduced by the stochastic solver. One approach is to consider the MCRT solver variance to be an additional uncertain input, rather than considering the MCRT solver variance as being introduced into the variance of each of the uncertain UQ inputs. This can be corroborated numerically by keeping the rng-seed of the MCRT solver constant when appropriate for the algorithm described in Section 1.3.

An alternative approach is similar to that described in Section 3.1, combining the deconvolved variance in Eq. (3.10) with the Saltelli equations to compute unbiased estimates of first order and total effect indices. In [22], we incorporated variance deconvolution into the Saltelli method, provide an unbiased sampling-based method for computing SIs when using an MCRT solver. From the definition of Sobol' indices in Eq. 1.2, we see that we need $\mathbb{V}ar_{\xi}\left[Q\right]$ and $V_u \forall u \in d$, where V_u is the conditional variance $\mathbb{V}ar\left[\mathbb{E}\left[Q|\xi_u\right]\right]$. To further understand the conditional variance of UQ parameter ξ_u from our variance deconvolution approach, we can break ξ down into its components $\xi_u, u = 1, 2, .., d$ such that $Q\left(\xi\right) = Q\left(\xi_u, \xi_{\sim u}\right)$. If we introduce additional notation for the expectation of the QoI as a function of just a variable of interest ξ_u, we can write

$$P(\xi_u) \triangleq \mathbb{E}_{\xi_{\sim u}}\left[Q(\xi_u, \xi_{\sim u})\right] \approx \frac{1}{N_{SI}} \sum_{k=1}^{N_{SI}} \tilde{Q}(\xi_u, {\xi_{\sim u}}^{(k)}) \triangleq \tilde{P}_{N_{SI}}(\xi_u), \tag{3.26}$$

and we can express Eqs. (3.8) and (1.2) as

$$V_u = \mathbb{V}ar\left[\tilde{P}_{N_{SI}}\right] - \frac{\mathbb{E}_{\xi_u}\left[\mathbb{V}ar_{\xi_{\sim u}}\left[\tilde{Q}\right]\right]}{N_{SI}} \quad \text{and} \quad S_u = \frac{\mathbb{V}ar\left[\tilde{P}_{N_{SI}}\right] - \frac{\mathbb{E}_{\xi_u}\left[\mathbb{V}ar_{\xi_{\sim u}}\left[\tilde{Q}\right]\right]}{N_{SI}}}{\mathbb{V}ar\left[\tilde{Q}\right] - \frac{\mathbb{E}_{\xi}\left[\sigma_{\eta}^2\right]}{N_{\eta}}}. \tag{3.27}$$

Computing V_u requires holding parameter ξ_u constant while re-sampling all other UQ parameters $\xi_{\sim u}$ N_{SI} times. For d main and d total effects, the total estimator cost is $C = N_{\xi} \times N_{SI} \times 2d \times N_{\eta}$.

Introducing variance deconvolution to Sobol' indices

To analyze sensitivity indices when using stochastic solvers, we apply the variance deconvolution estimator developed for UQ to a version of the Saltelli method. To compute sensitivity indices, we must have more than one uncertainty source to which the output variance can be apportioned. Therefore, our radiation transport example here is transmittance through an attenuation-only 1D slab with uncertain cross sections similar to that in Section 4.1, but also incorporates stochastic material mixing. We continue to use η to represent the stochastic behavior of the MCRT solver and let ξ denote cross section uncertainty, but introduce the random variable ω to denote the uncertainty due to the stochastic media (SM). To compute SIs, we need the variance of the quantity of interest (QoI) due to both sources of aleatoric uncertainty ξ and η, as well as the variance of the QoI due solely to ξ and solely to η.

As before, the QoI $Q(\xi,\omega)$ can only be approximated using a finite number of particle histories N_η:

$$Q(\xi,\omega) \triangleq \mathbb{E}_\eta\left[f(\xi,\omega,\eta)\right] \approx \tilde{Q}(\xi,\omega) \triangleq \frac{1}{N_\eta}\sum_{j=1}^{N_\eta} f\left(\xi,\omega,\eta^{(j)}\right), \tag{3.28}$$

where $f(\xi,\omega,\eta)$ is a function of a sample of the uncertainty sources and the MCRT solver. We introduce $\mathbb{P}_\mathbb{E}(\xi)$, the expectation of the transmittance over SM realizations, which can similarly only be approximated over a finite number of SM configurations N_ω:

$$\mathbb{P}_\mathbb{E}(\xi) \triangleq \mathbb{E}_\omega\left[Q(\xi,\omega)\right] \approx \tilde{\mathbb{P}}^{\mathbb{E}}_{N_\omega}(\xi) \triangleq \frac{1}{N_\omega}\sum_{k=1}^{N_\omega}\tilde{Q}(\xi,\omega^{(k)}). \tag{3.29}$$

In related work, collaborators solved for an expression for the variance due to the cross section uncertainty as a function of the expectation of the SM uncertainty [23]:

$$\mathbb{V}ar_\xi\left[\mathbb{P}_\mathbb{E}(\xi)\right] = \mathbb{V}ar_\xi\left[\tilde{\mathbb{P}}^{\mathbb{E}}_{N_\omega}(\xi)\right] - \frac{\mathbb{E}_\xi\left[\mathbb{V}ar_\omega\left[\tilde{Q}(\xi,\omega)\right]\right]}{N_\omega}, \tag{3.30}$$

in which $\mathbb{V}ar_\xi\left[\tilde{\mathbb{P}}^{\mathbb{E}}_{N_\omega}(\xi)\right]$ is a polluted estimate of $\mathbb{V}ar_\xi\left[\mathbb{P}_\mathbb{E}(\xi)\right]$ computed using N_η particle histories on each of N_ω SM realizations and $\frac{1}{N_\omega}\mathbb{E}_\xi\left[\mathbb{V}ar_\omega\left[\tilde{Q}(\xi,\omega)\right]\right]$ is the average statistical pollution caused by MCRT histories and SM variability. The final term in Eq. (3.30) can again be de-convolved into the total aleatoric variance $\mathbb{V}ar_{\xi,\omega}\left[Q(\xi,\omega)\right]$ and the contribution from the MCRT solver:

$$\mathbb{V}ar_{\xi,\omega}\left[\tilde{Q}(\xi,\omega)\right] = \mathbb{V}ar_{\xi,\omega}\left[Q(\xi,\omega)\right] + \mathbb{E}_{\xi,\omega}\left[\frac{1}{N_\eta}\sigma^2_\eta(\xi,\omega)\right]. \tag{3.31}$$

This is similar to Eq. (3.10) which de-convolved the total variance of $\tilde{Q}(\xi)$ into the parametric variance $\mathbb{V}ar_\xi[Q]$ and MCRT solver variance, but now with the additional aleatoric uncertainty source ω introduced. By combining Eqs. (3.30) and (3.31), we have all we need for an unbiased (de-polluted) estimate of the first-order sensitivity index of ξ on $Q(\xi,\omega)$:

$$S_\xi = \frac{\mathbb{V}ar_\xi\left[\mathbb{P}_\mathbb{E}(\xi)\right]}{\mathbb{V}ar_{\xi,\omega}\left[Q(\xi,\omega)\right]}. \tag{3.32}$$

It follows that, if we introduced an additional variable $\mathbb{P}_{\mathbb{E}}(\omega)$ to be the expectation of the transmittance over uncertain cross section realizations, we could follow the same process outlined for $\mathbb{P}_{\mathbb{E}}(\xi)$ to arrive at an unbiased estimate of the first-order sensitivity index of ω on $Q(\xi, \omega)$:

$$S_\omega = \frac{\mathbb{V}ar_\omega \left[\mathbb{P}_{\mathbb{E}}(\omega)\right]}{\mathbb{V}ar_{\xi,\omega}\left[Q(\xi,\omega)\right]}. \tag{3.33}$$

Through the law of total variance, we can also compute the Sobol total effects for both the aleatoric contributions:

$$S_\xi = \frac{\mathbb{V}ar_\xi \left[\mathbb{P}_{\mathbb{E}}(\xi)\right]}{\mathbb{V}ar_{\xi,\omega}\left[Q(\xi,\omega)\right]} = 1 - \frac{\mathbb{E}_\xi\left[\mathbb{V}ar_\omega\left[Q(\xi,\omega)\right]\right]}{\mathbb{V}ar_{\xi,\omega}\left[Q(\xi,\omega)\right]} = 1 - S_{T_\omega} \tag{3.34a}$$

$$S_\omega = \frac{\mathbb{V}ar_\omega \left[\mathbb{P}_{\mathbb{E}}(\omega)\right]}{\mathbb{V}ar_{\xi,\omega}\left[Q(\xi,\omega)\right]} 1 - \frac{\mathbb{E}_\omega\left[\mathbb{V}ar_\xi\left[Q(\xi,\omega)\right]\right]}{\mathbb{V}ar_{\xi,\omega}\left[Q(\xi,\omega)\right]} = 1 - S_{T_\xi}. \tag{3.34b}$$

These results are extendable to solve for the first-order and total SIs for any subset of aleatoric variances, with the caveat that to make practical use of this approach, it must be known how to hold ω constant while resampling ξ and vice-versa. Further work will build on this development by comparing its computational complexity and performance with that of the standard Saltelli approach to understand whether it warrants algorithmic changes to the standard Saltelli approach, or whether the most efficient route for GSA with stochastic solvers is to append variance deconvolution to the standard Saltelli approach.

3.2.2 Global sensitivity analysis - surrogate models

While we don't intend to develop novel methods for creating polynomial chaos expansion models using stochastic solvers, our collaborators at Sandia National Laboratories have been working to build PCE models using stochastic solvers [24]. We plan to build on the work in progress on developing PCE methods using stochastic solvers by comparing the accuracy and performance of the PCE surrogate models to that of the sampling-based approach outlined above.

3.3 Challenge problem application

This section outlines the methodology for demonstrating wider applicability of the developed UQ and GSA methods.

3.3.1 Complex cost models

Section 3.1.4 describes a method for finding the most cost-effective sampling allocation of N_ξ and N_η for a high-accuracy estimate of UQ statistics, using a linear cost model such that the total estimator cost is $\mathcal{C} = N_\xi \times N_\eta$. This optimization is based solely on how the estimator accuracy varies with N_η, assuming that all configurations of the linear cost model will be computationally equivalent. This is not necessarily the case in practice. For example, for a total estimator cost of $\mathcal{C} = 500$, 5 100-particle

simulations ($N_\xi = 5, N_\eta = 100$) and 100 5-particle simulations ($N_\xi = 100, N_\eta = 5$) would not have the same runtime. In going from Eq. (3.15) to Eq. (3.16), we substituted in the linear cost model to study how $\mathbb{V}ar\left[\tilde{S}^2\right]$ varied as a function of N_η. By incorporating estimates of cost models that include startup time and the difference between re-sampling time and MCRT runtime, we can understand how the sampling allocation of N_ξ and N_η are affected by complex cost models and what the cost-benefit is of using initial pilot studies to determine optimal allocation.

3.3.2 Complex radiation transport problems

These UQ and GSA methods have been used with 1D slab-geometry radiation transport simulations computing transmittance and reflectance with attenuation-only and scattering physics as proof-of-concept and numerical corroboration with theoretical findings. To show capability with more complex and realistic radiation transport problems, we plan to incorporate the variance deconvolution UQ and GSA frameworks into Monte Carlo Dynamic Code (MC/DC), a high-performance, Python-based, time-dependent Monte Carlo neutron transport software currently in development in the Center for Exascale Monte Carlo Neutron Transport (CEMeNT) [25]. The center's challenge problem is a three-dimensional, continuous energy, time-dependent neutron transport problem with moving control rods based on a NuScale-like small modular reactor (SMR). It is sectioned in time into four phases (see Figure 3.1) that simulate an over-withdrawal of control rods and a subsequent neutron excursion and reactor SCRAM.

We plan to test UQ and GSA capabilities and scaling using Phase 1, a time-dependent version of a typical steady-state fixed source problem that features an active neutron source and spatial asymmetry, shown with the stuck rods in Figure 3.2. Figure 3.3 shows total fission rate (produced by Ilham Variansyah [26] using MC/DC) for a simulation using $\sim 10^{10}$ particle histories on Quartz, an Intel CPU cluster at Lawrence Livermore National Laboratory [27]. Ultimately the center's goal is to have time-dependent, multi-group, pin-cell mesh tallies; this will require significantly more histories than the simulation that is shown, providing us with test cases for UQ and GSA performance and scaling for the simpler total fission rate problem and the scaled-up problem. This will present a challenge for the UQ and GSA aspect as additional tallies will be required to compute higher-order moments, likely impacting MC/DC's performance and scaling.

By incorporating the framework into an existing and active codebase, we will be able to test the UQ and GSA performance when both the physics and tallying complexity of the simulations are scaled up. MC/DC's existing capabilities include 3D geometry; time-dependence; tallies such as flux, current, fission density, and Eddington factors; and variance reduction techniques such as weight windows are in active development by collaborators. We will be able to collaborate with the software's main developer, Ilham Variansyah, to incorporate methods developed in this PhD research into MC/DC such that a user could perform reliable UQ or GSA studies using a highly capable Monte Carlo radiation transport solver and evaluate computational scaling with increased physics and tally requirements.

	Phase 1	Phase 2	Phase 3	Phase 4
t [seconds] $\in$	[0, 5]	[5, 10]	[10, 15]	[15, 20]
Regulating rods	Fully inserted (except stuck)	Fully inserted (except stuck)	9.71% withdrawn in 5s (except stuck)	Fully inserted in .0971s (except stuck)
Safety rods	Fully inserted	Fully withdrawn in 5s	Fully withdrawn	Fully inserted in 1s (except stuck)
Point source (Center, isotropic, highest energy)	Active	Active	Active	Inactive
k at the end	0.91032 $\pm$ 13 pcm	0.98500 $\pm$ 14 pcm	1.00512 $\pm$ 15 pcm	0.96619 $\pm$ 13 pcm

* Control rods are moved with constant speeds (piecewise linear)

Figure 3.1: The four phases of the CEMeNT challenge problem [26]; our work will focus on phase 1.

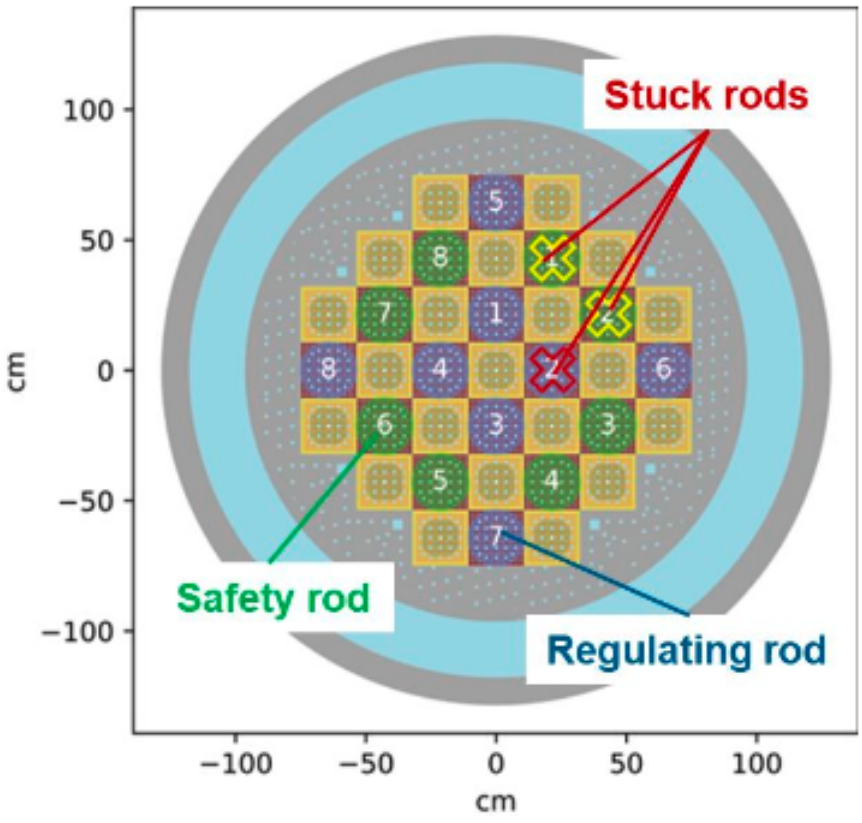

Figure 3.2: Cross-sectional view of the reactor test problem with rods highlighted [26].

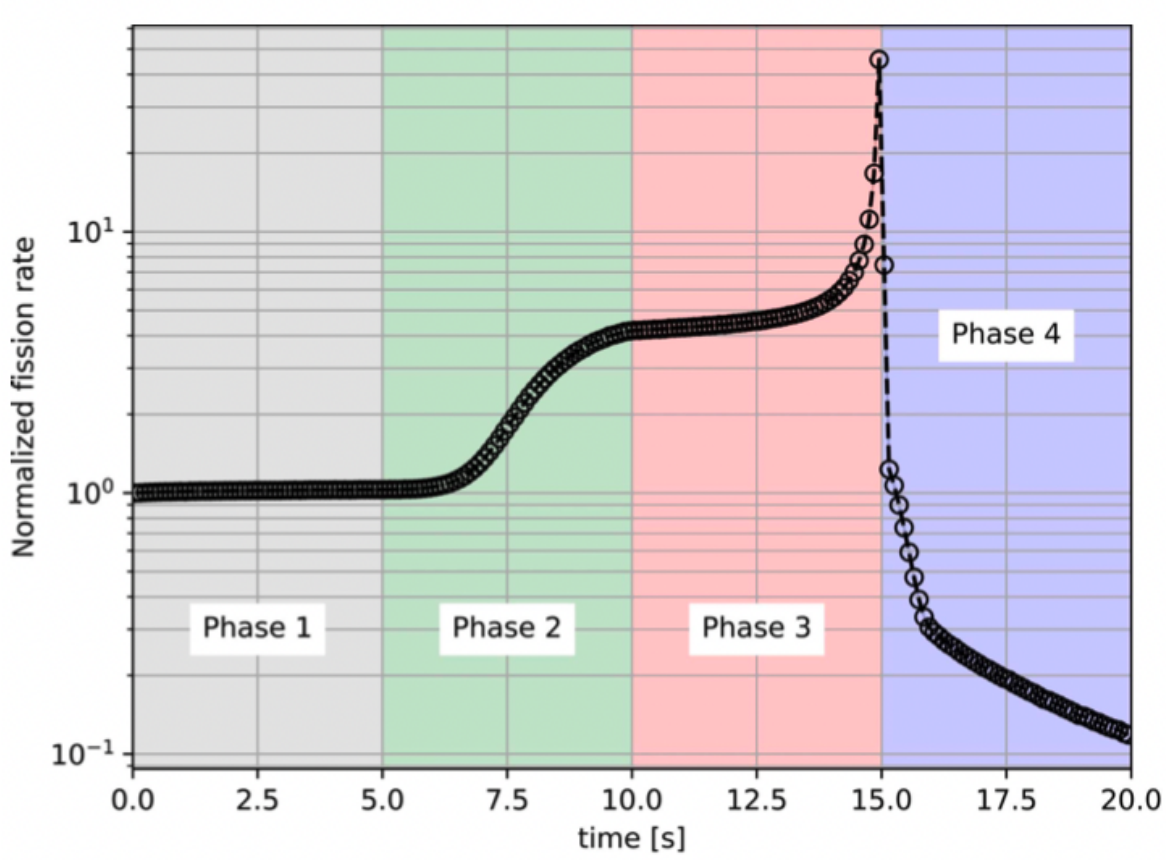

Figure 3.3: Total fission rate results from MC/DC with $\sim 10^{10}$ particle histories [26].

4 Preliminary results

4.1 Variance deconvolution for uncertainty quantification

4.1.1 Problem description

To verify the variance deconvolution method, we applied the UQ variance estimator in Eq. (3.10) (repeated below for convenience) to a radiation transport problem with an analytic solution to compare against. We solve the one-dimensional, neutral-particle, mono-energetic, steady-state radiation transport equation with a normally incident beam source of magnitude one:

$$\mu \frac{\partial \psi(x,\mu)}{\partial x} + \Sigma_t(x)\,\psi(x,\mu) = \int_{-1}^{1} d\mu' \psi(x,\mu') \frac{\Sigma_s(x,\mu' \to \mu)}{2}, \tag{4.1}$$

$$0 \leq x \leq L; \quad -1 \leq \mu \leq 1, \tag{4.2}$$

where $\psi(x,\mu)$ is angular flux, $\Sigma_t(x)$ is total cross section, $\Sigma_s(x,\mu)$ is scattering cross section, and x and μ respectively denote dependence on space and angle. The problem is a slab geometry with fixed boundaries $x \in [0, L]$ and fixed boundaries between material regions. The problem is solved for two different scenarios: attenuation-only in which $\Sigma_s(x,\mu) = 0$, and with both attenuation and isotropic scattering. We introduce stochasticity into the problem via the total cross section and, for the problem with scattering, the scattering ratio. As with the derivations in Section 3.1, we represent the stochasticity with the variable ξ. For both scenarios, the total cross section of each material is assumed to be uniformly distributed. In the scenario which also involves scattering, the ratio of scattering to total cross section c is distributed uniformly and independently of Σ_t. We consider a slab with a total of M materials, where for each region m the total cross section is defined as

$$\Sigma_{t,m}(\xi_m) = \bar{\Sigma}_{t,m} + \Sigma^{\Delta}_{t,m}\xi_m \tag{4.3}$$

with $\bar{\Sigma}_{t,m}$ representing the average total cross section and $\Sigma^{\Delta}_{t,m}$ the deviation from the mean value. Furthermore, a random parameter $\xi_m \sim \mathcal{U}[-1,1]$ is used to represent the variability of $\Sigma_{t,m}(\xi) \sim \mathcal{U}[\bar{\Sigma}_{t,m} - \Sigma^{\Delta}_{t,m}, \bar{\Sigma}_{t,m} + \Sigma^{\Delta}_{t,m}]$. For cases with scattering, the scattering ratio is defined analogously using

$$c_m(\xi_{M+m}) = \bar{c}_m + c^{\Delta}_m \xi_{M+m} \tag{4.4}$$

where $\xi_{M+m} \sim \mathcal{U}[-1,1]$, with $m = 1,\ldots,M$, is a uniformly distributed random variable. We note that in the attenuation-only case the problem contains a number of uncertain parameters equal to the number of materials, *i.e.* $\xi \in \mathbb{R}^d$ with $d = M$, whereas in the case of both attenuation and scattering $d = 2M$.

For the attenuation-only problem, we compare to an analytic solution for uncollided transmittance of a normally incident beam through a slab,

$$T(\xi) = \psi(L,1,\xi) = \exp\left[\sum_{m=1}^{M} \Sigma_{t,m}(\xi_m)\Delta x_m\right]. \tag{4.5}$$

The pth raw moment for the transmittance, as derived in [28], is

$$\mathbb{E}\left[T^p\right] = \prod_{m=1}^{d} \exp\left[-p\bar{\Sigma}_{t,m}\Delta x_m\right] \frac{\sinh\left[p\Sigma^{\Delta}_{t,m}\Delta x_m\right]}{p\bar{\Sigma}_{t,m}\Delta x_m}, \tag{4.6}$$

which allows for an exact evaluations of central moments by adopting the well-known transformations from raw to central moments. For instance, for the variance, which is the second central moment, we can write

$$\mathbb{V}ar\left[T\right] = \mathbb{E}\left[T^2\right] - \mathbb{E}\left[T\right]^2. \tag{4.7}$$

This example is well suited for verification as it is also possible to compute the variance $\mathbb{E}_{\xi}\left[\sigma^2_{\eta}\right]$ in closed form for this problem.

4.1.2 Numerical results

We consider a 1D slab with 3 material regions[1], and report in Table 4.1 the right boundary location, average total cross section, and deviation from the cross section mean for each of the material sections for both problems, as well as the analogous information for the scattering ratio for the isotropic scattering problem. In Table 4.2, we report the mean transmittance and parametric variance computed with closed-form solutions where available; numerical benchmark solutions with $N_\eta = 10^5$, $N_\xi = 10^3$ ($C = 10^8$); and using one typical repetition of our variance deconvolution method with $N_\eta = 10^1$, $N_\xi = 10^3$ ($C = 10^4$), for reference[2].

Table 4.1: Problem parameters.

Problem Parameters				Scattering Parameters	
	x_R	$\Sigma^0_{t,m}$	$\Sigma^{\Delta}_{t,m}$	$c^0_{s,m}$	$c^{\Delta}_{s,m}$
m = 1	2.0	0.90	0.70	0.50	0.40
m = 2	5.0	0.15	0.12	0.50	0.40
m = 3	6.0	0.60	0.50	0.50	0.40

[1]The approach can be extended to higher number of sections without any modifications to the algorithm.

[2]Note that for the deconvolved results, this is only one realization of a stochastic problem, which converges to the benchmark over many repetitions.

Table 4.2: Mean QoI and parametric variance. Numerical benchmark computed with $N_\eta = 10^5$, $N_\xi = 10^3$ ($C = 10^8$); variance deconvolution computed with $N_\eta = 10^1$, $N_\xi = 10^3$ ($C = 10^4$); and closed-form solutions where available.

Attenuation Only			
	Benchmark	Deconvolved	Analytic
$\mathbb{E}[T]$	8.915E-2	8.870E-2	8.378E-2
S_T^2	5.789E-3	5.768E-3	5.505E-3
Scattering			
	Benchmark	Deconvolved	-
$\mathbb{E}[T]$	1.299E-1	1.209E-1	-
S_T^2	9.710E-3	9.825E-3	-
$\mathbb{E}[R]$	1.386E-1	1.336E-1	-
S_R^2	8.251E-3	7.703E-3	-

To better understand where the variance of the novel estimator is minimized, we solve the described RT problem using Woodcock-delta tracking with analog Monte Carlo methods for an estimator cost $C = N_\xi \times N_\eta$ of 200, 500, 1000, 1500, 2000, and 5000 for a variety of N_η values. We repeat the estimator evaluation over 25,000 repetitions to evaluate its statistics. We report $\mathbb{V}ar[S^2]$ for both the attenuation-only and isotropic scattering case, where $S^2 = \mathbb{V}ar[T]$ or $\mathbb{V}ar[R]$, in Table 4.3. The exact parametric variance is calculable for the attenuation-only case, so we also compare the estimate of S^2 for the attenuation-only case to the analytic solution using Mean Square Error (MSE), which we also report in Table 4.3.

For the attenuation-only case, we see that $\mathbb{V}ar[S^2]$ first decreases as a function of N_η, reaches its minimum at $N_\eta = 10$, then gradually increases again. We only report up values up to $N_\eta = 100$, because after this $\mathbb{V}ar[S^2]$ just continues to increase. The varied N_η value is the number of histories per sample, meaning that even in the case where $N_\eta = 2$, the actual QoI (transmittance, reflectance) is still being calculated over the full estimator cost. To better see the trend, Figure 4.1 shows $\mathbb{V}ar[S^2]$ as a function of N_η on a log-log scale for the attenuation-only case. We can see clearly here that $\mathbb{V}ar[S^2]$ is not minimized by running with the lowest possible number of histories, and a tradeoff does indeed exist between the number of UQ samples N_ξ and the number of particle histories N_η; this is not the case for the previous estimator in [11] with most problems. We can see the same trend in the isotropic scattering case, and when $S^2 = \mathbb{V}ar[T]$, $\mathbb{V}ar[S^2]$ is also minimized at $N_\eta = 10$.

Table 4.3: The variance (and MSE, where applicable) of the estimate of S^2 over 25,000 repetitions for both the attenuation-only and scattering problems.

Attenuation-Only Problem									
	$\mathbb{V}ar\left[S^2\right]$					$MSE[S^2]$ (Exact $\mathbb{V}ar\left[T\right] = 5.505E-3$)			
N_η	Estimator Cost				N_η	Estimator Cost			
	200	500	2000	5000		200	500	2000	5000
2	9.584E-05	3.887E-05	9.626E-06	3.879E-06	2	1.332E-10	9.106E-13	3.176E-11	5.565E-11
5	3.970E-05	1.597E-05	3.907E-06	1.586E-06	5	1.119E-09	3.600E-14	3.734E-11	4.169E-11
10	**3.241E-05**	**1.303E-05**	**3.168E-06**	**1.297E-06**	10	7.155E-10	2.692E-10	5.997E-12	1.308E-11
20	3.568E-05	1.414E-05	3.482E-06	1.384E-06	20	2.576E-10	1.026E-10	8.893E-12	4.168E-11
100	1.327E-04	3.866E-05	9.218E-06	3.656E-06	100	3.678E-10	6.301E-09	1.424E-10	3.323E-11

Scattering Problem									
	$\mathbb{V}ar\left[S^2\right]$, Transmittance					$\mathbb{V}ar\left[S^2\right]$, Reflectance			
N_η	Estimator Cost				N_η	Estimator Cost			
	200	500	2000	5000		200	500	2000	5000
2	1.730E-04	6.921E-05	1.749E-05	6.996E-06	2	1.786E-04	7.085E-05	1.770E-05	7.140E-06
5	7.664E-05	2.963E-05	7.424E-06	2.882E-06	5	6.574E-05	2.592E-05	6.392E-06	2.591E-06
10	**6.329E-05**	**2.461E-05**	**6.175E-06**	**2.488E-06**	10	4.792E-05	1.852E-05	4.586E-06	1.861E-06
20	7.360E-05	2.775E-05	6.852E-06	2.753E-06	20	**4.656E-05**	**1.758E-05**	**4.303E-06**	**1.694E-06**
25	8.090E-05	3.102E-05	7.499E-06	3.012E-06	25	4.963E-05	1.836E-05	4.371E-06	1.771E-06
100	2.987E-04	8.572E-05	1.897E-05	7.456E-06	100	1.661E-04	4.169E-05	8.476E-06	3.241E-06

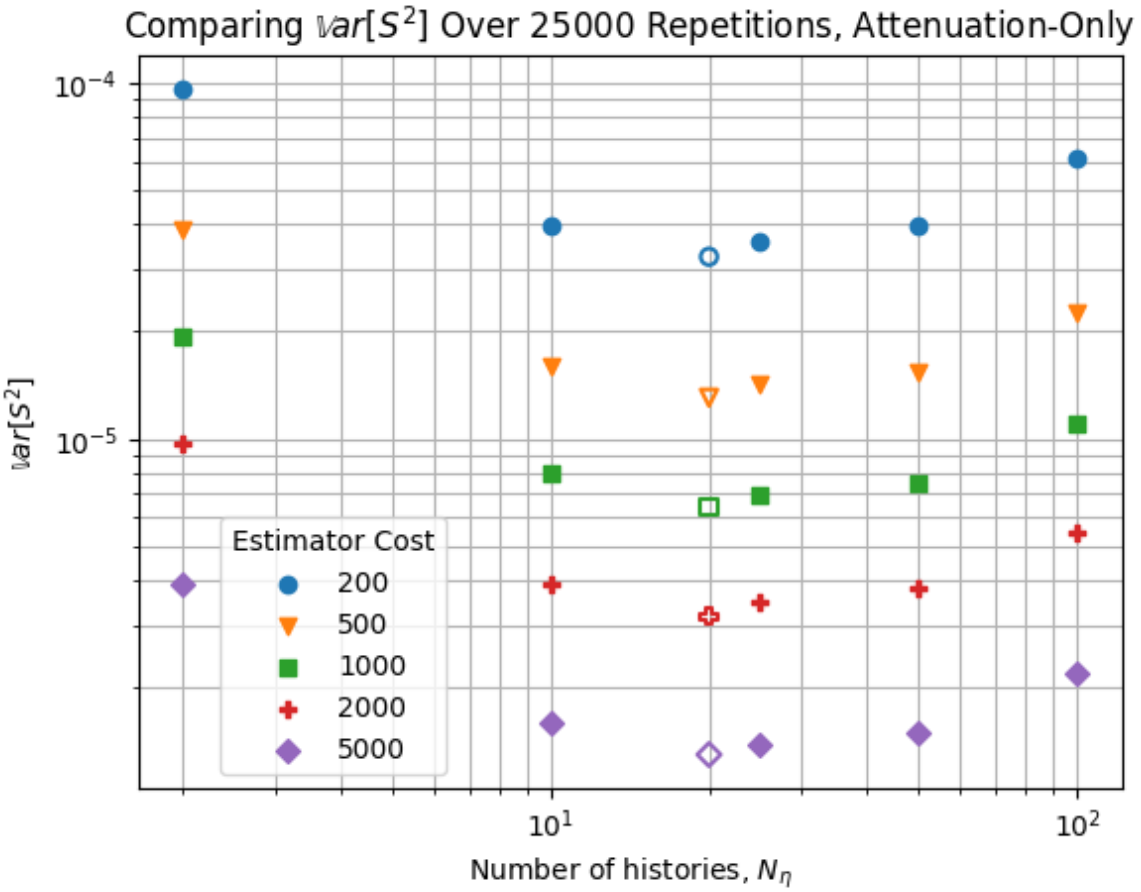

Figure 4.1: $\mathbb{V}ar\left[S^2\right]$ as a function of N_η for a variety of total estimator costs, log-log plot. Unfilled point is minimum $\mathbb{V}ar\left[S^2\right]$.

We see a similar trend for the isotropic scattering problem where S^2 is $\mathbb{V}ar\left[R\right]$, the parametric variance of the reflectance tally. However, in this case $\mathbb{V}ar\left[S^2\right]$ is minimized at $N_\eta = 20$, rather than $N_\eta = 10$. While both transmittance and reflectance are influenced by the addition of scattering and the stochastic scattering ratio, the reflectance tally is likely more sensitive to this scattering ratio, and requires more radiation transport tallies to resolve than the transmittance tally. This demonstrates that the optimal number of N_ξ and N_η can differ between different QoIs even within the same problem, motivating further investigation to allow the analyst to choose these parameters in an informed way. Figure 4.2 compares the trends for the attenuation-only estimate of $\mathbb{V}ar\left[T\right]$ to the isotropic scattering estimate of $\mathbb{V}ar\left[T\right]$ and $\mathbb{V}ar\left[R\right]$.

4.2 Global sensitivity analysis for stochastic solvers

4.2.1 Problem description

To verify the SI method, we can again use an analytic solution for uncollided transmittance of a normally incident beam through a slab from Eq. (4.5). This test problem

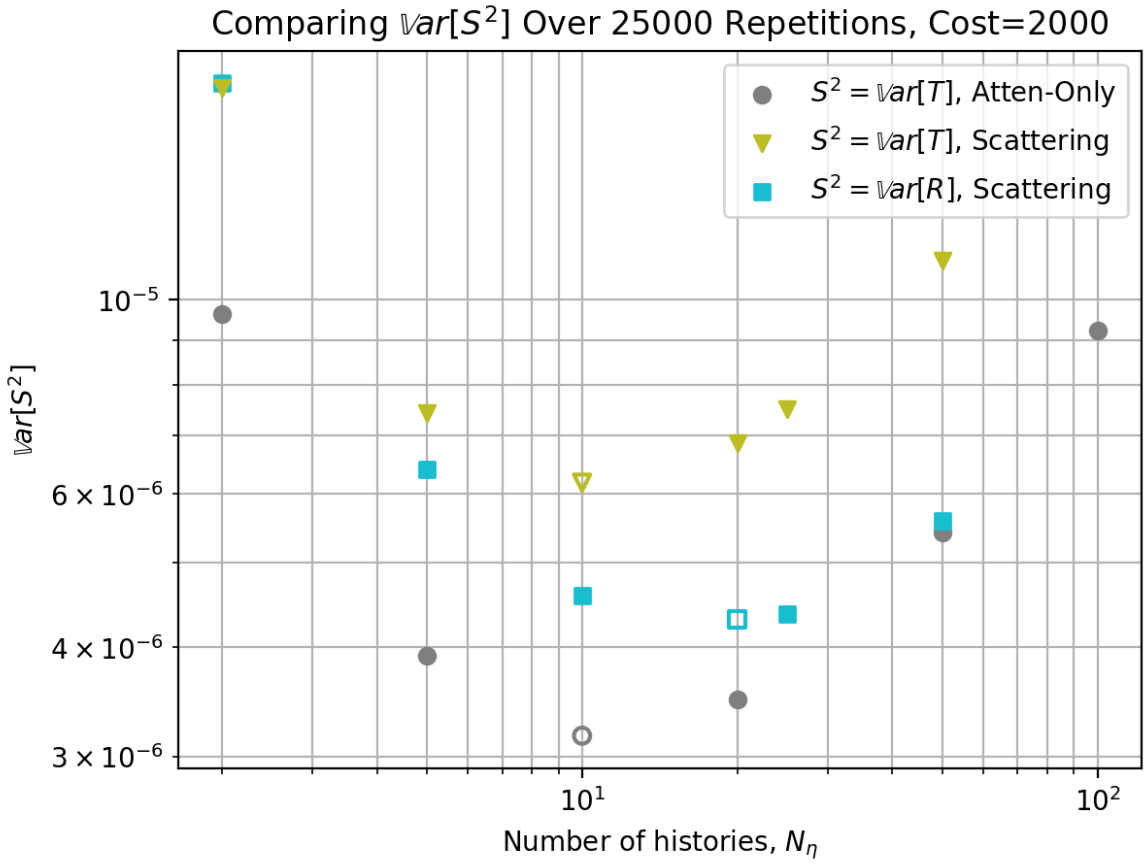

Figure 4.2: $\mathbb{V}ar\left[S^2\right]$ as a function of N_η for the attenuation-only and scattering cases. Log-log plot, estimator cost $N_\xi \times N_\eta = 2000$. Unfilled point is minimum $\mathbb{V}ar\left[S^2\right]$.

is a one-dimensional slab with three regions of thicknesses r_1, r_2 and r_3 and a mono-energetic beam source incident on the first region. The slab contains three absorption-only materials with total cross sections $\Sigma_{t,1}, \Sigma_{t,2}$ and $\Sigma_{t,3}$. Region 1 contains N_{tot} subcells of equal width $\Delta x = r_1/N_{tot}$, each of which can contain either Material 1 with probability p_1 or Material 2 with probability $(1 - p_1)$. The number of cells in Region 1 containing Material 1 in a realization of this stochastic medium can be represented as a sample from the binomial probability density function (PDF), $N_1(\omega) \sim \mathcal{B}\left(N_{tot}, p_1\right)$, where ω represents the non-parametric aleatoric uncertainty of N_1. Region 2 simply contains Material 2. Region 3 contains Material 3, whose cross section $\Sigma_{t,3}(\xi)$ is a function of parametric aleatoric uncertainty $\xi \sim \mathcal{U}\left(-1, 1\right)$.

The problem quantity of interest, transmittance T through the slab, is a function of the optical thickness τ of each region:

$$\begin{aligned} \tau_1 &= N_1(\omega)\Delta x \Sigma_{t,1} + (N_{tot} - N_1(\omega))\Delta x \Sigma_{t,2} \\ &= N_1(\omega)\Delta x \left(\Sigma_{t,1} - \Sigma_{t,2}\right) + r_1 \Sigma_{t,2} \end{aligned} \tag{4.8}$$

$$\tau_2 = r_2 \Sigma_{t,2} \tag{4.9}$$

$$\begin{aligned} \tau_3 = r_3 \Sigma_{t,3} &= r_3 \left(\Sigma^0_{t,3} + \Sigma^\Delta_{t,3} \xi\right) \\ &= r_3 \Sigma^0_{t,3} + r_3 \Sigma^\Delta_{t,3} \xi \end{aligned} \tag{4.10}$$

where $\Sigma_{t,3}(\xi) = \Sigma^0_{t,3} + \Sigma^{\Delta}_{t,3}\xi$, $\Sigma^0_{t,3}$ is the mean total cross section, and $\Sigma^{\Delta}_{t,3}$ the deviation from the mean. The transmittance is therefore a function of both the non-parametric and parametric aleatoric uncertainties,

$$T = T\left(\xi, \omega\right) = k \exp\left(-k_1 N_1(\omega)\right) \exp\left(-k_3 \xi\right) \tag{4.11}$$

where

$$k = \exp\left[-r_1\Sigma_{t,2} - r_2\Sigma_{t,2} - r_3\Sigma^0_{t,3}\right] \tag{4.12a}$$
$$k_1 = \Delta x\left(\Sigma_{t,1} - \Sigma_{t,2}\right) \tag{4.12b}$$
$$k_3 = -r_3\Sigma^{\Delta}_{t,3} \tag{4.12c}$$

The $p^{th}-$order raw moment of $T\left(\xi, \omega\right)$ is

$$\begin{aligned}\mathbb{E}_{\xi,\omega}[T^p(\xi,\omega)] &= \mathbb{E}_{\xi}\left[\mathbb{E}_{\omega}\left[T^p\left(\xi,\omega\right)\right]\right] \\ &= \int_{\omega}\int_{\xi} d\xi\, d\omega\, k^p \exp\left(-k_1 p N_1(\omega)\right) \exp\left(-k_3 p \xi\right) \\ &= k^p \frac{\sinh\left[k_3 p\right]}{k_3 p} \sum_{x=0}^{N_{tot}} B_{\omega}(x) \exp\left(-k_1 p x\right)\end{aligned} \tag{4.13}$$

where $B_{\omega}(x)$ represents the PDF of the binomial variable $N_1(\omega)$ being equal to x:

$$\begin{aligned}B_{\omega}(x) &\triangleq Pr\left(N_1 = x \,|\, N_{tot}, p_1\right) \\ &= \frac{N_{tot}!}{x!\left(N_{tot}-x\right)!} p_1^x \left(1-p_1\right)^{\left(N_{tot}-x\right)}\end{aligned} \tag{4.14}$$

Eq. (4.13) enables computation of the variance of $T\left(\xi, \omega\right)$ over both aleatoric uncertainties, $\mathbb{V}ar_{\xi,\omega}\left[T\left(\xi,\omega\right)\right]$, by expanding the expression for variance,

$$\mathbb{V}ar_{\xi,\omega}\left[T\left(\xi,\omega\right)\right] = \mathbb{E}_{\xi,\omega}\left[T^2\left(\xi,\omega\right)\right] - \mathbb{E}_{\xi,\omega}\left[T\left(\xi,\omega\right)\right]^2. \tag{4.15}$$

This is the denominator of the main and total effect SIs. For comparison with numerical results, we calculate analytic solutions for the numerators in Eqs. (3.34a) and (3.34b). Taking $\mathbb{V}ar_{\xi}\left[\mathbb{P}_{\mathbb{E}}(\xi)\right]$ to indicate the variance of the conditional mean of $T\left(\xi,\omega\right)$ given ξ, over all ξ, we find that

$$\begin{aligned}\mathbb{V}ar_{\xi}\left[\mathbb{P}_{\mathbb{E}}(\xi)\right] &= \mathbb{E}_{\xi}\left[{\mathbb{P}_{\mathbb{E}}}^2(\xi)\right] - \mathbb{E}_{\xi}\left[\mathbb{P}_{\mathbb{E}}(\xi)\right]^2 \\ &= \mathbb{E}_{\xi}\left[{\mathbb{P}_{\mathbb{E}}}^2(\xi)\right] - \mathbb{E}_{\xi,\omega}\left[T\left(\xi,\omega\right)\right]^2.\end{aligned} \tag{4.16}$$

The second term is the first-order raw moment of $T\left(\xi,\omega\right)$, calculable from Eq. (4.13). The first term, the second-order raw moment of $\mathbb{P}_{\mathbb{E}}(\xi)$, is

$$\begin{aligned}\mathbb{E}_{\xi}\left[{\mathbb{P}_{\mathbb{E}}}^2(\xi)\right] &= \int_{\xi} d\xi\, k^2 \exp(-k_3\xi)\left(\sum_{x=0}^{N_{tot}} B_{\omega}(x)\exp\left(-k_1 x\right)\right)^2 \\ &= \frac{k^2 \sinh\left[2k_3\right]}{2k_3}\left(\sum_{x=0}^{N_{tot}} B_{\omega}(x)\exp\left(-k_1 x\right)\right)^2\end{aligned} \tag{4.17}$$

Inserting Eqs. (4.15) and (4.16) into Eq. (3.34a) yields

$$S_\xi = \frac{\frac{k^2 \sinh[2k_3]}{2k_3}\left(\sum_{x=0}^{N_{tot}} B_\omega(x)\exp\left(-k_1 x\right)\right)^2 - \mathbb{E}_{\xi,\omega}\left[T\left(\xi,\omega\right)\right]^2}{\mathbb{E}_{\xi,\omega}\left[T^2\left(\xi,\omega\right)\right] - \mathbb{E}_{\xi,\omega}\left[T\left(\xi,\omega\right)\right]^2}. \tag{4.18}$$

Following the same process to calculate $\mathbb{V}ar_\omega\left[\mathbb{P}_\mathbb{E}(\omega)\right]$ yields

$$S_\omega = \frac{\frac{k^2 \sinh^2[k_3]}{k_3^2}\left(\sum_{x=0}^{N_{tot}} B_\omega(x)\exp\left(-2k_1 x\right)\right) - \mathbb{E}_{\xi,\omega}\left[T\left(\xi,\omega\right)\right]^2}{\mathbb{E}_{\xi,\omega}\left[T^2\left(\xi,\omega\right)\right] - \mathbb{E}_{\xi,\omega}\left[T\left(\xi,\omega\right)\right]^2}. \tag{4.19}$$

Given these closed-form solutions for the main effect SIs, Eqs. (3.34a) and (3.34b) provide closed-form solutions for the total effect SIs.

4.2.2 Numerical results

We solve two numerical problems each using the problem description from the previous section with $r_1 = r_2 = r_3 = 1.0$, $\Sigma_{t,1} = 3.0$, $\Sigma_{t,2} = 0.1$, $\Sigma^0_{t,3} = 1.0$, and $p_1 = 0.3$. We use two configurations, one with $N_{tot} = 10$ and $\Sigma^\Delta_{t,3} = 0.25$, and the other with $N_{tot} = 100$ and $\Sigma^\Delta_{t,3} = 0.75$. For each quantity on both problems, we use $N_\eta = 20$. For each problem, we first solve for the average transmittance ($\mathbb{E}_{\xi,\omega}\left[T(\xi,\omega)\right]$) and combined aleatoric variance ($\mathbb{V}ar_{\xi,\omega}\left[Q\left(\xi,\omega\right)\right]$) using 10,000 samples of the aleatoric uncertainty space (i.e., ξ and ω). We then use $N_\omega = 10$ and $N_\xi = 1000$, for a total of 10,000 aleatoric samples, to solve for $\mathbb{V}ar_\xi\left[\mathbb{P}_\mathbb{E}(\xi)\right]$. Next, we use $N_\xi = 10$ and $N_\omega = 1000$, for a total of 10,000 aleatoric samples, to solve for $\mathbb{V}ar_\omega\left[\mathbb{P}_\mathbb{E}(\omega)\right]$. For each of these numerically computed quantities, we average the computed quantities over 40 repetitions and use those repetitions to compute a standard error of the mean (SEM) for the quantity. To compute SI quantities from the total aleatoric variance and each conditional variance, statistical uncertainties are propagated using the standard error propagation formula for independent variables

$$s_f = \sqrt{\left(\frac{\partial f}{\partial x}\right)^2 s_x^2 + \left(\frac{\partial f}{\partial y}\right)^2 s_y^2 + \left(\frac{\partial f}{\partial z}\right)^2 s_z^2 + \ldots}. \tag{4.20}$$

Closed-form values, numerically computed values, and their error compared to the closed-form values are reported in Tables 4.4 and 4.5 for the first and second problem configurations, respectively.

Table 4.4: Closed-form and numerically computed results for the $N_{tot} = 10$ and $\Sigma^\Delta_{t,3} = 0.25$ problem.

	Closed	Numerical	Error
S_ω	0.8734261	0.8747955 ± 0.0103919	$-0.13\ \sigma$
S_ξ	0.1084529	0.1114180 ± 0.0025490	$-1.16\ \sigma$
S_{T_ω}	0.8915471	0.8885820 ± 0.0025490	$1.16\ \sigma$
S_{T_ξ}	0.1265739	0.1252045 ± 0.0103919	$0.13\ \sigma$

Table 4.5: Closed-form and numerically computed results for the $N_{tot} = 100$ and $\Sigma^{\Delta}_{t,3} = 0.75$ problem.

	Closed	Numerical	Error
S_ω	0.0873300	0.0879516 ± 0.0026643	$-0.23\ \sigma$
S_ξ	0.8968785	0.8969538 ± 0.0083963	$-0.01\ \sigma$
S_{T_ω}	0.1031215	0.1030462 ± 0.0083963	$0.01\ \sigma$
S_{T_ξ}	0.9126700	0.9120484 ± 0.0026643	$0.23\ \sigma$

None of the numerically computed SIs differ from the closed-form solutions by more than 1.16 standard deviations, the error is typically less than 1 standard deviation, and the even distribution between positive and negative error does not suggest a bias. The SIs of these two problems help us understand their practical value: while the transmittance and overall aleatoric variances for each problem are roughly the same, our numerically computed SIs provide a formal mechanism by which to measure that the SM contributes the majority of the variance (∼90%) in configuration 1 and, by contrast, the uncertain cross section provides the majority of the variance (∼90%) in configuration 2. Future work with this methodology will include comparing how this algorithm for computing SIs compares with the Saltelli approach outlined in Section 1.3 in accuracy and efficiency.

5 Planned schedule

Below is a Gantt chart indicating our proposed research milestones and timeline. Uncertainty quantification work for the first objective is complete, and a journal article for submission in the *Journal of Quantitative Spectroscopy and Radiative Transfer* (JQSRT) is in progress. It is in collaboration with two authors from Sandia National Laboratories, requiring an additional review and approval (R&A) process. We intend to submit to R&A by mid-February, and submit to JQSRT as soon as that process is complete. Work on the second objective, global sensitivity analysis, began with investigating the Saltelli approach as part of a submitted transactions for ANS Winter 2022. We also submitted an extended abstract on GSA to M&C 2023, and next steps are to extend that work into a full journal article. Objective two research work is approximately 30% complete with the beginning investigations into the Saltelli approach. Work on the third objective, the challenge problem and increased complexity, is underway as we have started integrating variance deconvolution UQ into MC/DC.

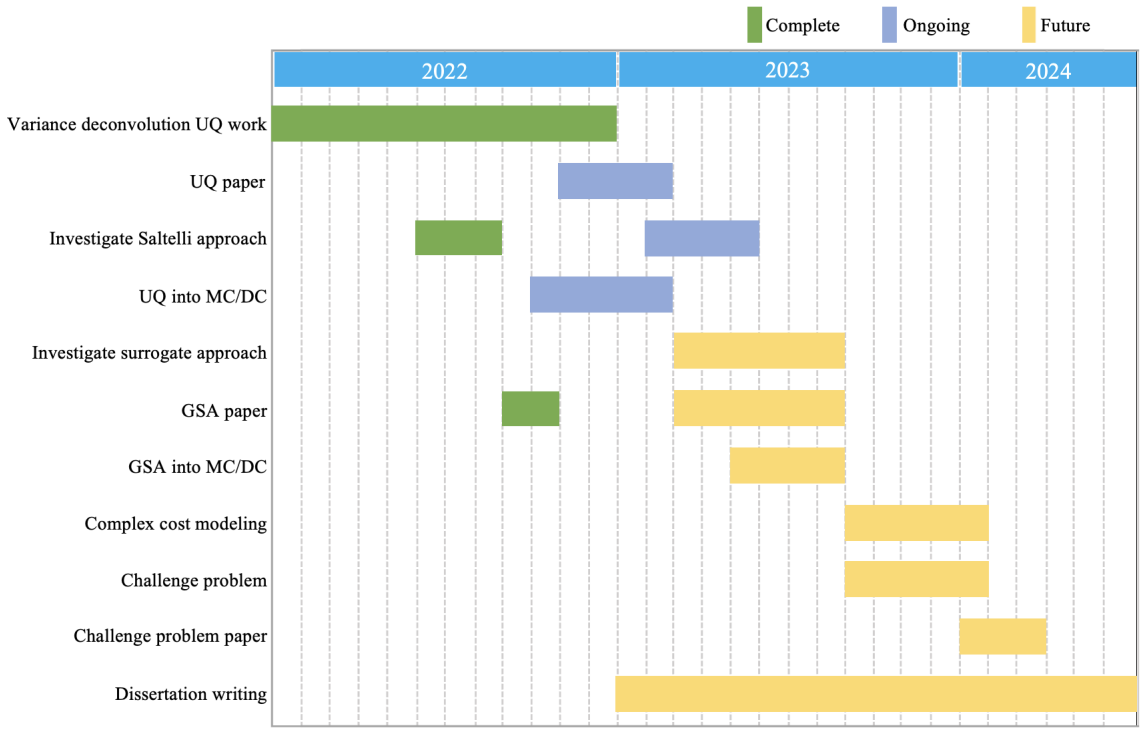

A Included papers

The following three included papers are, in order, a presented transactions from the American Nuclear Society 2022 Annual Meeting, the American Nuclear Society 2022 Winter Meeting, and a draft journal article intended for submission to the Journal of Quantitative Spectroscopy and Radiative Transfer.

I worked closely with mentors at Sandia National Laboratories and Dr. Palmer to produce all three papers. On the first transaction, I am first author and corroborated theoretical findings, performed numerical experiments, and wrote the transaction in tandem with Gianluca Geraci. On the second transaction, I am second author, as Aaron Olson and James Petticrew began the work prior to my joining the team. I corroborated theoretical findings, performed derivations for analytic solutions, corroborated numerical experiments, and wrote sections of the transaction. On the draft journal paper, I am first author and have performed many theoretical derivations and numerical experiments, and am writing the paper in tandem with Gianluca Geraci. Please note that the included paper is a rough draft that to show progress, with plans to submit in mid-February.

Numerical Investigation on the Performance of a Variance Deconvolution Estimator

Kayla Clements,[*,†] Gianluca Geraci,[†] and Aaron Olson,[†]

[*]*Oregon State University, clemekay@oregonstate.edu*
[†]*Sandia National Laboratories, ggeraci@sandia.gov, aolson@sandia.gov*

INTRODUCTION

In radiation transport problems, uncertainty quantification (UQ) can be used to characterize and propagate the effects of uncertain input parameters; we refer to this variance caused by uncertain parameters as parametric variance. Monte Carlo (MC) sampling is one method to obtain statistics of the system's quantities of interest (QoIs) that we wish to evaluate with UQ. In the case of a QoI obtained from Monte Carlo radiation transport (MC RT) computations, UQ MC sampling can function as a wrapper around the MC RT solver. MC RT solvers produce results whose variance is inversely proportional to the square root of the number of particle histories used; we refer to this variance as statistical variability. Though increasing the number of particle histories will decrease this statistical variability, it is often necessary to control the growth of the overall computational burden by limiting the number of particle histories used in each MC RT computation. In this contribution, we show how the statistical variability from this limited number of particle histories propagates to the variance of the QoI, compounding with the parametric variance, and that this increase must be accounted for to obtain reliable UQ results. We named this process –estimating and removing the MC RT statistical variability from the measured total variance –variance deconvolution.

Recently, we developed a novel variance deconvolution estimator which uses tallies already generated during MC RT computations to accurately and efficiently estimate the parametric variance, without carrying the contribution of the statistical variability [1]. Preliminary results suggested that the most efficient variance estimator can be obtained for given computational cost by using specific numbers of UQ samples and particle histories. In this work, we present thorough numerical studies for RT problems with and without scattering to further develop our understanding of how this trade-off affects estimator performance.

VARIANCE DECONVOLUTION

We first develop some background on the variance deconvolution estimator following the presentation in [1]. In the case of a general RT problem, the quantity of interest Q can be understood as a function of a vector of d input parameters, $\xi \in \Xi \subseteq \mathcal{R}^d$. Several code evaluations can be performed for values of ξ sampled from the joint probability density function $p(\xi)$. These samples are then used to evaluate the desired statistics, *e.g.* mean and variance. The interested reader can refer to [2] for an in depth presentation of MC sampling estimators or [3] for an in depth review of MC RT. The non-deterministic behavior of MC RT codes provides a challenge to this process. Each UQ realization $Q(\xi^{(i)})$ from an MC RT code is the result of an averaging over a finite number of particle histories. If we use $f(\xi^{(i)}, \eta^{(j)})$ to indicate the jth particle history corresponding to the ith sample, the QoI can be approximated as

$$Q(\xi^{(i)}) \overset{\text{def}}{=} \mathbb{E}_\eta \left[f(\xi^{(i)}, \eta) \right] \approx \frac{1}{N_\eta} \sum_{j=1}^{N_\eta} f(\xi^{(i)}, \eta^{(j)}) \overset{\text{def}}{=} \tilde{Q}(\xi^{(i)}), \quad (1)$$

where N_η indicates the number of particle histories per parameter sample and $\mathbb{E}_\eta[\cdot]$ is a shorthand to indicate the expected value over realizations drawn with respect to the variable η. We note here that η is used here only to notionally represent the MC RT stochastic behavior and that its value may not be, in general, controllable or known.

Straightforward computation of the parametric variance from the samples of $\tilde{Q}$ unfortunately does not yield accurate results. Instead, the limited number of particle histories N_η embeds a statistical variability that propagates to the measurable variance of $\tilde{Q}$. Although $\mathbb{V}ar_\xi[\tilde{Q}] \to \mathbb{V}ar_\xi[Q]$ as $N_\eta \to \infty$, we want to understand how to accurately compute the parametric variance of $\tilde{Q}$ using a limited, and possibly small, number of histories N_η. This result can be obtained rigorously by applying the Law of Total Variance to $\mathbb{V}ar[\tilde{Q}]$,

$$\begin{aligned} \mathbb{V}ar\left[\tilde{Q}\right] &= \mathbb{V}ar_\xi\left[\mathbb{E}_\eta\left[\tilde{Q}\right]\right] + \mathbb{E}_\xi\left[\mathbb{V}ar_\eta\left[\tilde{Q}\right]\right] \\ &= \mathbb{V}ar_\xi\left[Q\right] + \mathbb{E}_\xi\left[\frac{\sigma_\eta^2}{N_\eta}\right] \\ &= \mathbb{V}ar_\xi\left[Q\right] + \mathbb{E}_\xi\left[\sigma^2_{RT,N_\eta}\right], \end{aligned} \quad (2)$$

where σ_η^2 is defined as the variance of the histories over N_η for each fixed UQ parameter, *i.e.* $\sigma_\eta^2(\xi) \overset{\text{def}}{=} \mathbb{V}ar_\eta[f(\xi, \eta)]$, and $\sigma^2_{RT,N_\eta}(\xi) \overset{\text{def}}{=} \sigma_\eta^2(\xi)/N_\eta$ is the corresponding MC RT solver variance [1]. The expression above relates the true parametric variance of the QoI, $\mathbb{V}ar_\xi[Q]$, and the expected value (over the parameter space) of the statistical variability introduced by the MC RT computations, σ^2_{RT,N_η}. Both terms contribute to the total variance $\mathbb{V}ar[\tilde{Q}]$, the only variance directly observable from numerical experiments.

Practical implementation

As previously discussed, the QoI Q can only be approximated with $\tilde{Q}$, the variance of which can be considered to be polluted by the MC RT statistical variability. On the other hand, $\tilde{Q}$ can be re-evaluated for several samples of ξ, making $\mathbb{V}ar_\xi[\tilde{Q}]$ an accessible quantity; unlike $\mathbb{V}ar_\xi[Q]$, it can be directly estimated by taking the variance over the number of UQ samples N_ξ. Similarly, given multiple particle histories per UQ sample, it is possible to estimate the term $\sigma_\eta^2 = \mathbb{V}ar_\eta[f]$ at each ith UQ parameter location, and therefore estimate σ^2_{RT,N_η}. The true parametric variance can then be obtained.

As $\mathbb{V}ar[\tilde{Q}]$ and $\mathbb{E}_\xi[\sigma^2_{RT,N_\eta}]$ are exact only at the limit of infinite N_ξ, a sample estimator counterpart of the variance deconvolution in Equation 2 is necessary,

$$\mathbb{V}ar_\xi[Q] \approx S^2 = \tilde{S}^2 - \hat{\mu}_{\sigma^2_{RT,N_\eta}}, \tag{3}$$

where S^2 and $\tilde{S}^2$ represent the sample estimators for the true parametric (*i.e.* inaccessible) and polluted variances, respectively, and $\hat{\mu}_{\sigma^2_{RT,N_\eta}}$ indicates the sample mean of the MC RT variance over N_ξ. Assuming the tallies of each particle history are accessible, we can define the two estimators as

$$\begin{aligned} \tilde{S}^2 &= \frac{1}{N_\xi - 1}\sum_{i=1}^{N_\xi}\left(\tilde{Q}(\xi^{(i)}) - \frac{1}{N_\xi}\sum_{k=1}^{N_\xi}\tilde{Q}(\xi^{(k)})\right)^2 \\ \hat{\mu}_{\sigma^2_{RT,N_\eta}} &= \frac{1}{N_\xi}\sum_{i=1}^{N_\xi}\frac{\sigma^2_\eta(\xi^{(i)})}{N_\eta}, \end{aligned} \tag{4}$$

where the term σ^2_η is approximated, for each ith UQ sample, with an additional sample variance estimator

$$\begin{aligned} \sigma^2_\eta(\xi^{(i)}) &\approx \hat{\sigma}^2_\eta(\xi^{(i)}) \\ &= \frac{1}{N_\eta - 1}\sum_{j=1}^{N_\eta}\left(f(\xi^{(i)},\eta^{(j)}) - \frac{1}{N_\eta}\sum_{k=1}^{N_\eta}f(\xi^{(i)},\eta^{(k)})\right)^2. \end{aligned} \tag{5}$$

By solving for $\tilde{S}^2$, σ^2_η, and $\hat{\mu}_{\sigma^2_{RT,N_\eta}}$, we can calculate S^2, and estimate of $\mathbb{V}ar_\xi[Q]$. Ref. [1] shows that S^2 is an unbiased estimator for $\mathbb{V}ar_\xi[Q]$.

The idea of the variance deconvolution, in RT applications, was previously introduced in [4] and presented in the context of an embedded UQ strategy dubbed Embedded VAriance DEconvolution (EVADE). Moreover, EVADE has been successfully adopted in RT computations in the presence of stochastic media, as in [5]. The original EVADE estimator presented in [4] was derived for an approximation of $\tilde{Q}$ obtained with a single particle history. The interested reader can refer to [1] for an in depth discussion of the relationship between the two estimators and numerical comparisons. Both estimators are unbiased, although the variance of the newer estimator summarized thus far is smaller in all analysis scenarios we have considered.

In the present work, we significantly extend our understanding of the deconvolution strategy by investigating the trade-off between the number of UQ samples N_ξ and the number of particle histories N_η. Because only one history was used to calculate the total polluted variance in the original EVADE estimator, the variance of an estimate of S^2 using a prescribed estimator cost $C = N_\xi \times N_\eta$ was minimized when the lowest possible number of particle histories was used. Preliminary results from [1] found that the minimum variance of the newer estimator did not necessarily correspond to the minimum number of histories in the tested problem. To investigate this, we performed numerical studies varying the ratio of N_η to N_ξ for a prescribed estimator cost for a given problem, results of which are discussed in the numerical section.

PROBLEM DESCRIPTION

A short description of the problem used in the numerical investigation follows. We consider the stochastic, one-dimensional, neutral-particle, mono-energetic, steady-state radiation transport equation with a normally incident beam source of magnitude one. The slab has fixed boundaries, i.e. $x \in [0, L]$, and contains a total of M material sections separated by fixed boundaries. The problem is solved both as an attenuation-only problem and with isotropic scattering included. For both scenarios, the stochastic total cross section of each material is assumed to be uniformly distributed. In the scenario which includes scattering, the ratio $c = \Sigma_s/\Sigma_t$ of scattering to total cross section is distributed uniformly and independently of Σ_t. For each region m, Σ_t and c are defined using

$$\Sigma_{t,m}(\xi_m) = \Sigma^0_{t,m} + \Sigma^\Delta_{t,m}\xi_m \tag{6a}$$

$$c_m(\xi_m) = c^0_m + c^\Delta_m\xi_m \tag{6b}$$

where $\cdot^0$ represents the average value and $\cdot^\Delta$ the deviation from the mean. Furthermore, a random parameter $\xi_m \sim \mathcal{U}[-1, 1]$ is used to represent the variability of $\Sigma_{t,m}(\xi) \sim \mathcal{U}[\Sigma^0_{t,m} - \Sigma^\Delta_{t,m}, \Sigma^0_{t,m} + \Sigma^\Delta_{t,m}]$. For cases with scattering, the scattering ratio c_m is defined analogously. In the attenuation-only case, the number of uncertain parameters is equal to the number of materials, *i.e.* $\xi \in \mathbb{R}^d$ with $d = M$, whereas in the case of both attenuation and scattering $d = 2M$.

For the attenuation-only case, the estimate S^2 can be compared to its analytic counterpart. By using the pth raw moment for the transmittance, as shown in [4],

$$\mathbb{E}[T^p] = \prod_{m=1}^{d} exp\left[-p\Sigma^0_{t,m}\Delta x_m\right]\frac{sinh\left[p\Sigma^\Delta_{t,m}\Delta x_m\right]}{p\Sigma^0_{t,m}\Delta x_m}, \tag{7}$$

the parametric variance can be obtained as $\mathbb{V}ar[T] = \mathbb{E}[T^2] - \mathbb{E}[T]^2$. It is also possible to compute the variance $\mathbb{E}_\xi[\sigma^2_{RT,N_\eta}]$ in closed form for this problem, using $\sigma^2_{RT,N_\eta} = \frac{T(\xi)}{N_\eta}(1 - T(\xi))$.

NUMERICAL RESULTS

In this section, we present the performance of the described variance estimator for two UQ analysis scenarios, attenuation-only and attenuation with scattering. We consider a 1D slab with 3 material sections[1], and report in Table I the right boundary location, average total cross section, and deviation from the cross section mean for each of the material sections for both problems, as well as the analogous information for the scattering ratio for the isotropic scattering problem. In Table II, we report the mean QoI and parametric variance computed with closed-form solutions where available; numerical benchmark solutions with $N_\eta = 10^5$, $N_\xi = 10^3$ ($C = 10^8$); and using one typical repetition of our variance deconvolution method with $N_\eta = 10^1$, $N_\xi = 10^3$ ($C = 10^4$), for reference[2].

[1] The approach can be extended to higher number of sections without any modifications to the algorithm.

[2] Note that for the deconvolved results, this is only one realization of a stochastic problem, which converges to the benchmark over many repetitions.

TABLE I. Problem parameters.

Problem Parameters				Scattering Parameters	
	x_R	$\Sigma^0_{t,m}$	$\Sigma^\Delta_{t,m}$	$c^0_{s,m}$	$c^\Delta_{s,m}$
m = 1	2.0	0.90	0.70	0.50	0.40
m = 2	5.0	0.15	0.12	0.50	0.40
m = 3	6.0	0.60	0.50	0.50	0.40

TABLE II. Mean QoI and parametric variance. Numerical benchmark computed with $N_\eta = 10^5$, $N_\xi = 10^3$ ($C = 10^8$); variance deconvolution computed with $N_\eta = 10^1$, $N_\xi = 10^3$ ($C = 10^4$); and closed-form solutions where available.

Attenuation Only			
	Benchmark	Deconvolved	Analytic
$\mathbb{E}[T]$	8.915E-2	8.870E-2	8.378E-2
S^2_T	5.789E-3	5.768E-3	5.505E-3
Scattering			
	Benchmark	Deconvolved	-
$\mathbb{E}[T]$	1.299E-1	1.209E-1	-
S^2_T	9.710E-3	9.825E-3	-
$\mathbb{E}[R]$	1.386E-1	1.336E-1	-
S^2_R	8.251E-3	7.703E-3	-

To better understand where the variance of the novel estimator is minimized, we solve the described RT problem using Woodcock-delta tracking with analog Monte Carlo methods for an estimator cost $C = N_\xi \times N_\eta$ of 200, 500, 1000, 1500, 2000, and 5000 for a variety of N_η values. We repeat the estimator evaluation over 25,000 repetitions to evaluate its statistics. We report $\mathbb{V}ar[S^2]$ for both the attenuation-only and isotropic scattering case, where $S^2 = \mathbb{V}ar[T]$ or $\mathbb{V}ar[R]$, in Table III. The exact parametric variance is calculable for the attenuation-only case, so we also compare the estimate of S^2 for the attenuation-only case to the analytic solution using Mean Square Error (MSE), which we also report in Table III.

For the attenuation-only case, we see that $\mathbb{V}ar[S^2]$ first decreases as a function of N_η, reaches its minimum at $N_\eta = 10$, then gradually increases again. We only report up values up to $N_\eta = 100$, because after this $\mathbb{V}ar[S^2]$ just continues to increase. The varied N_η value is the number of histories per sample, meaning that even in the case where $N_\eta = 2$, the actual QoI (transmittance, reflectance) is still being calculated over the full estimator cost. To better see the trend, Figure 1 shows $\mathbb{V}ar[S^2]$ as a function of N_η on a log-log scale for the attenuation-only case. We can see clearly here that $\mathbb{V}ar[S^2]$ is not minimized by running with the lowest possible number of histories, and a tradeoff does indeed exist between the number of UQ samples N_ξ and the number of particle histories N_η; this is not the case for the previous estimator in [1] with most problems. We can see the same trend in the isotropic scattering case, and when $S^2 = \mathbb{V}ar[T]$, $\mathbb{V}ar[S^2]$ is also minimized at $N_\eta = 10$.

We see a similar trend for the isotropic scattering problem where S^2 is $\mathbb{V}ar[R]$, the parametric variance of the reflectance tally. However, in this case $\mathbb{V}ar[S^2]$ is minimized at $N_\eta = 20$, rather than $N_\eta = 10$. While both transmittance and reflectance are influenced by the addition of scattering and the stochastic

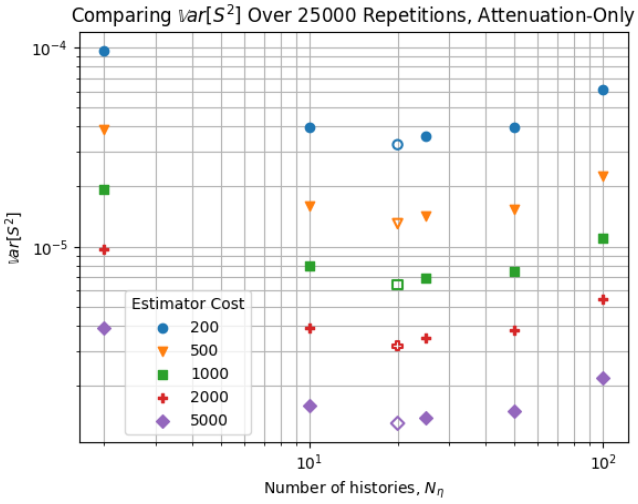

Fig. 1. $\mathbb{V}ar[S^2]$ as a function of N_η for a variety of total estimator costs, log-log plot. Unfilled point is minimum $\mathbb{V}ar[S^2]$.

scattering ratio, the reflectance tally is likely more sensitive to this scattering ratio, and requires more radiation transport tallies to resolve than the transmittance tally. This demonstrates that the optimal number of N_ξ and N_η can differ between different QoIs even within the same problem, motivating further investigation to allow the analyst to choose these parameters in an informed way. Figure 2 compares the trends for the attenuation-only estimate of $\mathbb{V}ar[T]$ to the isotropic scattering estimate of $\mathbb{V}ar[T]$ and $\mathbb{V}ar[R]$.

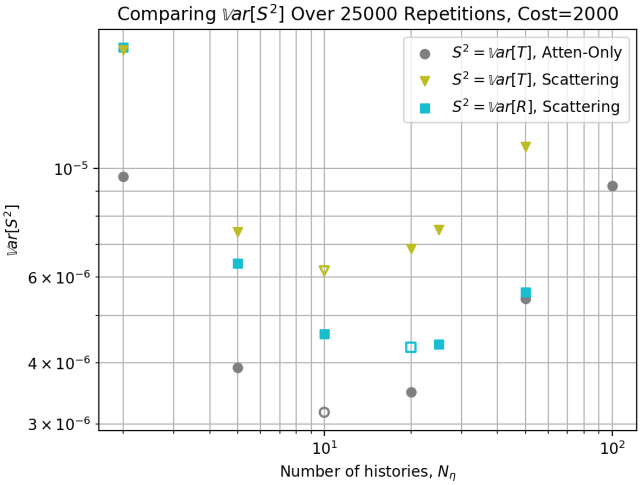

Fig. 2. $\mathbb{V}ar[S^2]$ as a function of N_η for the attenuation-only and scattering cases. Log-log plot, estimator cost $N_\xi \times N_\eta = 2000$. Unfilled point is minimum $\mathbb{V}ar[S^2]$.

CONCLUSIONS AND FUTURE WORK

For a stochastic radiation transport problem solved using MC RT methods, simply performing uncertainty quantification with MC sampling would over-estimate the parametric

TABLE III. The variance (and MSE, where applicable) of the estimate of S^2 over 25,000 repetitions for both the attenuation-only and scattering problems.

Attenuation-Only Problem									
	$\mathbb{V}ar[S^2]$					$MSE[S^2]$ (Exact $\mathbb{V}ar[T] = 5.505E-3$)			
N_η	Estimator Cost				N_η	Estimator Cost			
	200	500	2000	5000		200	500	2000	5000
2	9.584E-05	3.887E-05	9.626E-06	3.879E-06	2	1.332E-10	9.106E-13	3.176E-11	5.565E-11
5	3.970E-05	1.597E-05	3.907E-06	1.586E-06	5	1.119E-09	3.600E-14	3.734E-11	4.169E-11
10	**3.241E-05**	**1.303E-05**	**3.168E-06**	**1.297E-06**	10	7.155E-10	2.692E-10	5.997E-12	1.308E-11
20	3.568E-05	1.414E-05	3.482E-06	1.384E-06	20	2.576E-10	1.026E-10	8.893E-12	4.168E-11
100	1.327E-04	3.866E-05	9.218E-06	3.656E-06	100	3.678E-10	6.301E-09	1.424E-10	3.323E-11

Scattering Problem									
	$\mathbb{V}ar[S^2]$, Transmittance					$\mathbb{V}ar[S^2]$, Reflectance			
N_η	Estimator Cost				N_η	Estimator Cost			
	200	500	2000	5000		200	500	2000	5000
2	1.730E-04	6.921E-05	1.749E-05	6.996E-06	2	1.786E-04	7.085E-05	1.770E-05	7.140E-06
5	7.664E-05	2.963E-05	7.424E-06	2.882E-06	5	6.574E-05	2.592E-05	6.392E-06	2.591E-06
10	**6.329E-05**	**2.461E-05**	**6.175E-06**	**2.488E-06**	10	4.792E-05	1.852E-05	4.586E-06	1.861E-06
20	7.360E-05	2.775E-05	6.852E-06	2.753E-06	20	**4.656E-05**	**1.758E-05**	**4.303E-06**	**1.694E-06**
25	8.090E-05	3.102E-05	7.499E-06	3.012E-06	25	4.963E-05	1.836E-05	4.371E-06	1.771E-06
100	2.987E-04	8.572E-05	1.897E-05	7.456E-06	100	1.661E-04	4.169E-05	8.476E-06	3.241E-06

variance; it fails to consider that the total variance has been polluted by the statistical variability of the MC RT solver. In [1], we developed a novel variance deconvolution method which estimates the parametric variance of a QoI by removing this statistical variability from the polluted total variance. Preliminary numerical investigations showed that the variance of this estimate of parametric variance could be minimized by optimizing the ratio of UQ samples N_ξ to particle histories N_η, providing the most accurate estimate for a given computational cost.

In this work, we performed numerical studies for an attenuation-only and isotropic scattering problem over a range of total computational costs, using Woodcock-delta tracking with analog Monte Carlo. We found that the variance of the estimate of $\mathbb{V}ar[T]$ followed a consistent trend of decreasing as N_η increased, reaching a minimum, then increasing again, for the problem defined with and without scattering. In both the attenuation-only and scattering cases, this minimum was at $N_\eta = 10$ across all tested costs. A similar trend was observed in the isotropic scattering case for a QoI of reflectance, though the minimum was at $N_\eta = 20$. Though further investigation is needed, these studies allow us to better understand how to apply this variance deconvolution method for the most accurate estimate of parametric variance. As we continue developing this estimator, we hope to corroborate these numerical findings with an analytic, closed-form solution for the variance of the estimate of $\mathbb{V}ar[S^2]$.

ACKNOWLEDGMENTS

This work was supported by the Laboratory Directed Research and Development program at Sandia National Laboratories, a multimission laboratory managed and operated by National Technology and Engineering Solutions of Sandia LLC, a wholly owned subsidiary of Honeywell International Inc. for the U.S. Department of Energy's National Nuclear Security Administration under contract DE-NA0003525. This paper describes objective technical results and analysis. Any subjective views or opinions that might be expressed in the paper do not necessarily represent the views of the U.S. Department of Energy or the United States Government. This work was supported by the Center for Exascale Monte-Carlo Neutron Transport (CEMeNT) a PSAAP-III project funded by the Department of Energy, grant number DE-NA003967.

REFERENCES

1. K. CLEMENTS, G. GERACI, and A. J. OLSON, "A Variance Deconvolution Approach to Sampling Uncertainty Quantification for Monte Carlo Radiation Transport Solvers," in "Computer Science Research Institute Summer Proceedings 2021," (2021), Technical Report SAND2022-0653R, pp. 293–307, `https://cs.sandia.gov/summerproceedings/CCR2021.html`.
2. A. B. OWEN, *Monte Carlo theory, methods and examples* (2013).
3. Los Alamos National Laboratory, *MCNP - A General Monte Carlo N-Particle Transport Code, Version 5* (2008).
4. A. J. OLSON, "Calculation of parametric variance using variance deconvolution," in "Transactions of the American Nuclear Society," (2019), vol. 120, pp. 461–464.
5. E. H. VU and A. J. OLSON, "Conditional Point Sampling: A stochastic media transport algorithm with full geometric sampling memory," *Journal of Quantitative Spectroscopy and Radiative Transfer*, **272**, 107767 (2021).

A sampling-based approach to solve Sobol' Indices using variance deconvolution for arbitrary uncertainty distributions

Aaron J. Olson,[*] Kayla B. Clements,[*,†] and James M. Petticrew[‡]

[*]*Sandia National Laboratories, aolson@sandia.edu*
[†]*Oregon State University, clemekay@oregonstate.edu*
[‡]*University of Sheffield, jmpetticrew1@sheffield.ac.uk*

INTRODUCTION

Global sensitivity analysis (GSA) seeks to assess the relative contributions of various uncertainty sources to the uncertainty in one or more computation outputs. Such rank-ordering of contributions enables informed decisions such as downselection of which uncertainty sources to further study and identification of where to invest additional effort in reducing the overall uncertainty. Perhaps the most common tool for GSA are Sobol' Indices (SI) [1]. Common approaches to computing SI include through the Saltelli sampling methods [2] and direct computation following the construction of a polynomial chaos surrogate model [3].

We seek to compute SI using a stochastic solver, here a Monte Carlo radiation transport (MC RT) solver, that describe the relative variance contributions from two different aleatoric uncertainty sources, which are sources for which the uncertainty is due to real random effects as opposed to epistemic uncertainty where the uncertainty is due to lack of knowledge. We examine a parametric aleatoric uncertainty source (e.g., an uncertain cross section value) and a non-parametric uncertainty source (e.g., stochastic media). Stochastic media (SM) are comprised of constituent materials that are modeled as being randomly mixed within the medium–except in special cases, they cannot be described by a distribution on an interval.

While the Saltelli sampling methods have been carefully optimized for application with deterministic solvers, their optimization does not consider selection of parameters that drive the statistical noise produced by stochastic solvers. Likewise, while surrogate-based approaches, such as use of a polynomial chaos expansion, can be efficient for uncertainty sources for which the probability basis function is known and well-behaved, they cannot be straightforwardly applied when one or more of the uncertainty sources cannot be easily characterized with a well-behaved probability basis. Therefore, we seek to develop efficient methods for computing SI in the presence of stochastic solver noise (e.g., MC RT) and non-parametric aleatoric uncertainty (e.g., SM) that are amenable to embedding within a stochastic solver.

In [4] and previous, related work, we proposed a variance deconvolution approach by which to remove stochastic solver noise from a numerically computed output variance driven by an aleatoric uncertainty source and thereby enable unbiased computation of aleatoric uncertainty when using a stochastic solver. We successfully applied an early version of this method to stochastic media transport problems [5] to enable characterization of the variance caused by the stochastic material mixing. In Ref. [6], we applied variance deconvolution to solve for SI in a transport problem with uniformly distributed uncertainty sources and demonstrated that the method was more efficient than the Saltelli approach when using a stochastic solver for at least some cases. In recent work, we proposed a symbolic notation for describing the difference between parametric and non-parametric uncertainty sources and derived expressions to solve for conditional variance terms [7].

In this contribution, we propose a new, unbiased, sampling-based method for solving SI when using a stochastic solver via application of variance deconvolution that is applicable even when involving non-parametric aleatoric uncertainty sources. This approach is simpler than our previous iteration [6] for using variance deconvolution to solve for SI with stochastic solvers; incorporates our improved variance deconvolution estimator [4]; builds on our recently proposed notation and derivations for describing different types of aleatoric uncertainty sources [7]; and demonstrates not only computation of variance caused by a non-parametric uncertainty source [5], but also the ability to solve relative variance contributions of parametric and non-parametric uncertainty sources through SI. We numerically corroborate the method by proposing a new, attenuation-only transport problem involving stochastic material mixing and an uncertain cross section and deriving closed-form transport solutions. We use the same example problem to demonstrate the usefulness of the method for ranking the importance of uncertainty contributions. We leave as topics for future work the optimization of model parameter selection and efficiency comparison with other methods such as the Saltelli and surrogate-based approaches.

Whereas we present cross section uncertainty and stochastic media as, respectively, a parametric and a non-parametric uncertainty source, it is worth noting that the numerical model we present for each is actually parametric, that our method does not rely on the parametric property of either (but our closed-form solutions rely on both), and that these designations have been chosen primarily to be illustrative since stochastic media is often a non-parametric uncertainty source.

SI GENERATION

As we recently proposed [4, 7], let η denote statistical sampling of a stochastic solver, ω denote dependence on an aleatoric uncertainty source that we cannot–or choose to assume that we cannot–characterize with a known distribution on an interval, and let ξ represent an aleatoric uncertainty source that we can characterize with a known distribution on an interval. Without loss of generality, in this summary, η denotes sampling of a Monte Carlo radiation transport (MC RT) solver, ω denotes dependence on stochastic media (SM) configuration, and ξ denotes cross section uncertainty.

We seek to characterize a quantity of interest (QoI), in our problem transmittance through a slab, that is dependent on

the aleatoric uncertainty sources: $Q(\xi, \omega)$. The transmittance is the expectation of transmittance tallies, though, in practice, only a finite number (N_η) of particle histories can be simulated to approximate $Q(\xi, \omega)$:

$$Q(\xi,\omega) \overset{\text{def}}{=} \mathbb{E}_\eta\left[f(\xi,\omega,\eta)\right] \approx \tilde{Q}_{N_\eta}(\xi,\omega) \overset{\text{def}}{=} \frac{1}{N_\eta}\sum_{j=1}^{N_\eta} f\left(\xi,\omega,\eta^{(j)}\right), \tag{1}$$

where the tilde represents an approximation polluted with MC RT sampling noise and $f(\xi, \omega, \eta)$ is a function of a sample of the aleatoric uncertainty sources and the MC RT solver.

Similarly, the expectation of the QoI as a function of the cross section uncertainty is

$$\mathbb{P}_{\mathbb{E}}(\xi) \overset{\text{def}}{=} \mathbb{E}_\omega\left[Q(\xi,\omega)\right] \approx \tilde{\mathbb{P}}^{\mathbb{E}}_{N_\omega}(\xi) \overset{\text{def}}{=} \frac{1}{N_\omega}\sum_{k=1}^{N_\omega} \tilde{Q}_{N_\eta}(\xi,\omega^{(k)}), \tag{2}$$

where $\mathbb{P}_{\mathbb{E}}(\xi)$ is the expectation of the QoI averaged over N_ω SM realizations for a value of the uncertain cross section and $\tilde{\mathbb{P}}^{\mathbb{E}}_{N_\omega}(\xi)$ is an approximation of that quantity polluted by MC RT and SM sampling noise.

We recently solved for an expression for the variance due to the parametric uncertainty as a function of the expectation of the non-parametric uncertainty [7]:

$$\mathbb{V}ar_\xi\left[\mathbb{P}_{\mathbb{E}}(\xi)\right] = \mathbb{V}ar_\xi\left[\tilde{\mathbb{P}}^{\mathbb{E}}_{N_\omega}(\xi)\right] - \frac{\mathbb{E}_\xi\left[\mathbb{V}ar_\omega\left[\tilde{Q}_{N_\eta}(\xi,\omega)\right]\right]}{N_\omega}, \tag{3}$$

in which $\mathbb{V}ar_\xi\left[\tilde{\mathbb{P}}^{\mathbb{E}}_{N_\omega}(\xi)\right]$ is a polluted estimate of $\mathbb{V}ar_\xi\left[\mathbb{P}_{\mathbb{E}}(\xi)\right]$ computed using N_η particle histories on each of N_ω SM realizations and $\frac{1}{N_\omega}\mathbb{E}_\xi\left[\mathbb{V}ar_\omega\left[\tilde{Q}_{N_\eta}(\xi,\omega)\right]\right]$ is the average statistical pollution caused by MC RT histories and SM variability. While $\mathbb{V}ar_\xi\left[\mathbb{P}_{\mathbb{E}}(\xi)\right]$ cannot be correctly computed by sampling with a finite number of N_η and N_ω, it is straightforward to compute a de-polluted (unbiased) estimator for the desired conditional variance by tallying the other two terms and finding the difference. We have called this process of deconvolving an easily computed, but polluted, variance into a noise term and the desired de-polluted variance "variance deconvolution."

A minor conceptual step of recognizing that aleatoric variance can be comprised of both parametric and non-parametric contributions enables us to generalize another of our previously established applications of variance deconvolution [4] to solve for the total aleatoric variance while de-polluting from MC RT noise. This is expressed as

$$\mathbb{V}ar_{\xi,\omega}\left[Q(\xi,\omega)\right] = \mathbb{V}ar_{\xi,\omega}\left[\tilde{Q}_{N_\eta}(\xi,\omega)\right] - \mathbb{E}_{\xi,\omega}\left[\sigma^2_{RT,N_\eta}(\xi,\omega)\right], \tag{4}$$

where $\mathbb{V}ar_{\xi,\omega}\left[Q(\xi,\omega)\right]$ is the total aleatoric variance, $\mathbb{V}ar_{\xi,\omega}\left[\tilde{Q}_{N_\eta}(\xi,\omega)\right]$ is a polluted estimate of it when using N_η MC RT histories, and $\sigma^2_{RT,N_\eta}(\xi,\omega)$ is the 1-sigma statistical uncertainty (aka, standard error of the mean) on an estimate of $Q(\xi,\omega)$ when using N_η histories: $\sigma^2_{RT,N_\eta}(\xi,\omega) \overset{\text{def}}{=} \frac{1}{N_\eta}\mathbb{V}ar_\eta[f(\xi,\omega,\eta)]$.

We make the new observation that Eqs. (3) and (4) enable unbiased (de-polluted) computation of the Sobol main effect for the parametric contribution to the aleatoric uncertainty:

$$S_\xi = \frac{\mathbb{V}ar_\xi\left[\mathbb{P}_{\mathbb{E}}(\xi)\right]}{\mathbb{V}ar_{\xi,\omega}\left[Q(\xi,\omega)\right]}. \tag{5}$$

Furthermore, we contribute the new observation that it is mathematically valid to switch all occurrences of ξ with ω and all occurrences of ω with ξ in Eqs. (1)-(5). The result of this observation is that we not only have the means to compute unbiased estimates of the Sobol main effect for the parametric contribution to the total aleatoric variance in the presence of MC RT noise, but, through the law of total variance, we can compute the Sobol main and total effects for both the parametric and non-parametric contributions:

$$S_\xi = \frac{\mathbb{V}ar_\xi\left[\mathbb{P}_{\mathbb{E}}(\xi)\right]}{\mathbb{V}ar_{\xi,\omega}\left[Q(\xi,\omega)\right]} = 1 - \frac{\mathbb{E}_\xi\left[\mathbb{V}ar_\omega[Q(\xi,\omega)]\right]}{\mathbb{V}ar_{\xi,\omega}\left[Q(\xi,\omega)\right]} = 1 - S_{T_\omega} \tag{6a}$$

$$S_\omega = \frac{\mathbb{V}ar_\omega\left[\mathbb{P}_{\mathbb{E}}(\omega)\right]}{\mathbb{V}ar_{\xi,\omega}\left[Q(\xi,\omega)\right]} = 1 - \frac{\mathbb{E}_\omega\left[\mathbb{V}ar_\xi[Q(\xi,\omega)]\right]}{\mathbb{V}ar_{\xi,\omega}\left[Q(\xi,\omega)\right]} = 1 - S_{T_\xi} \tag{6b}$$

A caveat is that, to make practical use of this approach to solve for $\mathbb{V}ar_\omega\left[\mathbb{P}_{\mathbb{E}}(\omega)\right]$, it must be known how to hold ω constant while resampling ξ. For example, depending on the SM model used, it may not be known how to maintain the same SM realization while resampling a ξ parameter such as the average chord length of a constituent material.

Though we do not demonstrate here, this procedure can be used to solve for the Sobol main and total effects for any subset of parametric and non-parametric contributions to the total aleatoric variance.

CLOSED-FORM SOLUTIONS

To verify the accuracy of the method described in the previous section, we propose a simple test problem and derive closed-form solutions to various terms of interest. For brevity, we show only key steps in deriving closed-form solutions.

The test problem geometry is a one-dimensional slab with three regions of thicknesses r_1, r_2 and r_3 and a mono-energetic beam source incident on the first region. The slab contains three absorption-only materials with total cross sections $\Sigma_{t,1}, \Sigma_{t,2}$ and $\Sigma_{t,3}$. Region 1 contains N_{tot} subcells of equal width $\Delta x = r_1/N_{tot}$, each of which can contain either Material 1 with probability p_1 or Material 2 with probability $(1 - p_1)$. The number of cells in Region 1 containing Material 1 in a realization of this stochastic medium can be represented as a sample from the binomial probability density function (PDF), $N_1(\omega) \sim \mathcal{B}(N_{tot}, p_1)$, where ω represents the non-parametric aleatoric uncertainty of N_1. Region 2 simply contains Material 2. Region 3 contains Material 3, whose cross section $\Sigma_{t,3}(\xi)$ is a function of parametric aleatoric uncertainty $\xi \sim \mathcal{U}(-1, 1)$.

The problem quantity of interest, transmittance T through the slab, is a function of the optical thickness τ of each region:

$$\begin{aligned}\tau_1 &= N_1(\omega)\Delta x\Sigma_{t,1} + (N_{tot} - N_1(\omega))\Delta x\Sigma_{t,2} \\ &= N_1(\omega)\Delta x\left(\Sigma_{t,1} - \Sigma_{t,2}\right) + r_1\Sigma_{t,2}\end{aligned} \tag{7}$$

$$\tau_2 = r_2\Sigma_{t,2} \tag{8}$$

$$\begin{aligned}\tau_3 &= r_3\Sigma_{t,3} = r_3\left(\Sigma^0_{t,3} + \Sigma^\Delta_{t,3}\xi\right) \\ &= r_3\Sigma^0_{t,3} + r_3\Sigma^\Delta_{t,3}\xi\end{aligned} \tag{9}$$

where $\Sigma_{t,3}(\xi) = \Sigma^0_{t,3} + \Sigma^\Delta_{t,3}\xi$, $\Sigma^0_{t,3}$ is the mean total cross section, and $\Sigma^\Delta_{t,3}$ the deviation from the mean. The transmittance is

therefore a function of both the non-parametric and parametric aleatoric uncertainties,

$$T = T(\xi, \omega) = k \exp(-k_1 N_1(\omega)) \exp(-k_3 \xi) \tag{10}$$

where

$$k = \exp\left[-r_1 \Sigma_{t,2} - r_2 \Sigma_{t,2} - r_3 \Sigma^0_{t,3}\right] \tag{11a}$$
$$k_1 = \Delta x (\Sigma_{t,1} - \Sigma_{t,2}) \tag{11b}$$
$$k_3 = -r_3 \Sigma^{\Delta}_{t,3} \tag{11c}$$

The $p^{th}-$order raw moment of $T(\xi, \omega)$ is

$$\begin{aligned} \mathbb{E}_{\xi,\omega}[T^p(\xi,\omega)] &= \mathbb{E}_{\xi}\left[\mathbb{E}_{\omega}\left[T^p(\xi,\omega)\right]\right] \\ &= \int_{\omega}\int_{\xi} d\xi\, d\omega\, k^p \exp(-k_1 p N_1(\omega)) \exp(-k_3 p \xi) \\ &= k^p \frac{\sinh[k_3 p]}{k_3 p} \sum_{x=0}^{N_{tot}} B_{\omega}(x) \exp(-k_1 p x) \end{aligned} \tag{12}$$

where $B_\omega(x)$ represents the PDF of the binomial variable $N_1(\omega)$ being equal to x:

$$\begin{aligned} B_{\omega}(x) &\overset{\text{def}}{=} Pr(N_1 = x \,|\, N_{tot}, p_1) \\ &= \frac{N_{tot}!}{x!\,(N_{tot}-x)!} p_1^x (1-p_1)^{(N_{tot}-x)} \end{aligned} \tag{13}$$

Eq. (12) enables computation of the variance of $T(\xi, \omega)$ over both aleatoric uncertainties, $\mathbb{V}ar_{\xi,\omega}[T(\xi,\omega)]$, by expanding the expression for variance,

$$\mathbb{V}ar_{\xi,\omega}[T(\xi,\omega)] = \mathbb{E}_{\xi,\omega}\left[T^2(\xi,\omega)\right] - \mathbb{E}_{\xi,\omega}[T(\xi,\omega)]^2 . \tag{14}$$

This is the denominator of the main and total effect SIs. For comparison with numerical results, we calculate analytic solutions for the numerators in Eqs. (6a) and (6b). Taking $\mathbb{V}ar_{\xi}[\mathbb{P}_{\mathbb{E}}(\xi)]$ to indicate the variance of the conditional mean of $T(\xi, \omega)$ given ξ, over all ξ, we find that

$$\begin{aligned} \mathbb{V}ar_{\xi}[\mathbb{P}_{\mathbb{E}}(\xi)] &= \mathbb{E}_{\xi}\left[{\mathbb{P}_{\mathbb{E}}}^2(\xi)\right] - \mathbb{E}_{\xi}[\mathbb{P}_{\mathbb{E}}(\xi)]^2 \\ &= \mathbb{E}_{\xi}\left[{\mathbb{P}_{\mathbb{E}}}^2(\xi)\right] - \mathbb{E}_{\xi,\omega}[T(\xi,\omega)]^2 . \end{aligned} \tag{15}$$

The second term is the first-order raw moment of $T(\xi, \omega)$, calculable from Eq. (12). The first term, the second-order raw moment of $\mathbb{P}_{\mathbb{E}}(\xi)$, is

$$\begin{aligned} \mathbb{E}_{\xi}\left[{\mathbb{P}_{\mathbb{E}}}^2(\xi)\right] &= \int_{\xi} d\xi\, k^2 \exp(-k_3\xi)\left(\sum_{x=0}^{N_{tot}} B_{\omega}(x)\exp(-k_1 x)\right)^2 \\ &= \frac{k^2 \sinh[2k_3]}{2k_3}\left(\sum_{x=0}^{N_{tot}} B_{\omega}(x)\exp(-k_1 x)\right)^2 \end{aligned} \tag{16}$$

Inserting Eqs. (14) and (15) into Eq. (6a) yields

$$S_{\xi} = \frac{\frac{k^2\sinh[2k_3]}{2k_3}\left(\sum_{x=0}^{N_{tot}} B_{\omega}(x)\exp(-k_1 x)\right)^2 - \mathbb{E}_{\xi,\omega}[T(\xi,\omega)]^2}{\mathbb{E}_{\xi,\omega}[T^2(\xi,\omega)] - \mathbb{E}_{\xi,\omega}[T(\xi,\omega)]^2} . \tag{17}$$

Following the same process to calculate $\mathbb{V}ar_{\omega}[\mathbb{P}_{\mathbb{E}}(\omega)]$ yields

$$S_{\omega} = \frac{\frac{k^2\sinh^2[k_3]}{k_3^2}\left(\sum_{x=0}^{N_{tot}} B_{\omega}(x)\exp(-2k_1 x)\right) - \mathbb{E}_{\xi,\omega}[T(\xi,\omega)]^2}{\mathbb{E}_{\xi,\omega}[T^2(\xi,\omega)] - \mathbb{E}_{\xi,\omega}[T(\xi,\omega)]^2} . \tag{18}$$

Given these closed-form solutions for the main effect SIs, Eqs. (6a) and (6b) provide closed-form solutions for the total effect SIs.

RESULTS

We solve two numerical problems each using the problem description from the previous section with $r_1 = r_2 = r_3 = 1.0$, $\Sigma_{t,1} = 3.0$, $\Sigma_{t,2} = 0.1$, $\Sigma^0_{t,3} = 1.0$, and $p_1 = 0.3$. For Problem 1, $N_{tot} = 10$ and $\Sigma^{\Delta}_{t,3} = 0.25$. For Problem 2, $N_{tot} = 100$ and $\Sigma^{\Delta}_{t,3} = 0.75$.

For each quantity on both problems, we use $N_\eta = 20$. For each problem, we first solve for the average transmittance ($\mathbb{E}_{\xi,\omega}[T(\xi,\omega)]$) and combined aleatoric variance ($\mathbb{V}ar_{\xi,\omega}[Q(\xi,\omega)]$) using 10,000 samples of the aleatoric uncertainty space (i.e., ξ and ω). We then use $N_\omega = 10$ and $N_\xi = 1000$, for a total of 10,000 aleatoric samples, to solve for $\mathbb{V}ar_{\xi}[\mathbb{P}_{\mathbb{E}}(\xi)]$. Next, we use $N_\xi = 10$ and $N_\omega = 1000$, for a total of 10,000 aleatoric samples, to solve for $\mathbb{V}ar_{\omega}[\mathbb{P}_{\mathbb{E}}(\omega)]$. For each of these numerically computed quantities, we average the computed quantities over 40 repetitions and use those repetitions to compute a standard error of the mean (SEM) for the quantity. Closed-form values, numerically computed mean and SEM values, and error in numerical values reported as number of 1-sigma SEMs are reported in Table I. In addition to the above-mentioned quantities, to enable numerical interrogation and reproducibility, we report intermediate computed values for $\mathbb{V}ar_{\xi,\omega}\left[\tilde{Q}_{N_\eta}(\xi,\omega)\right]$ and $\mathbb{E}_{\xi,\omega}\left[\sigma^2_{RT,N_\eta}(\xi,\omega)\right]$.

SI are computed using Eq. (6). To compute these quantities from the total aleatoric variance and each conditional variance, statistical uncertainties are propagated using the standard error propagation formula for independent variables

$$s_f = \sqrt{\left(\frac{\partial f}{\partial x}\right)^2 s_x^2 + \left(\frac{\partial f}{\partial y}\right)^2 s_y^2 + \left(\frac{\partial f}{\partial z}\right)^2 s_z^2 + \ldots .} \tag{19}$$

Error is computed compared to closed-form solutions in terms of number of standard deviations and listed in Table I.

We first observe that all numerically computed values agree with closed-form solutions within no more than 1.58 standard deviations, that the error is usually less than 1 standard deviation, and that the error is stochastically either positive or negative. This degree and form of agreement with closed-form solutions corroborates the new numerical method.

We secondly observe the SI of these two problems to gain insight to their practical value: whereas the transmittance and overall aleatoric variance for each problem are roughly the same, our numerically computed SI provide a formal mechanism by which to measure that the SM provide the majority of the variance (~90%) in Problem 1 and, by contrast, the uncertain cross section provides the majority of the variance (~90%) in Problem 2.

TABLE I. Closed-form and Numerically Computed Values

	Problem 1				Problem 2			
	Closed	Numerical	SEM	Error	Closed	Numerical	SEM	Error
	Unconditional Mean and Variance				Unconditional Mean and Variance			
$\mathbb{E}_{\xi,\omega}\left[T(\xi,\omega)\right]$	0.1387816	0.1387030	0.0001423	0.55 σ	0.1395753	0.1396815	0.0001744	−0.61 σ
$\mathbb{V}ar_{\xi,\omega}\left[\tilde{Q}_{N_\eta}(\xi,\omega)\right]$	N/A	0.0094396	0.0000240	N/A	N/A	0.0097554	0.0000291	N/A
$\mathbb{E}_{\xi,\omega}\left[\sigma^2_{RT,N_\eta}(\xi,\omega)\right]$	N/A	0.0057908	0.0000048	N/A	N/A	0.0058113	0.0000058	N/A
$\mathbb{V}ar_{\xi,\omega}\left[Q(\xi,\omega)\right]$	0.0036845	0.0036488	0.0000226	1.58 σ	0.0039277	0.0039441	0.0000271	−0.61 σ
	Conditional Variance Values				Conditional Variance Values			
$\mathbb{V}ar_{\omega}\left[\mathbb{P}_{\mathbb{E}}(\omega)\right]$	0.0032181	0.0031919	0.0000324	0.81 σ	0.0003430	0.0003469	0.0000102	−0.38 σ
$\mathbb{V}ar_{\xi}\left[\mathbb{P}_{\mathbb{E}}(\xi)\right]$	0.0003996	0.0004065	0.0000090	−0.77 σ	0.0035227	0.0035377	0.0000225	−0.67 σ
	Sobol Indices				Sobol Indices			
S_ω	0.8734261	0.8747955	0.0103919	−0.13 σ	0.0873300	0.0879516	0.0026643	−0.23 σ
S_ξ	0.1084529	0.1114180	0.0025490	−1.16 σ	0.8968785	0.8969538	0.0083963	−0.01 σ
S_{T_ω}	0.8915471	0.8885820	0.0025490	1.16 σ	0.1031215	0.1030462	0.0083963	0.01 σ
S_{T_ξ}	0.1265739	0.1252045	0.0103919	0.13 σ	0.9126700	0.9120484	0.0026643	0.23 σ

CONCLUSIONS

We leverage the recently established variance deconvolution method to propose a new, unbiased method for computing SI when using a stochastic solver such as a MC RT solver. We demonstrate that, since this method does not rely on the parametric property of uncertainty sources, as long as samples of each uncertainty source can be kept constant while the other uncertainty sources are resampled, this approach can not only solve SI for well-behaved parametric aleatoric uncertainty sources such as uncertain cross section values, but also for challenging non-aleatoric uncertainty sources such as stochastic media. To enable numerical testing of the new method, we derive closed-form solutions for a radiation transport test problem involving stochastic media and an uncertain cross section value. Numerical results agree with closed-form solutions within statistical uncertainty corroborating the numerical approach. Via two numerical test problems, we demonstrate the ability of SI to rank the fractional contribution of each uncertain input (including SM) to the output uncertainty.

In future work, we plan to examine applications with more than two aleatoric uncertainty sources, to compare the method's efficiency to other methods, to optimize the method's efficiency by re-using samples to contribute to computing more than one term, and to apply the method to more complicated transport problems such as those with scattering.

ACKNOWLEDGMENTS

Sandia National Laboratories is a multimission laboratory managed and operated by National Technology & Engineering Solutions of Sandia, LLC, a wholly owned subsidiary of Honeywell International Inc., for the U.S. Department of Energy's National Nuclear Security Administration under contract DE-NA0003525. This paper describes objective technical results and analysis. Any subjective views or opinions that might be expressed in the paper do not necessarily represent the views of the U.S. Department of Energy or the United States Government. This work was supported by the Center for Exascale Monte-Carlo Neutron Transport (CEMeNT) a PSAAP-III project funded by the Department of Energy, grant number DE-NA003967. The third author made significant contributions to this work while employed by AWE: UK Ministry of Defence © Crown Owned Copyright 2022/AWE. The authors thank Dr. Jacquilyn Weeks of World Tree Consulting for writing consultation in the preparation of this document.

REFERENCES

1. I. SOBOL, "Sensitivity estimates for nonlinear mathematical models," *Mathematical Modeling and Computational Experiment*, **1**, 407–414 (1993).
2. A. SALTELLI, P. ANNONI, I. AZZINI, F. CAMPOLONGO, M. RATTO, and S. TARANTOLA, "Variance based sensitivity analysis of model output. Design and estimator for the total sensitivity index," *Computer Physics Communications*, **181**, 259–270 (2010).
3. B. SUDRET, "Global sensitivity analysis using polynomial chaos expansion," *Reliability Engineering and System Safety*, **93**, 964–979 (2000).
4. K. B. CLEMENTS, G. GERACI, and A. J. OLSON, "Numerical investigation on the performance of a variance deconvolution estimator," *Trans. Am. Nucl. Soc.*, **126**, 344–347 (2022).
5. E. H. VU and A. J. OLSON, "Conditional Point Sampling: A stochastic media transport algorithm with full geometric sampling memory," *J. Quant. Spectrosc. and Rad. Transfer*, **272**, 107767 (2021).
6. J. M. PETTICREW and A. J. OLSON, "Computation of Sobol'Indices using Embedded Variance Deconvolution," in "M&C 2021," American Nuclear Society, Raleigh, NC (October 2021).
7. G. GERACI and A. J. OLSON, "Deconvolution strategies for efficient parametric variance estimation in stochastic media transport problems," *Trans. Am. Nucl. Soc.*, **126**, 279–282 (2022).

Highlights

A variance deconvolution estimator for efficient uncertainty quantification in Monte Carlo radiation transport applications

Kayla B. Clements, Gianluca Geraci, Aaron J. Olson, Todd S. Palmer

- A variance deconvolution strategy is introduced to eliminate the stochastic error introduced by under-resolved MC RT computations
- Statistical assessment of the estimator (bias, variance) and its comparison with brute-force approaches that need to revolve the MC RT computations
- Resource allocation and the estimator's performance are discussed for the attenuation-only and scattering regime
- Derivation of closed-form solutions for several estimators in the attenuation-only case

A variance deconvolution estimator for efficient uncertainty quantification in Monte Carlo radiation transport applications

Kayla B. Clements[a,b,*], Gianluca Geraci[b,*], Aaron J. Olson[b], Todd S. Palmer[a]

[a]*Oregon State University, Address, Corvallis, XXX, OR, USA*
[b]*Sandia National Laboratories, P.O. Box 5800, Mail Stop 1318, Albuquerque, 87185-1318, NM, USA*

Abstract

UPDATE at the end Monte Carlo radiation transport solvers are at the heart of many analyses and workflows for high-fidelity systems. Despite their large computational cost, their use is often mandated by the complexity of the systems and they cannot be efficiently replaced by deterministic solvers, e.g., discrete ordinate methods. Unfortunately, forward computations alone cannot be relied for high-consequence systems and the sources of uncertainty affecting transport computations need to be characterized and propagated to obtain reliable estimates for the quantities of interest. Uncertainty Quantification (UQ) is routinely used for this task, but, in the context of Monte Carlo transport solvers, additional challenges need to be faced. In fact, under-resolved Monte Carlo transport computations introduce a stochastic error that corrupt the statistics of interest for UQ. In this contribution, we propose and analyze a sampling estimator that allow for the accurate and precise computation of the variance of the quantities of interest without requiring the full convergence of the Monte Carlo transport computations. We rigorously derive the statistical properties of the new estimator, compare its performance with the standard estimator, and demonstrate its use on an array of radiation transport model problems involving both attenuation and scattering.

Keywords: Monte Carlo, uncertainty quantification, radiation transport

1. Introduction

UPDATE at the end In general, uncertainty quantification (UQ) is the process of propagating sources of uncertainty through computational simulation codes in order to evaluate the statistics of Quantities of Interest (QoIs) with respect to those uncertain sources. The UQ workflow is well established [source for UQ], and requires repeated evaluations of numerical codes to compute statistics of the QoI. However, if traditional UQ methods are applied to evaluating codes that are not deterministic, *i.e.* some component of the solver is stochastic, the subsequent statistical analysis can be considered "polluted" by the variability introduced by the solver itself. One such case is in the use of Monte Carlo radiation transport (MCRT) solvers, wherein the behavior of fixed number of particles is simulated and averaged to produce a QoI with some variability as a function of the number of particles used. MCRT solvers are widely used across the nuclear engineering landscape, and in fact are sometimes preferred over deterministic solvers **when?**. When integrating MCRT codes into a UQ workflow, a brute-force method to overcome the introduction of the solver variability is to drive down the solver variability by increasing the number of particle histories far past what one might use just to solve for the QoI. With this method, the variability contribution from the MCRT solver is assumed to be negligible compared to the variability one hopes to analyze, and the UQ workflow proceeds. Unfortunately, this increases the computational expense of a single MCRT run to the point of intractability when combined with the repeated runs necessary for UQ.

Instead, we have developed a variance deconvolution framework that allows us to effectively compute the variance contribution from a stochastic solver, subtract it from the total "polluted" variance, and therefore calculate the desired

*Corresponding authors
Email addresses: clemekay@oregonstate.edu,kbcleme@sandia.gov (Kayla B. Clements), ggeraci@sandia.gov (Gianluca Geraci), aolson@sandia.gov (Aaron J. Olson), todd.palmer@oregonstate.edu (Todd S. Palmer)

variance introduced by the uncertain inputs. This is far more cost effective than the brute-force approach, and uses an unbiased estimator for the variance introduced by the solver and for the UQ variance (referred to from here as parametric variance). We have applied this variance deconvolution UQ workflow here to MCRT problems, but as we'll show, the method is not specific to radiation transport and is widely applicable with solvers that use a Monte Carlo method.

2. Mathematical background

In this work the focus is the quantification of statistics for a scalar QoI $Q : \mathbb{R}^d \to \mathbb{R}$, which is is a function of a vector of uncertain variables $\xi \in \Xi \subseteq \mathbb{R}^d$, where $d \in \mathbb{N}$, the number of uncertain variables, can be arbitrarily large. Moreover, arbitrary joint distribution functions are considered for the input parameters $p(\xi)$, including the case of correlated ones, i.e., non-independent variables. The final goal of the analysis is the precise quantification of the first two statistical moments of Q, i.e., the mean and variance of Q, which are defined as

$$\begin{aligned} \mathbb{E}[Q] &= \int_\Xi Q(\xi)\, p(\xi)\, \mathrm{d}\xi \quad \text{and} \\ \mathbb{V}ar[Q] &= \int_\Xi (Q(\xi) - \mathbb{E}[Q])^2\, p(\xi)\, \mathrm{d}\xi. \end{aligned} \tag{1}$$

In particular, we will design estimators capable of efficiently resolve the variance of Q, whenever the underlying solver is stochastic. In the presence of stochastic solvers, direct observations of Q, as function of ξ, are not possible, either because the response is corrupted by noise ([**?**]) or because the quantity of interest is defined as a statistic of events associated to the solver. This latter case emerges naturally in the presence of MC RT solvers and, without loss of generality, this application scenario will serve as the motivation for the following presentation. MC RT solvers will be discussed more in details in Sec. 5, however, from an abstract mathematical perspective, it suffices to idealize them as it follows. For each given realization of the random uncertainty parameters, the QoI Q can be obtained by post-processing statistics associated to particle trajectories. Each trajectory undergoes a series of random events that we can notionally represent with a random variable $\eta \in H \subset \mathbb{R}^{d'}$, whose distribution is unknown, i.e., it cannot be sampled, but whose events $f : H \to \mathbb{R}$ are observable. For instance, an event f can be defined as a particle passing through a slab. Several radiation transport QoIs, e.g., transmittance, reflectance, fluxes, *etc.*, can be defined starting from the events f as

$$Q(\xi) = \mathbb{E}[f(\xi, \eta) \mid \xi] \stackrel{\text{def}}{=} \mathbb{E}_\eta[f(\xi, \eta)], \tag{2}$$

where hereinafter we will indicate with a subscript the integration variable. It follows that, to evaluate the statistics of Q with respect to the uncertain parameters ξ Eq.(1), one needs to include the definition of the QoI Eq. (2). Unfortunately, the accurate convergence of Eq. (2) with MC RT solvers requires a large collection of events f, which corresponds to the propagation of a large ensemble of particles. For high-fidelity and complex applications, this cost cannot be afforded for multiple realizations of ξ, which effectively prevents the use of UQ within radiation transport applications with MC RT solvers. This challenge is illustrated in the next section.

2.1. Monte Carlo sampling estimation

Several techniques for UQ [**?**] allow for an efficient computations of statistics like the ones presented in Eq. (1); however, in the presence of large dimensional spaces and noisy QoIs like the ones of interest for radiation transport, MC sampling is the most robust choice despite its slow convergence rate. In the context of this work, MC simply consists in drawing N_ξ samples of ξ from $p(\xi)$, evaluating the corresponding QoI $Q(\xi)$, and postprocessing their values to evaluate the statistics (1) as

$$\begin{aligned} \mathbb{E}[Q] &\approx \frac{1}{N_\xi} \sum_{i=1}^{N_\xi} Q(\xi^{(i)}) \stackrel{\text{def}}{=} \hat{Q}_\xi \\ \mathbb{V}ar[Q] &\approx \frac{1}{N_\xi - 1} \sum_{i=1}^{N_\xi} \left(Q(\xi^{(i)}) - \frac{1}{N_\xi} \sum_{k=1}^{N_\xi} Q(\xi^{(k)}) \right)^2 \stackrel{\text{def}}{=} \hat{\sigma}^2_\xi. \end{aligned} \tag{3}$$

Since the MC estimators depend on a finite number of realizations for $Q(\xi)$, at different set of N_ξ realizations would correspond a different value for the estimator. Hence, an MC estimator is itself a random variable; as such, it is important to characterize an MC estimator with its statistical properties of bias and variance, which correspond to the accuracy and precision of the estimator. The estimators presented in Eq. (6) are both unbiased (for the variance the Bessel's correction is introduced for achieving this property; see [**?**]), i.e., $\mathbb{E}\left[\hat{Q}_\xi\right] = \mathbb{E}[Q]$ and $\mathbb{E}\left[\hat{\sigma}^2_\xi\right] = \mathbb{V}ar[Q]$. In the radiation transport context an additional estimator needs to be introduced. The evaluation of the QoI (2) is indeed obtained as

$$Q(\xi^{(i)}) \approx \frac{1}{N_\eta}\sum_{j=1}^{N_\eta} f(\xi^{(i)}, \eta^{(j)}) \stackrel{\text{def}}{=} \tilde{Q}_{N_\eta}\left(\xi^{(i)}\right). \tag{4}$$

The convergence of this estimator is directly linked to the variance of f with respect to η, i.e.,

$$\mathbb{V}ar_\eta\left[f(\xi^{(i)}, \eta)\right] \stackrel{\text{def}}{=} \sigma^2_\eta(\xi^{(i)}), \tag{5}$$

as $\left|Q(\xi^{(i)}) - \tilde{Q}_{N_\eta}\left(\xi^{(i)}\right)\right| \sim \mathcal{N}\left(0, \sigma^2_\eta(\xi^{(i)})/N_\eta\right)$, i.e. its standard error converge only as ${N_\eta}^{-1/2}$. Unfortunately, for problem with enough variability this error might not be made arbitrarily small under computational budget constraints; it follows that it should be included (and propagated) in the UQ evaluation of statistics. In fact, by combining Eq. (6) and Eq. (17) is it possible to obtain

$$\begin{aligned}
\mathbb{E}_\xi[Q] \approx \mathbb{E}_\xi\left[\tilde{Q}_{N_\eta}\right] \approx \frac{1}{N_\xi}\sum_{i=1}^{N_\xi}\tilde{Q}_{N_\eta}(\xi^{(i)}) = \frac{1}{N_\xi}\sum_{i=1}^{N_\xi}\left(\frac{1}{N_\eta}\sum_{j=1}^{N_\eta} f(\xi^{(i)}, \eta^{(j)})\right) \stackrel{\text{def}}{=} \left\langle \tilde{Q}_{N_\eta}\right\rangle_{N_\xi} \\
\mathbb{V}ar_\xi[Q] \approx \mathbb{V}ar_\xi\left[\tilde{Q}_{N_\eta}\right] \approx \frac{1}{N_\xi - 1}\sum_{i=1}^{N_\xi}\left(\tilde{Q}_{N_\eta}(\xi^{(i)}) - \frac{1}{N_\xi}\sum_{k=1}^{N_\xi}\tilde{Q}_{N_\eta}(\xi^{(k)})\right)^2 \stackrel{\text{def}}{=} \tilde{S}^2.
\end{aligned} \tag{6}$$

Since the estimators in Eqs. (6) are based on an approximation of Q, obtained with a finite number (often limited) of N_η evaluations for f, we refer to these estimator as *polluted*. In this work, the main focus is to obtain an efficient estimation of $\mathbb{V}ar_\xi[Q]$ from its polluted approximation $\tilde{S}^2$; our novel estimator will be introduced in the next section, while here we summarize some results concerning the statistical properties of $\left\langle \tilde{Q}_{N_\eta}\right\rangle_{N_\xi}(\xi^{(i)})$ (previously introduced in [**?**]).

Proposition 2.1. *The polluted estimator* $\left\langle \tilde{Q}_{N_\eta}\right\rangle_{N_\xi}$ *is unbiased, i.e.,* $\mathbb{E}\left[\left\langle \tilde{Q}_{N_\eta}\right\rangle_{N_\xi}\right] = \mathbb{E}_\xi[Q]$.

Proof. This results follows directly from the linearity of expected value. □

Proposition 2.2. *The variance of the* $\left\langle \tilde{Q}_{N_\eta}\right\rangle_{N_\xi}$ *is equal to*

$$\mathbb{V}ar\left[\left\langle \tilde{Q}_{N_\eta}\right\rangle_{N_\xi}\right] = \frac{\mathbb{V}ar\left[\tilde{Q}_{N_\eta}\right]}{N_\xi}, \tag{7}$$

where

$$\mathbb{V}ar\left[\tilde{Q}_{N_\eta}\right] = \mathbb{V}ar_\xi[Q] + \frac{\mathbb{E}_\xi\left[\sigma^2_\eta\right]}{N_\eta}. \tag{8}$$

Proof. This results follows from the law of total variance as...**complete this** □

From Proposition 2.2 it also follows the following corollary.

Corollary 2.1. *Under the assumption of equal cost between two particles generate at multiple parameter locations...**write this** for a prescribed total budget of* $C = N_\xi \times N_\eta$, *the variance of* $\left\langle \tilde{Q}_{N_\eta}\right\rangle_{N_\xi}$ *is minimized for* $N_\eta = 1$.

Proof. **Add this** □

As it will be demonstrated in the next sections, the combination between the linearity of the expected value estimator and the assumption of a simplified cost model (that does not include any data transfer or restart cost) produces a trivial result for the optimal allocation of resources (Corollary 2.1). This result will not hold for our novel variance estimator, even under the same simplistic assumption regarding the cost model. This result will be rigorously demonstrated in the next section.

3. Variance deconvolution estimator for under-resolved stochastic computations

Section ToC:

- New estimator definition
- Practical consideration (implementation)
- Statistical properties
- Performance for prescribed computational budget (optimal resources allocation)

1. What is the 'brute force' approach, ie what could you do today without this? What is the drawback? It's biased, and reducing the bias is expensive. Write out statistical properties.
2. Introduce variance deconvolution estimator. Introduce its statistics, including that it is unbiased. (Include closed-form here if we get it, but if we can't it can be in the numerical estimator section.)
3. Discussion on variance reduction techniques for MCRT. If we consider the variance reduction to scale with α, we consider $\alpha(\xi)$.

3.1. A variance deconvolution estimator

In Proposition 2.2, we used the law of total variance for determining the variance of $\tilde{Q}_{N_\eta}$ as

$$\mathbb{V}ar\left[\tilde{Q}_{N_\eta}\right] = \mathbb{V}ar_\xi\left[Q\right] + \frac{\mathbb{E}_\xi\left[\sigma_\eta^2\right]}{N_\eta}. \tag{9}$$

Since the variance of the QoI $\mathbb{V}ar_\xi\left[Q\right]$ is unknown, the previous expression only expresses the fact that the under-resolved MC RT solutions are contributing an additional term $\frac{\mathbb{E}_\xi\left[\sigma_\eta^2\right]}{N_\eta}$, which augments the observable polluted variance $\mathbb{V}ar\left[\tilde{Q}_{N_\eta}\right]$. We propose to use this expression to define a novel estimator that accounts for the additional variance's contribution introduced by the under-resolved MC RT computations. This idea has been introduced in a series of contributions [?] and, in particular, in [**?**] the term *variance deconvolution* has been coined; we will adopt this designation in this article.

Before defining the new estimator we define the terms needed for its evaluation; first, it is possible to show that $\mathbb{V}ar\left[\tilde{Q}_{N_\eta}\right]$ can be estimated from $\mathbb{V}ar_\xi\left[\tilde{Q}_{N_\eta}\right]$, if the particle realizations at each sample location are independent, as illustrated in the next proposition.

Proposition 3.1. *Given N_η independent realizations for the particles trajectories used at each uncertain location ξ, the total variance for the polluted QoI $\mathbb{V}ar\left[\tilde{Q}_{N_\eta}\right]$ can be approximated by its variance over the uncertain parameters, i.e.,*

$$\mathbb{V}ar\left[\tilde{Q}_{N_\eta}\right] = \mathbb{V}ar_\xi\left[\tilde{Q}_{N_\eta}\right]. \tag{10}$$

Proof. **Complete the proof** 1) Write the sampling estimator for $\mathbb{V}ar\left[\tilde{Q}_{N_\eta}\right]$, 2) assume independence over j, 3) and show equivalence. □

By combining Eqs. (9) and (10) one can write

$$\begin{aligned}\mathbb{V}ar_{\xi}\left[Q\right] &= \mathbb{V}ar\left[\tilde{Q}_{N_\eta}\right] - \frac{\mathbb{E}_{\xi}\left[\sigma_{\eta}^2\right]}{N_\eta} \\ &= \mathbb{V}ar_{\xi}\left[\tilde{Q}_{N_\eta}\right] - \frac{\mathbb{E}_{\xi}\left[\sigma_{\eta}^2\right]}{N_\eta}.\end{aligned} \tag{11}$$

From Eq. (11) we can immediately realize that $\mathbb{V}ar_{\xi}\left[\tilde{Q}_{N_\eta}\right] \approx \tilde{S}^2$, whereas an estimator for $\mathbb{E}_{\xi}\left[\sigma_{\eta}^2\right]$ can be easily defined from the sampling estimator for $\mathbb{V}ar_{\eta}\left[f\right]$

$$\sigma_{\eta}^2(\xi^{(i)}) \approx \frac{1}{N_\xi - 1}\sum_{j=1}^{N_\eta}\left(f(\xi^{(i)},\eta^{(j)}) - \tilde{Q}_{N_\eta}(\xi^{(i)})\right)^2 \stackrel{\text{def}}{=} \hat{\sigma}_{\eta}^2(\xi^{(i)}), \tag{12}$$

and

$$\mathbb{E}_{\xi}\left[\sigma_{\eta}^2\right] \approx \frac{1}{N_\xi}\sum_{i=1}^{N_\xi}\hat{\sigma}_{\eta}^2(\xi^{(i)}). \tag{13}$$

Moreover, to simplify the notation, since the number of particles N_η is assumed to be constant, we use the shorthand

$$\hat{\mu}_{\sigma^2_{RT,N_\eta}} \stackrel{\text{def}}{=} \frac{1}{N_\eta}\frac{1}{N_\xi}\sum_{i=1}^{N_\xi}\hat{\sigma}_{\eta}^2(\xi^{(i)}). \tag{14}$$

Finally, the variance deconvolution estimator is defined as

$$\mathbb{V}ar_{\xi}\left[Q\right] = \mathbb{V}ar_{\xi}\left[\tilde{Q}_{N_\eta}\right] - \frac{\mathbb{E}_{\xi}\left[\sigma_{\eta}^2\right]}{N_\eta} \approx \tilde{S}^2 - \hat{\mu}_{\sigma^2_{RT,N_\eta}} \stackrel{\text{def}}{=} S^2. \tag{15}$$

In the following we demonstrate that ...

In this work we propose to exploit this relationship to obtain an efficient estimation of the $\mathbb{V}ar_{\xi}\left[Q\right]$.

In the case of a non-deterministic solver, our QoI is obtained as statistics of elementary and observable events. We consider observing a single elementary realization $f(\xi,\eta)$. We have introduced the random variable η, possibly a random vector, to notionally represent the code's stochastic behavior; unlike with ξ, knowledge of η is neither implied nor required. For a single realization of ξ, multiple runs of the solver will produce different and independent results, representing different realizations of η. In the case of radiation transport, $f(\xi,\eta)$ can be considered the result of a single particle history, and η describes the inaccessible vector of random variables used by the solver to generate the particle's random walk. One sample of QoI $Q(\xi)$ is therefore obtained as an expected value of elementary events f over multiple realizations of η,

$$Q(\xi) = \mathbb{E}\left[f(\xi,\eta) \mid \xi\right] \stackrel{\text{def}}{=} \mathbb{E}_{\eta}\left[f(\xi,\eta)\right]. \tag{16}$$

We have defined the shorthand notation $\mathbb{E}_X\left[\cdot\right]$ to indicate the expected value drawn over realizations drawn with respect to the variable X. For a radiation transport application, this corresponds to an averaging over the number of particle histories. In practice, the elementary event will have a finite number of realizations, so $Q(\xi)$ is approximated using a finite number of particles N_η,

$$Q(\xi^{(i)}) \approx \frac{1}{N_\eta}\sum_{j=1}^{N_\eta} f(\xi^{(i)},\eta^{(j)}) \stackrel{\text{def}}{=} \tilde{Q}_{N_\eta}\left(\xi^{(i)}\right). \tag{17}$$

Combining Eqs. (6) and (17) provides an approximations for the expected value of the QoI,

$$\begin{aligned}\mathbb{E}\left[Q\right] &\approx \frac{1}{N_\xi}\sum_{i=1}^{N_\xi}\tilde{Q}_{N_\eta}(\xi^{(i)}) \\ &= \frac{1}{N_\xi}\sum_{i=1}^{N_\xi}\left(\frac{1}{N_\eta}\sum_{j=1}^{N_\eta} f(\xi^{(i)},\eta^{(j)})\right) \stackrel{\text{def}}{=} \hat{Q}\end{aligned} \tag{18}$$

nesting the MC approximation for $Q(\xi)$ inside the MC approximations for the UQ statistics of interest. The contribution of this work is to understand how this nested MC-MC approximation propagates through the UQ results by evaluating several features of these estimators, under the assumption that the number of histories N_η is constant for each UQ sample[1].

3.2. Statistical properties of the MC-MC estimator

We first consider the effects of the nested sampling estimator by studying its bias, taking the expected value of the estimator over both spaces,

$$\begin{aligned}
\mathbb{E}\left[\hat{Q}\right] &= \mathbb{E}\left[\frac{1}{N_\xi}\sum_{i=1}^{N_\xi}\left(\frac{1}{N_\eta}\sum_{j=1}^{N_\eta} f(\xi^{(i)},\eta^{(j)})\right)\right] \\
&= \frac{1}{N_\xi}\sum_{i=1}^{N_\xi}\left(\frac{1}{N_\eta}\sum_{j=1}^{N_\eta}\mathbb{E}_\xi\left[\mathbb{E}_\eta\left[f(\xi^{(i)},\eta^{(j)})\right]\right]\right) \\
&= \frac{1}{N_\xi}\sum_{i=1}^{N_\xi}\left(\frac{1}{N_\eta}\sum_{j=1}^{N_\eta}\mathbb{E}_\xi\left[Q(\xi^{(i)})\right]\right) \\
&= \frac{1}{N_\xi}\sum_{i=1}^{N_\xi}\mathbb{E}_\xi\left[Q(\xi^{(i)})\right] = \mathbb{E}_\xi\left[Q(\xi)\right].
\end{aligned} \tag{19}$$

By taking advantage of the linearity of the expected value operator, *i.e.* $\mathbb{E}\left[X_1 + X_2 + \cdots + X_j\right] = \mathbb{E}\left[X_1\right] + \mathbb{E}\left[X_2\right] + \cdots + \mathbb{E}\left[X_j\right]$ [cite], we see that the nested MC-MC sampling estimator for $\mathbb{E}\left[Q\right]$ is unbiased. We next consider the variance of nested sampling estimator, using the known property of the variance of a linear combination [cite],

$$\begin{aligned}
\mathbb{V}ar\left[\hat{Q}\right] &= \mathbb{V}ar\left[\frac{1}{N_\xi}\sum_{i=1}^{N_\xi}\left(\frac{1}{N_\eta}\sum_{j=1}^{N_\eta} f(\xi^{(i)},\eta^{(j)})\right)\right] \\
&= \mathbb{V}ar\left[\frac{1}{N_\xi}\sum_{i=1}^{N_\xi}\tilde{Q}_{N_\eta}(\xi^{(i)})\right] \\
&= \frac{1}{{N_\xi}^2}\sum_{i=1}^{N_\xi}\mathbb{V}ar\left[\tilde{Q}_{N_\eta}(\xi^{(i)})\right] \\
&= \frac{1}{N_\xi}\mathbb{V}ar\left[\tilde{Q}_{N_\eta}(\xi)\right].
\end{aligned} \tag{20}$$

Because $\tilde{Q}_{N_\eta}(\xi)$ is the average of elementary observable events which depend on η, we can apply the law of total variance [citation] to $\tilde{Q}_{N_\eta}(\xi)$ to evaluate further:

$$\begin{aligned}
\mathbb{V}ar\left[Y\right] &= \mathbb{E}\left[\mathbb{V}ar\left[Y|X\right]\right] + \mathbb{V}ar\left[\mathbb{E}\left[Y|X\right]\right] \\
\mathbb{V}ar\left[\tilde{Q}_{N_\eta}(\xi)\right] &= \mathbb{E}_\xi\left[\mathbb{V}ar_\eta\left[\tilde{Q}_{N_\eta}(\xi)\right]\right] + \mathbb{V}ar_\xi\left[\mathbb{E}_\eta\left[\tilde{Q}_{N_\eta}(\xi)\right]\right] \\
&= \mathbb{E}_\xi\left[\mathbb{V}ar_\eta\left[\frac{1}{N_\eta}\sum_{j=1}^{N_\eta} f(\eta^{(j)},\xi)\right]\right] + \mathbb{V}ar_\xi\left[Q(\xi)\right] \\
&= \mathbb{E}_\xi\left[\frac{1}{{N_\eta}^2}\sum_{j=1}^{N_\eta}\mathbb{V}ar_\eta\left[f(\eta^{(j)},\xi)\right]\right] + \mathbb{V}ar_\xi\left[Q(\xi)\right] \\
&= \mathbb{E}_\xi\left[\frac{1}{N_\eta}\mathbb{V}ar_\eta\left[f(\xi,\eta)\right]\right] + \mathbb{V}ar_\xi\left[Q(\xi)\right].
\end{aligned} \tag{21}$$

[1] This assumption is not strictly required, but simplifies derivations.

Combined with Eq.(20), the variance of the MC-MC estimator is

$$\mathbb{V}ar\left[\hat{Q}\right] = \frac{\mathbb{E}_\xi\left[\mathbb{V}ar_\eta\left[f\right]\right] + N_\eta \mathbb{V}ar_\xi\left[Q\right]}{N_\xi} \tag{22}$$

These evaluations allow us to better understand the effects of the nested MC-MC estimator on UQ statistics. It is known that given population mean μ, population variance σ^2, and sample mean $\bar{X}$ over sample size n, $\mathbb{E}\left[\bar{X}\right] = \mu$ and $\mathbb{V}ar\left[\bar{X}\right] = \sigma^2/n$. If we think of the nested MC-MC estimator of $\mathbb{E}\left[Q\right]$ as a nested sample mean with nested sample sizes N_ξ and N_η, it follows that $\mathbb{E}\left[\hat{Q}\right] = \mathbb{E}\left[Q\right]$. Similarly, it follows that $\mathbb{V}ar\left[\hat{Q}\right] = \mathbb{V}ar\left[\tilde{Q}_{N_\eta}\right]/N_\xi$. Perhaps the less intuitive result is that the variance of $\tilde{Q}_{N_\eta}$, also a sample estimator, decomposed into two distinct contributions: $\mathbb{V}ar_\xi\left[Q(\xi)\right]$, which we may think of as the parametric variance of the QoI; and $\mathbb{E}_\xi\left[\frac{1}{N_\eta}\mathbb{V}ar_\eta\left[f(\xi,\eta)\right]\right]$, which we may think of as the variance contribution from the stochastic solver.

3.3. Variance deconvolution and practical implementation

The typical sampling-based UQ workflow is to collect evaluations of the QoI over the UQ space $Q(\xi)$, then approximate $\mathbb{E}\left[Q\right]$ and $\mathbb{V}ar\left[Q\right]$ with MC estimators. When a stochastic solver is introduced, $Q(\xi)$ becomes inaccessible and may only be approximated by $\tilde{Q}_{N_\eta}(\xi)$. This does not present a problem in computing $\mathbb{E}\left[Q\right]$, because as we've shown, $\hat{Q}$ provides an unbiased estimate. For $\mathbb{V}ar\left[Q\right]$, this is not the case – Eq. (21) shows that the stochastic solver introduces a bias, $\mathbb{E}_\xi\left[\mathbb{V}ar_\eta\left[f(\xi,\eta)\right]\right]/N_\eta$. Existing methods [citation] have used a brute-force approach to this issue, increasing the number of elementary event realizations N_η such that the noise contribution from the stochastic solver can be assumed to be negligible, approximating $\lim_{N_\eta\to\infty}\mathbb{V}ar_\eta\left[f(\xi,\eta)\right] = 0$. In many application spaces, increasing N_η enough that this assumption holds can increase computational cost to the point of intractability. In that sense, perhaps the most important result of Eq. (21) is a practical path to a fully unbiased estimate of $\mathbb{V}ar\left[Q\right]$. Given that $\tilde{Q}_{N_\eta}$ is an accessible quantity, $\mathbb{V}ar\left[\tilde{Q}_{N_\eta}\right]$ is calculable by taking the variance of several evaluations of $\tilde{Q}_{N_\eta}(\xi)$. Similarly, $\mathbb{V}ar_\eta\left[f(\xi,\eta)\right]$ is calculable given N_η realizations of $f(\xi,\eta)$ per UQ sample, making $\mathbb{E}_\xi\left[\mathbb{V}ar_\eta\left[f(\xi,\eta)\right]\right]$. Re-arranging Eq. (21), an unbiased estimate of $\mathbb{V}ar\left[Q\right]$ can be estimated by removing the stochastic solver noise from the total polluted variance,

$$\mathbb{V}ar\left[Q\right] = \mathbb{V}ar_\xi\left[Q\right] = \mathbb{V}ar\left[\tilde{Q}_{N_\eta}\right] - \frac{\mathbb{E}_\xi\left[\sigma_\eta^2\right]}{N_\eta}, \tag{23}$$

where σ_η^2 is defined as the variance of the histories for one fixed UQ parameter, *i.e.* $\sigma_\eta^2 \overset{\text{def}}{=} \mathbb{V}ar_\eta\left[f(\xi,\eta)\right]$. To practically implement this method for computing $\mathbb{V}ar\left[Q\right]$, we will use several sample-estimator counterparts,

$$\begin{aligned}
\mathbb{V}ar\left[\tilde{Q}_{N_\eta}\right] &\approx \frac{1}{N_\xi - 1}\sum_{i=1}^{N_\xi}\left(\tilde{Q}_{N_\eta}(\xi^{(i)}) - \hat{Q}\right)^2 \overset{\text{def}}{=} \tilde{S}^2 \\
\sigma_\eta^2(\xi^{(i)}) &\approx \frac{1}{N_\xi - 1}\sum_{j=1}^{N_\eta}\left(f(\xi^{(i)},\eta^{(j)}) - \tilde{Q}_{N_\eta}(\xi^{(i)})\right)^2 \overset{\text{def}}{=} \hat{\sigma}_\eta^2(\xi^{(i)}) \\
\frac{\mathbb{E}_\xi\left[\sigma_\eta^2\right]}{N_\eta} &\approx \frac{1}{N_\eta}\frac{1}{N_\xi}\sum_{i=1}^{N_\xi}\hat{\sigma}_\eta^2(\xi^{(i)}) \overset{\text{def}}{=} \hat{\mu}_{\sigma^2_{RT,N_\eta}}.
\end{aligned} \tag{24}$$

The sample estimator counterpart of Eq. (23) is then

$$\mathbb{V}ar\left[Q\right] \approx S^2 = \tilde{S}^2 - \hat{\mu}_{\sigma^2_{RT,N_\eta}}. \tag{25}$$

3.4. Prescribing a computational budget

The goal of a precise estimator is to obtain statistics with the lowest possible variance for a prescribed computational budget. In the case of this MC-MC estimator, assuming a linear cost model with a constant N_η for all N_ξ UQ

runs, the total computational budget is $C = N_\xi \times N_\eta$. Eq. (20) suggests that the variance of the estimator, $\mathbb{V}ar\left[\hat{Q}\right]$, is minimized when $\mathbb{V}ar\left[\tilde{Q}_{N_\eta}\right]$ is; the most effective computational budget for $\hat{Q}$ is that which minimizes $\mathbb{V}ar\left[\tilde{Q}_{N_\eta}\right]$. In practical implementation, the most effective computational budget for $\hat{Q}$ is that which minimizes the variance of $\tilde{Q}_{N_\eta}$'s sample estimator, $\tilde{S}^2$.

Before presenting the derivation for minimizing $\mathbb{V}ar\left[\tilde{S}^2\right]$, we introduce some notation:

$$\begin{aligned}
\mu\left[X\right] &\overset{\text{def}}{=} \mathbb{E}\left[X\right] \\
\mu_k\left[X\right] &\overset{\text{def}}{=} \mathbb{E}\left[\left(X-\mu\right)^k\right] \\
\mu_{\eta,k}\left[X\right] &\overset{\text{def}}{=} \mathbb{E}_\eta\left[\left(X-\mu_\eta\right)^k\right] \\
\sigma^2\left[X\right] &= \mu_2\left[X\right]
\end{aligned} \tag{26}$$

Given that $\tilde{S}^2$ is a sample variance, its variance is [cite]:

$$\mathbb{V}ar\left[\tilde{S}^2\right] = \frac{\mu_4\left[\tilde{Q}_{N_\eta}\right]}{N_\xi} - \frac{\sigma^4\left[\tilde{Q}_{N_\eta}\right]\left(N_\xi-3\right)}{N_\xi(N_\xi-1)}. \tag{27}$$

Introducing the shorthand notation $\tilde{\mu}_k \overset{\text{def}}{=} \mu_k\left[\tilde{Q}_{N_\eta}\right]$,

$$\mathbb{V}ar\left[\tilde{S}^2\right] = \frac{\tilde{\mu}_4}{N_\xi} - \frac{\tilde{\sigma}^4(N_\xi-3)}{N_\xi(N_\xi-1)}. \tag{28}$$

Our objective is to study Eq. (28) for a fixed cost, as a function of N_η to answer the question: how much should we resolve each stochastic code run to minimize $\mathbb{V}ar\left[\tilde{S}^2\right]$, and therefore $\mathbb{V}ar\left[\hat{Q}\right]$, under a given cost constraint? We start by considering a simple linear cost model in which the start-up time is negligible, *i.e.* $C = N_\xi \times N_\eta$ and we re-write Eq. (28) as a function of N_η (while C is kept constant)

$$\mathbb{V}ar\left[\tilde{S}^2\right] = N_\eta\frac{\tilde{\mu}_4}{C} - \frac{\tilde{\sigma}^4 N_\eta\left(C-3N_\eta\right)}{C\left(C-N_\eta\right)}. \tag{29}$$

We want to solve $\partial\mathbb{V}ar\left[\tilde{S}^2\right]/\partial N_\eta = 0$, which is

$$\frac{\partial\mathbb{V}ar\left[\tilde{S}^2\right]}{\partial N_\eta} = \frac{\tilde{\mu}_4}{C} + \frac{N_\eta}{C}\frac{\partial\tilde{\mu}_4}{\partial N_\eta} - \frac{\partial\tilde{\sigma}^4}{\partial N_\eta}\frac{N_\eta\left(C-3N_\eta\right)}{C\left(C-N_\eta\right)} - \tilde{\sigma}^4\frac{\partial N_\eta\left(C-3N_\eta\right)}{\partial C\left(C-N_\eta\right)}, \tag{30}$$

where the statistics of interest are

$$\begin{aligned}
\tilde{\mu}_4 &= \mathbb{E}\left[\tilde{Q}^4_{N_\eta}\right] - 4\mathbb{E}\left[\tilde{Q}^3_{N_\eta}\right]\mathbb{E}\left[Q\right] + 6\mathbb{E}\left[\tilde{Q}^2_{N_\eta}\right]\mathbb{E}\left[Q\right]^2 - 3\mathbb{E}\left[Q\right]^4 \\
\mathbb{E}\left[\tilde{Q}^4\right] &= \mathbb{E}\left[Q^4\right] + \frac{1}{{N_\eta}^4}\left[{6N_\eta}^3\mathbb{E}_\xi\left[Q^2\sigma_\eta^2\right] + {4N_\eta}^2\mathbb{E}_\xi\left[Q\mu_{\eta,3}[f]\right] + N_\eta\mathbb{E}_\xi\left[\mu_{\eta,4}[f] + 3\left(N_\eta-1\right)(\sigma_\eta^2)^2\right]\right] \\
\mathbb{E}\left[\tilde{Q}^3\right] &= \mathbb{E}\left[Q^3\right] + \frac{3}{N_\eta}\mathbb{E}_\xi\left[Q\sigma_\eta^2\right] + \frac{1}{{N_\eta}^2}\mathbb{E}_\xi\left[\mu_{\eta,3}\right] \\
\mathbb{E}\left[\tilde{Q}^2\right] &= \mathbb{V}ar\left[\tilde{Q}_{N_\eta}\right] + \mathbb{E}_\xi\left[Q\right]^2 = \mathbb{V}ar_\xi\left[Q\right] + \frac{\mathbb{E}_\xi\left[\sigma_\eta^2\right]}{N_\eta} + \mathbb{E}_\xi\left[Q\right]^2 = \mathbb{E}_\xi\left[Q^2\right] + \frac{1}{N_\eta}\mathbb{E}_\xi\left[\sigma_\eta^2\right] \\
\tilde{\sigma}^4 &= \mathbb{V}ar_\xi\left[Q\right]^2 + 2\mathbb{V}ar_\xi\left[Q\right]\mathbb{E}_\xi\left[\sigma^2_{RT,N_\eta}\right] + \mathbb{E}_\xi\left[\sigma^2_{RT,N_\eta}\right]^2 = \left(\mathbb{V}ar\left[\tilde{Q}_{N_\eta}\right]\right)^2
\end{aligned} \tag{31}$$

and the derivatives are

$$\begin{aligned}
\frac{\partial \tilde{\mu}_4}{\partial N_\eta} &= \frac{\partial \mathbb{E}\left[\tilde{Q}^4_{N_\eta}\right]}{\partial N_\eta} - 4\mathbb{E}\left[Q\right]\frac{\partial \mathbb{E}\left[\tilde{Q}^3_{N_\eta}\right]}{\partial N_\eta} + 6\mathbb{E}\left[Q\right]^2\frac{\partial \mathbb{E}\left[\tilde{Q}^2_{N_\eta}\right]}{\partial N_\eta} \\
\frac{\partial \mathbb{E}\left[\tilde{Q}_4\right]}{\partial N_\eta} &= -\frac{6}{{N_\eta}^2}\mathbb{E}_\xi\left[Q^2\sigma^2_\eta\right] - \frac{8}{{N_\eta}^3}\mathbb{E}_\xi\left[Q\mu_{\eta,3}\right] - \frac{3}{{N_\eta}^4}\mathbb{E}_\xi\left[\mu_{\eta,4}\right] - \frac{3}{{N_\eta}^3}\left(2-\frac{3}{N_\eta}\right)\mathbb{E}_\xi\left[\left(\sigma^2_\eta\right)^2\right] \\
\frac{\partial \mathbb{E}\left[\tilde{Q}^3_{N_\eta}\right]}{\partial N_\eta} &= -\frac{3}{{N_\eta}^2}\mathbb{E}_\xi\left[Q\sigma^2_\eta\right] - \frac{2}{{N_\eta}^3}\mathbb{E}_\xi\left[\mu_{\eta,3}\right] \\
\frac{\partial \mathbb{E}\left[\tilde{Q}^2_{N_\eta}\right]}{\partial N_\eta} &= -\frac{1}{{N_\eta}^2}\mathbb{E}_\xi\left[\sigma^2_\eta\right] \\
\frac{\partial \tilde{\sigma}^4}{\partial N_\eta} &= -\frac{2}{{N_\eta}^2}\mathbb{V}ar_\xi\left[Q\right]\mathbb{E}_\xi\left[\sigma^2_\eta\right] - \frac{2}{{N_\eta}^3}\left(\mathbb{E}_\xi\left[\sigma^2_\eta\right]\right)^2 = -\frac{2}{{N_\eta}^2}\left(\mathbb{V}ar_\xi\left[Q\right] + \frac{\mathbb{E}_\xi\left[\sigma^2_\eta\right]}{N_\eta}\right) \\
\frac{\partial\left(N_\eta\left(C-3N_\eta\right)\right)}{\partial\left(C\left(C-N_\eta\right)\right)} &= \frac{C^2 - 6CN_\eta + 3{N_\eta}^2}{C\left(C-N_\eta\right)^2}.
\end{aligned} \tag{32}$$

The previous expressions suggest which statistics one needs to compute in order to solve the resource allocation problem.

3.4.1. Unbiased estimators for analytical terms

In practical application, one would aim to run a pilot study to compute the necessary terms needed to find the optimal cost configuration for a subsequent UQ study. After developing the analytical expressions, we need to find unbiased estimators to compute these analytical terms from available tallies.

We introduce some notation for a (biased) sample central moment:

$$m_k[X] = \frac{1}{N}\sum_{i=1}^{N}(x_i - m)^k \tag{33}$$

where m is the sample central mean. We use the notation $\hat{\cdot}$ to indicate a sample estimator. The unbiased central moments over N_η are:

$$\begin{aligned}
\hat{\sigma}^2_\eta &= \frac{N_\eta}{N_\eta - 1}m_{\eta,2} \\
\hat{\mu}_{\eta,3} &= \frac{{N_\eta}^2}{(N_\eta-1)(N_\eta-2)} \\
\hat{\mu}_{\eta,4} &= \frac{N_\eta\left[\left({N_\eta}^2 - 2N_\eta + 3\right)m_{\eta,4} - 3\left(2N_\eta - 3\right)m^2_{\eta,2}\right]}{(N_\eta-1)(N_\eta-2)(N_\eta-3)} \\
\hat{\sigma}^4_\eta &= \frac{N_\eta\left[\left({N_\eta}^2 - 3N_\eta + 3\right)m^2_{\eta,2} - \left(N_\eta - 1\right)m_{\eta,4}\right]}{(N_\eta-1)(N_\eta-2)(N_\eta-3)}
\end{aligned} \tag{34}$$

such that

$$\begin{aligned}
\mathbb{E}\left[\hat{\sigma}^2_\eta\right] &= \mathbb{E}_\xi\left[\sigma^2_\eta\right], \\
\mathbb{E}\left[\hat{\mu}_{\eta,3}\right] &= \mathbb{E}_\xi\left[\mu_{\eta,3}\right], \\
\mathbb{E}\left[\hat{\mu}_{\eta,4}\right] &= \mathbb{E}_\xi\left[\mu_{\eta,4}\right], \text{and} \\
\mathbb{E}\left[\hat{\sigma}^4_\eta\right] &= \mathbb{E}_\xi\left[\sigma^4_\eta\right].
\end{aligned} \tag{35}$$

Equations (31) give us unbiased estimators for $\mathbb{E}\left[Q^2\right]$, $\mathbb{E}\left[Q^3\right]$, and $\mathbb{E}\left[Q^4\right]$, leaving us needing to compute estimators for $\mathbb{E}\left[Q\sigma_\eta^2\right]$, $\mathbb{E}\left[Q\mu_{\eta,3}\right]$, and $\mathbb{E}\left[Q^2\sigma_\eta^2\right]$ from the available $\tilde{Q}_{N_\eta}\hat{\sigma}_\eta^2$, $\tilde{Q}_{N_\eta}\hat{\mu}_{\eta,3}$, and $\tilde{Q}_{N_\eta}^2\hat{\sigma}_\eta^2$. Note - what level of detail should I include here?

$$
\begin{aligned}
m_{\eta,2} &= \frac{1}{N_\eta}\sum_{j=1}^{N_\eta}\left(f-\tilde{Q}_{N_\eta}\right)^2 = \frac{1}{N_\eta}\left(\sum_{j=1}^{N_\eta} j=1f^2 - N_\eta\tilde{Q}_{N_\eta}^2\right)\\
\hat{\sigma}_\eta^2 &= \frac{1}{N_\eta-1}\left(\sum_{j=1}^{N_\eta} j=1f^2 - N_\eta\tilde{Q}_{N_\eta}^2\right)\\
\mathbb{E}_\eta\left[\tilde{Q}_{N_\eta}\hat{\sigma}_\eta^2\right] &= \frac{1}{N_\eta-1}\left(\mathbb{E}_\eta\left[\tilde{Q}_{N_\eta}\sum_{j=1}^{N_\eta} j=1f^2\right] - N_\eta\mathbb{E}_\eta\left[\tilde{Q}_{N_\eta}^3\right]\right)\\
&= \ldots = Q\sigma_\eta^2 + \frac{1}{N_\eta}\mu_{\eta,3}\\
\mathbb{E}_\xi\left[Q\sigma_\eta^2\right] &= \mathbb{E}\left[\tilde{Q}_{N_\eta}\hat{\sigma}_\eta^2\right] - \frac{1}{N_\eta}\mathbb{E}\left[\hat{\mu}_{\eta,3}\right]
\end{aligned}
\tag{36}
$$

$$
\begin{aligned}
m_{\eta,3} &= \frac{1}{N_\eta}\sum_{j=1}^{N_\eta}\left(f-\tilde{Q}_{N_\eta}\right)^3 = \frac{1}{N_\eta}\left(\sum_{j=1}^{N_\eta} j=1f^3 - 3\tilde{Q}_{N_\eta}\sum_{j=1}^{N_\eta} j=1f^2 + 2N_\eta\tilde{Q}_{N_\eta}^3\right)\\
\hat{\mu}_{\eta,3} &= \frac{N_\eta}{(N_\eta-1)(N_\eta-2)}\left(\sum_{j=1}^{N_\eta} j=1f^3 - 3\tilde{Q}_{N_\eta}\sum_{j=1}^{N_\eta} j=1f^2 + 2N_\eta\tilde{Q}_{N_\eta}^3\right)\\
\mathbb{E}_\eta\left[\tilde{Q}_{N_\eta}\hat{\mu}_{\eta,3}\right] &= \frac{N_\eta}{(N_\eta-1)(N_\eta-2)}\left(\mathbb{E}_\eta\left[\tilde{Q}_{N_\eta}\sum_{j=1}^{N_\eta} j=1f^3\right] - 3\mathbb{E}_\eta\left[\tilde{Q}_{N_\eta}^2\sum_{j=1}^{N_\eta} j=1f^2\right] + 2N_\eta\mathbb{E}_\eta\left[\tilde{Q}_{N_\eta}^4\right]\right)\\
&= \ldots = Q\mu_{\eta,3} + \frac{1}{N_\eta}\mu_{\eta,4} + \frac{2-3N_\eta}{N_\eta(N_\eta-2)}(\sigma_\eta^2)^2\\
\mathbb{E}_\xi\left[Q\mu_{\eta,3}\right] &= \mathbb{E}\left[\tilde{Q}_{N_\eta}\hat{\mu}_{\eta,3}\right] - \frac{1}{N_\eta}\mathbb{E}\left[\hat{\mu}_{\eta,4}\right] - \frac{2-3N_\eta}{N_\eta(N_\eta-2)}\mathbb{E}_\xi\left[(\hat{\sigma}_\eta^2)^2\right]
\end{aligned}
\tag{37}
$$

$$
\begin{aligned}
m_{\eta,2} &= \frac{1}{N_\eta}\sum_{j=1}^{N_\eta}\left(f-\tilde{Q}_{N_\eta}\right)^2 = \frac{1}{N_\eta}\left(\sum_{j=1}^{N_\eta} j=1f^2 - N_\eta\tilde{Q}_{N_\eta}^2\right)\\
\hat{\sigma}_\eta^2 &= \frac{1}{N_\eta-1}\left(\sum_{j=1}^{N_\eta} j=1f^2 - N_\eta\tilde{Q}_{N_\eta}^2\right)\\
\mathbb{E}_\eta\left[\tilde{Q}_{N_\eta}^2\hat{\sigma}_\eta^2\right] &= \frac{1}{N_\eta-1}\left(\mathbb{E}_\eta\left[\tilde{Q}_{N_\eta}^2\sum_{j=1}^{N_\eta} j=1f^2\right] - N_\eta\mathbb{E}_\eta\left[\tilde{Q}_{N_\eta}^4\right]\right)\\
&= \ldots = Q^2\sigma_\eta^2 + \frac{2}{N_\eta}Q\mu_{\eta,3} + \frac{1}{{N_\eta}^2}\mu_{\eta,4} + \frac{N_\eta-3}{{N_\eta}^2}(\sigma_\eta^2)^2\\
\mathbb{E}_\xi\left[Q^2\sigma_\eta^2\right] &= \mathbb{E}\left[\tilde{Q}_{N_\eta}^2\hat{\sigma}_\eta^2\right] - \frac{2}{N_\eta}\mathbb{E}\left[\tilde{Q}_{N_\eta}\hat{\mu}_{\eta,3}\right] + \frac{1}{{N_\eta}^2}\mathbb{E}\left[\hat{\mu}_{\eta,4}\right] - \frac{(N_\eta+1)^2}{{N_\eta}^2(N_\eta-2)}\mathbb{E}\left[(\hat{\sigma}_\eta^2)^2\right]
\end{aligned}
\tag{38}
$$

To conduct a pilot study, the workflow is to:

1. For a single $\xi^{(i)}$, run a MC simulation
2. Compute $\hat{\mu}_{\eta,3,i}$, $\hat{\mu}_{\eta,4,i}$, and $\hat{\sigma}_{\eta,i}^4$ using the equations above, in addition to $\hat{\sigma}_{\eta,i}^2$ and $\tilde{Q}_{N_\eta}(\xi^{(i)})$.

3. After all N_ξ have run, average $\hat{\mu}_{\eta,3,i}$, $\hat{\mu}_{\eta,4,i}$, $\hat{\sigma}^4_{\eta,i}$, $\hat{\sigma}^2_{\eta,i}$, and $\tilde{Q}_{N_\eta}(\xi^{(i)})$ over N_ξ for unbiased estimates of $\mathbb{E}_\xi\left[\sigma^2_\eta\right]$, $\mathbb{E}_\xi\left[\mu_{\eta,3}\right]$, $\mathbb{E}_\xi\left[\mu_{\eta,4}\right]$, $\mathbb{E}_\xi\left[(\sigma^2_\eta)^2\right]$, and $\mathbb{E}\left[Q\right]$.
4. Use the equations above to compute unbiased estimates of $\mathbb{E}\left[Q^2\right]$, $\mathbb{E}\left[Q^3\right]$, $\mathbb{E}\left[Q^4\right]$, $\mathbb{E}\left[Q\sigma^2_\eta\right]$, $\mathbb{E}\left[Q\mu_{\eta,3}\right]$, and $\mathbb{E}\left[Q^2\sigma^2_\eta\right]$.
5. Pass these terms to a function that will compute $\tilde{\mu}_4$, $\frac{\partial\tilde{\mu}_4}{\partial N_\eta}$, $\tilde{\sigma}^4$, and $\frac{\partial\tilde{\sigma}^4}{\partial N_\eta}$ to optimize $\frac{\partial\mathbb{V}ar[\tilde{S}^2]}{\partial N_\eta}$ as a function of N_η.

From here, one would ideally have computed the optimum N_η at which to run a full UQ study, and assign the number of UQ samples in accordance with the prescribed total estimator cost.

4. Transport solvers

Directly from CSRI The MC-MC estimator is applied here to an example radiation transport problem in which the inner MC loop is a Monte Carlo radiation transport solver. Our goal is to provide an estimate of the variance of the QoI, over the UQ parameter space, which for this example problem is transmittance through a slab.

4.1. Problem Description

We solve the stochastic, one-dimensional, neutral-particle, mono-energetic, steady-state radiation transport equation with a normally incident beam source of magnitude one:

$$\mu\frac{\partial\psi(x,\mu,\xi)}{\partial x} + \Sigma_t(x,\xi)\psi(x,\mu,\xi) = \int_{-1}^{1} d\mu'\psi(x,\mu',\xi)\frac{\Sigma_s(x,\mu'\rightarrow\mu,\xi)}{2}, \tag{39}$$

$$0 \le x \le L; \quad -1 \le \mu \le 1, \tag{40}$$

$$\psi(0,\mu,\xi) = 1, \mu > 0; \quad \psi(L,\mu,\xi) = 0, \mu < 0 \tag{41}$$

where $\psi(x,\mu,\xi)$ is angular flux, $\Sigma_t(x,\xi)$ is total cross section, $\Sigma_s(x,\mu,\xi)$ is scattering cross section, and x, μ, and ξ respectively denote dependence on space, angle, and the vector of independent uncertain variables. The problem boundaries are fixed, i.e. $x \in [0, L]$, as are the locations between material regions. The problem is solved for two different scenarios: attenuation only, in which $\Sigma_s(x,\mu,\xi) = 0$; and with both attenuation and isotropic scattering. For both scenarios, the total cross section of each material is assumed to be uniformly distributed. In the scenario which also involves scattering, the ratio of scattering to total cross section c is distributed uniformly and independently of Σ_t. We consider a slab with a total of M materials, where for each region m the total cross section is defined as

$$\Sigma_{t,m}(\xi_m) = \bar{\Sigma}_{t,m} + \Sigma^\Delta_{t,m}\xi_m \tag{42}$$

with $\bar{\Sigma}_{t,m}$ representing the average total cross section and $\Sigma^\Delta_{t,m}$ the deviation from the mean value. Furthermore, a random parameter $\xi_m \sim \mathcal{U}[-1,1]$ is used to represent the variability of $\Sigma_{t,m}(\xi) \sim \mathcal{U}[\bar{\Sigma}_{t,m} - \Sigma^\Delta_{t,m}, \bar{\Sigma}_{t,m} + \Sigma^\Delta_{t,m}]$. For cases with scattering, the scattering ratio is defined analogously using

$$c_m(\xi_{M+m}) = \bar{c}_m + c^\Delta_m\xi_{M+m} \tag{43}$$

where $\xi_{M+m} \sim \mathcal{U}[-1,1]$, with $m = 1,\ldots,M$, is a uniformly distributed random variable. We note that in the attenuation-only case the problem contains a number of uncertain parameters equal to the number of materials, *i.e.* $\xi \in \mathbb{R}^d$ with $d = M$, whereas in the case of both attenuation and scattering $d = 2M$.

4.2. Monte Carlo Particle Transport and Woodcock Delta Tracking

Though Equation 39 can be thought of as the governing equation for this example problem, Section **??** points out that an estimate of our quantity of interest is obtained not by analytically or numerically solving the Boltzmann equation, but by averaging the tallied responses of individual particles [**?**]. In this example problem, the tallied QoI is transmittance; a response is tallied when a particle exits the far end of the slab, and a history is terminated when a particle is either absorbed or scatters to exit back through the beam-incident side of the slab. The series of random

samples used to determine when the particle will reach a position of interest and what will happen when it does is described stochastically using η, as outlined in Section **??**.

Particles' 'random walks' begin with the initial conditions in Eq. (39). They're moved through the system by randomly sampling the distance to their next collision[2], d_c ,

$$d_c = \frac{-ln(\Gamma)}{\Sigma_t}, \ \Gamma \in [0, 1) \tag{44}$$

where Γ is a randomly sampled number on [0,1) [**?**]. Equation 44, and therefore the calculated distance to collision, remains accurate as long as Σ_t is constant. For homogeneous media where $\Sigma_{t,m}$ is constant across material m, this is uncomplicated [3]. However, for heterogeneous media modeled as having different material sections separated by boundaries, this can become computationally expensive [**?**]. If the distance to a boundary is less than the calculated distance to collision and the particle would move from material m to material m', traditional collision-distance tracking methods only move the particle so far as the boundary location, then re-calculate d_c using $\Sigma_{t,m'}$ [**?**].

Instead, Woodcock-delta tracking calculates d_c using a majorant cross section Σ_M, which is typically taken to be the largest total cross section the particle might encounter along its direction of travel. Using the largest possible cross-section renders checking whether a particle has crossed a material boundary unecessary; the probability of collision is either correct or overestimated, making the calculated distance to collision either correct or underestimated. This is corrected for by taking the ratio between Σ_t at the collision site and Σ_M to be the probability of whether the collision has actually occurred. For a particle moved to a possible collision site in material i, if for a randomly sampled $\omega \in [0, 1)$,

$$\omega < \frac{\Sigma_{t,i}}{\Sigma_M} \ , \tag{45}$$

the collision has actually occurred and is evaluated accordingly. Otherwise the collision is rejected as hypothetical (also referred to as "delta-collisions") and a new distance to collision is sampled [**?**]. Eventually, the particle will either exit the system via the right-hand-side and be tallied for transmittance, or exit the system in some other way and not be tallied for this problem. The transmittance is averaged over all histories in the sample, and this is then repeated N_ξ times for UQ analysis.

5. Verification transport problems: the attenuation-only case

For a problem in which $\Sigma_s(x) = 0$, i.e. attenuation-only, an analytic solution for uncollided transmittance of a normally incident beam through a slab is

$$T(\xi) = \psi(L, 1, \xi) = \exp\left[\sum_{m=1}^{M} \Sigma_{t,m}(\xi_m)\Delta x_m\right]. \tag{46}$$

The pth raw moment for the transmittance, as derived in [**?**], can be written as

$$\mathbb{E}\left[T^p\right] = \prod_{m=1}^{d} exp\left[-p\bar{\Sigma}_{t,m}\Delta x_m\right] \frac{sinh\left[p\Sigma^{\Delta}_{t,m}\Delta x_m\right]}{p\bar{\Sigma}_{t,m}\Delta x_m}, \tag{47}$$

which allows for an exact evaluations of central moments by adopting the well-known transformations from raw to central moments. For instance, for the variance, which is the second central moment, we can write

$$\mathbb{V}ar\left[T\right] = \mathbb{E}\left[T^2\right] - \mathbb{E}\left[T\right]^2. \tag{48}$$

Moreover, as it is also possible to compute the variance $\mathbb{E}_\xi\left[\sigma^2_{RT,N_\eta}\right]$ in closed form for this problem, this example is well suited for verification purposes.

[2] Readers interested in the derivation of the distance to collision can see ref [**?**], and a detailed derivation of Monte Carlo transport methods can be found in Ch. 9 of [**?**].

[3] Our problem assumes constant $\Sigma_{t,m}$ across material m. However, $\Sigma_{t,m}$ in reality can vary with energy, temperature, density, or changing material composition [**?**].

6. Numerical results

Section ToC:

- Attenuation-only
- Scattering
- Performance (resource allocation)

CSRI: In this section we present the performance of the variance estimators described in the previous sections for two UQ analysis scenarios, namely attenuation-only and attenuation with scattering. We consider a 1D slab with 3 material sections[4] and fixed boundaries between them. Each problem is solved using a fixed computational cost of $N_\xi \times N_\eta = 1500$ particle histories, however we consider different combinations of N_ξ and N_η. Moreover, we run 25 000 repetitions of the estimators, which correspond to realizations of all random variables, both ξ and η, to generate estimators' distributions and statistics.

6.1. Scenario 1: Attenuation only

In Table 1, we report the right boundary location, average total cross section, and deviation from the mean for the cross section for each of the material sections. In Table 2, we report the statistics (mean and variance) for the new estimator S^2 and previous estimator S_I^2 of $\mathbb{V}ar[T]$ where T is the calculated transmittance, obtained over 25 000 repetitions of the estimator and for different combinations of N_ξ and N_η. We also compare the calculated variance to the analytic solution outlined in Section 5 using the mean squared error (MSE), which measures both the bias and variance of the estimator distribution, thus providing combined metrics for both the accuracy and precision of our estimator. It should be noted again here that no matter the number of histories run for calculation of other QoI such as transmittance, the previous method [**?**] specifies the use of only one history (typically the first one) to calculate total polluted variance.

	m = 1	m = 2	m = 3
x_R	2.0	5.0	6.0
$\bar{\Sigma}_{t,m}$	0.90	0.15	0.60
$\Sigma^{\Delta}_{t,m}$	0.70	0.12	0.50

Table 1: Stochastic Attenuation Problem Parameters

(N_ξ, N_η)	(100,15)	(300,5)	(500,3)	(750,2)	Exact
$\mathbb{E}\left[S^2\right]$	5.506e-03	5.501e-03	5.519e-03	5.498e-03	5.505e-03
$\mathbb{E}\left[S_I^2\right]$	5.557e-03	5.446e-03	5.522e-03	5.508e-03	5.505e-03
$\mathbb{V}ar\left[S^2\right]$	4.328e-06	5.172e-06	7.636e-06	1.276e-05	-
$\mathbb{V}ar\left[S_I^2\right]$	4.716e-04	1.392e-04	7.270e-05	4.543e-05	-
$\mathbb{V}ar\left[S_I^2\right]/\mathbb{V}ar\left[S^2\right]$	108.96	26.91	9.52	3.56	-
MSE$[S^2]$	4.328e-06	5.172e-06	7.636e-06	1.276e-05	-
MSE$[S_I^2]$	4.716e-04	1.392e-04	7.270e-05	4.542e-05	-

Table 2: Parametric variance ($\mathbb{V}ar[T]$) results for the stochastic attenuation-only problem using 25000 repetitions. Note that the previous estimator [**?**] specifies the use of one history to calculate total polluted variance, causing the higher variance and mean squared error.

We first note that one would expect the MSE of an unbiased estimator to be equal to the variance, as it is possible to observe in Table 2, corroborating the unbiased nature of both estimators. We also observe from these results that for the same computational cost $N_\xi \times N_\eta = 1500$, the variance and MSE of S^2 using the novel estimator increase as the number of histories decreases. We observe the opposite using the previous estimator. Because the previous estimator's lower precision results from the use of only one history to estimate the total variance, as the number of

[4]The approach can be extended to higher number of sections without any modifications to the algorithm.

histories gets closer to 1 this effect is minimized. Even with $\mathbb{V}ar\left[S^2\right]$ increasing as $\mathbb{V}ar\left[S_I^2\right]$ decreasing, each of the four cases shows a reduction in $\mathbb{V}ar\left[S^2\right]$ when using the new estimator over the old.

In Figure 1, we provide the results of the 25 000 repetitions, considering all tested combinations of N_ξ and N_η, for both estimators and we compare them with the exact solutions which is available for this problems.

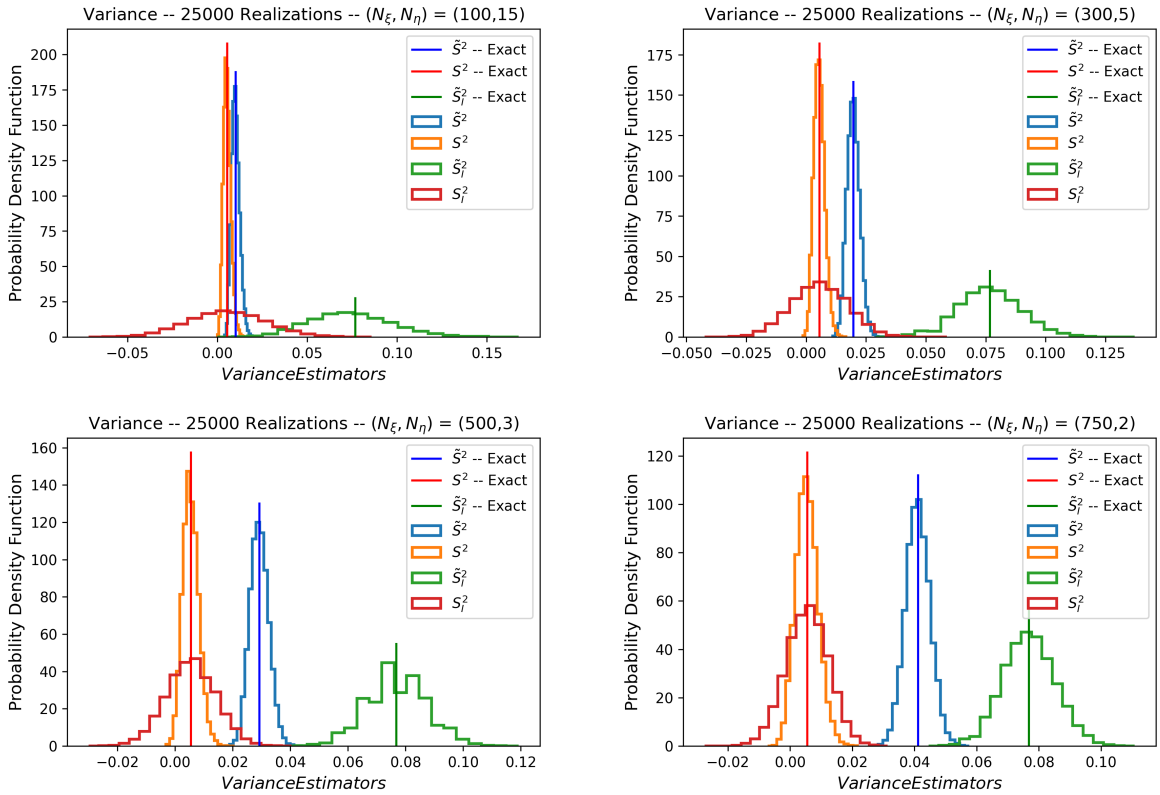

Figure 1: 1D radiation transport problem with absorption only ($d = 3$). 25 000 repetitions for the estimators: the new S^2 and the previous S_I^2, [**?**], estimators are reported. Exact solutions are reported as vertical lines.

The distributions from both methods centering around the analytic solution for $\mathbb{V}ar\left[T\right]$ provides additional evidence that both estimators are unbiased. However, $\mathbb{V}ar\left[T\right]$ calculated using our novel method has a tighter distribution around the analytic variance, corresponding with its higher statistical reliability. This is also evident from looking at the ratio between $\mathbb{V}ar\left[S_I^2\right]$ and $\mathbb{V}ar\left[S^2\right]$ reported in Table 2, which for this case varies approximately from 3 to 100. This holds even when comparing the estimators' respective most efficient cases, $\mathbb{V}ar\left[S_I^2\right](100, 15)/\mathbb{V}ar\left[S^2\right](750, 2)$ = 10.50, approximately an order of magnitude of improvement. In a practical application, we would only be able to obtain a single realization for S^2 or S_I^2; therefore, it is preferable to use an estimator with a higher precision, *i.e.* smaller variance thus higher probability of being closer to the true statistics.

6.2. Case 2: Attenuation and scattering

For this test case, in Table 3 we report the right boundary location, average total cross section and deviation from its mean, and average scattering ratio $c_{s,m}$ and deviation from its mean for each of the material sections. The results of the estimators are summarized in Table 4. It is worth noting that though the mean variance appears to systemically change as a function of N_η, this is not the case; all of the solutions are within the statistical uncertainty, and for this series of repetitions happened to increase as N_η does. All calculated variances are higher than their attenuation-only counterparts, caused by the inclusion of the second stochastic parameter for each of the materials, the scattering ratio.

As with Case 1, $\mathbb{V}ar\left[S^2\right]$ decreases as the number of histories increases, and $\mathbb{V}ar\left[S_I^2\right]$ behaves inversely. Though $\mathbb{V}ar\left[S_I^2\right]/\mathbb{V}ar\left[S^2\right]$ is higher in Case 1 than Case 2, we still observe improvement when using the new estimator over the old, and the ratio of their respective best cases $\mathbb{V}ar\left[S_I^2\right](100,15)/\mathbb{V}ar\left[S^2\right](750,2) = 9.11$, still close to an order of magnitude of difference.

	m = 1	m = 2	m = 3
x_R	2.0	5.0	6.0
$\bar{\Sigma}_{t,m}$	0.90	0.15	0.60
$\Sigma^{\Delta}_{t,m}$	0.70	0.12	0.50
$\bar{c}_{s,m}$	0.50	0.50	0.50
$c^{\Delta}_{s,m}$	0.40	0.40	0.40

Table 3: Stochastic Absorption and Scattering Problem Parameters

(N_ξ, N_η)	(100,15)	(300,5)	(500,3)	(750,2)
$\mathbb{E}\left[S^2\right]$	9.689e-03	9.148e-03	8.201e-03	6.587e-03
$\mathbb{E}\left[S_I^2\right]$	9.879e-03	9.098e-03	8.345e-03	6.591e-03
$\mathbb{V}ar\left[S^2\right]$	9.143e-06	9.830e-06	1.158e-05	1.555e-05
$\mathbb{V}ar\left[S_I^2\right]$	5.481e-04	1.611e-04	8.327e-05	4.965e-05
$\mathbb{V}ar\left[S_I^2\right]/\mathbb{V}ar\left[S^2\right]$	59.95	16.39	7.19	3.19

Table 4: Parametric variance ($\mathbb{V}ar\left[T\right]$) results for the attenuation and scattering problem using 25000 repetitions. Note that the previous estimator [**?**] specifies the use of one history to calculate total polluted variance, causing the higher variance.

In Figure 2, we show the distributions of S^2 and $\tilde{S}^2$ over 25 000 repetitions for all tested combinations of (N_ξ, N_η). The variance is about an order of magnitude larger compared to the attenuation-only case, reported in Figure 1. This is further evidence of the increased variability induced by the second parameter for each material section.

Although there is no analytic solution for comparison, it is evident that the variance distributions are wider when calculated using the previous method compared to those from the novel one, as expected. We also note that the advantage of the novel estimator grows as N_η increases since it can take advantage of the additional particle histories to decrease the variability of the term $\mathbb{V}ar\left[\tilde{S}^2\right]$. Moreover, the contribution of the MC RT estimator variance is better resolved and, therefore, the polluted variance and the parametric variance are closer when the number of particle histories increases.

6.3. ANS2022

In this section, we present the performance of the described variance estimator for two UQ analysis scenarios, attenuation-only and attenuation with scattering. We consider a 1D slab with 3 material sections[5], and report in Table 5 the right boundary location, average total cross section, and deviation from the cross section mean for each of the material sections for both problems, as well as the analogous information for the scattering ratio for the isotropic scattering problem. In Table 6, we report the mean QoI and parametric variance computed with closed-form solutions where available; numerical benchmark solutions with $N_\eta = 10^5$, $N_\xi = 10^3$ ($C = 10^8$); and using one typical repetition of our variance deconvolution method with $N_\eta = 10^1$, $N_\xi = 10^3$ ($C = 10^4$), for reference[6].

To better understand where the variance of the novel estimator is minimized, we solve the described RT problem using Woodcock-delta tracking with analog Monte Carlo methods for an estimator cost $C = N_\xi \times N_\eta$ of 200, 500, 1000, 1500, 2000, and 5000 for a variety of N_η values. We repeat the estimator evaluation over 25,000 repetitions to evaluate its statistics. We report $\mathbb{V}ar\left[S^2\right]$ for both the attenuation-only and isotropic scattering case, where $S^2 = \mathbb{V}ar\left[T\right]$ or $\mathbb{V}ar\left[R\right]$, in Table 7. The exact parametric variance is calculable for the attenuation-only case, so we also compare the

[5]The approach can be extended to higher number of sections without any modifications to the algorithm.

[6]Note that for the deconvolved results, this is only one realization of a stochastic problem, which converges to the benchmark over many repetitions.

Table 5: Problem parameters.

Problem Parameters				Scattering Parameters	
	x_R	$\Sigma^0_{t,m}$	$\Sigma^\Delta_{t,m}$	$c^0_{s,m}$	$c^\Delta_{s,m}$
m = 1	2.0	0.90	0.70	0.50	0.40
m = 2	5.0	0.15	0.12	0.50	0.40
m = 3	6.0	0.60	0.50	0.50	0.40

Table 6: Mean QoI and parametric variance. Numerical benchmark computed with $N_\eta = 10^5$, $N_\xi = 10^3$ ($C = 10^8$); variance deconvolution computed with $N_\eta = 10^1$, $N_\xi = 10^3$ ($C = 10^4$); and closed-form solutions where available.

Attenuation Only			
	Benchmark	Deconvolved	Analytic
$\mathbb{E}[T]$	8.915E-2	8.870E-2	8.378E-2
S^2_T	5.789E-3	5.768E-3	5.505E-3
Scattering			
	Benchmark	Deconvolved	-
$\mathbb{E}[T]$	1.299E-1	1.209E-1	-
S^2_T	9.710E-3	9.825E-3	-
$\mathbb{E}[R]$	1.386E-1	1.336E-1	-
S^2_R	8.251E-3	7.703E-3	-

estimate of S^2 for the attenuation-only case to the analytic solution using Mean Square Error (MSE), which we also report in Table 7.

For the attenuation-only case, we see that $\mathbb{V}ar\left[S^2\right]$ first decreases as a function of N_η, reaches its minimum at $N_\eta = 10$, then gradually increases again. We only report up values up to $N_\eta = 100$, because after this $\mathbb{V}ar\left[S^2\right]$ just continues to increase. The varied N_η value is the number of histories per sample, meaning that even in the case where $N_\eta = 2$, the actual QoI (transmittance, reflectance) is still being calculated over the full estimator cost. To better see the trend, Figure 3 shows $\mathbb{V}ar\left[S^2\right]$ as a function of N_η on a log-log scale for the attenuation-only case. We can see clearly here that $\mathbb{V}ar\left[S^2\right]$ is not minimized by running with the lowest possible number of histories, and a tradeoff does indeed exist between the number of UQ samples N_ξ and the number of particle histories N_η; this is not the case for the previous estimator in [**?**] with most problems. We can see the same trend in the isotropic scattering case, and when $S^2 = \mathbb{V}ar[T]$, $\mathbb{V}ar\left[S^2\right]$ is also minimized at $N_\eta = 10$.

We see a similar trend for the isotropic scattering problem where S^2 is $\mathbb{V}ar[R]$, the parametric variance of the reflectance tally. However, in this case $\mathbb{V}ar\left[S^2\right]$ is minimized at $N_\eta = 20$, rather than $N_\eta = 10$. While both transmittance and reflectance are influenced by the addition of scattering and the stochastic scattering ratio, the reflectance tally is likely more sensitive to this scattering ratio, and requires more radiation transport tallies to resolve than the transmittance tally. This demonstrates that the optimal number of N_ξ and N_η can differ between different QoIs even within the same problem, motivating further investigation to allow the analyst to choose these parameters in an informed way. Figure 4 compares the trends for the attenuation-only estimate of $\mathbb{V}ar[T]$ to the isotropic scattering estimate of $\mathbb{V}ar[T]$ and $\mathbb{V}ar[R]$.

7. Conclusions

1. For GSA, the fact that the number of histories is constant is killing us. If I'm wanting to do this for my thesis, maybe it's something to investigate adaptive number of histories especially for higher order tallies.
2. More and more we start doing the embedding, want to understand at some point how much the constant histories per UQ sample is hurting us.

Table 7: The variance (and MSE, where applicable) of the estimate of S^2 over 25,000 repetitions for both the attenuation-only and scattering problems.

Attenuation-Only Problem									
	$\mathbb{V}ar\left[S^2\right]$					$MSE[S^2]$ (Exact $\mathbb{V}ar[T] = 5.505E-3$)			
N_η	Estimator Cost				N_η	Estimator Cost			
	200	500	2000	5000		200	500	2000	5000
2	9.584E-05	3.887E-05	9.626E-06	3.879E-06	2	1.332E-10	9.106E-13	3.176E-11	5.565E-11
5	3.970E-05	1.597E-05	3.907E-06	1.586E-06	5	1.119E-09	3.600E-14	3.734E-11	4.169E-11
10	**3.241E-05**	**1.303E-05**	**3.168E-06**	**1.297E-06**	10	7.155E-10	2.692E-10	5.997E-12	1.308E-11
20	3.568E-05	1.414E-05	3.482E-06	1.384E-06	20	2.576E-10	1.026E-10	8.893E-12	4.168E-11
100	1.327E-04	3.866E-05	9.218E-06	3.656E-06	100	3.678E-10	6.301E-09	1.424E-10	3.323E-11

Scattering Problem									
	$\mathbb{V}ar\left[S^2\right]$, Transmittance					$\mathbb{V}ar\left[S^2\right]$, Reflectance			
N_η	Estimator Cost				N_η	Estimator Cost			
	200	500	2000	5000		200	500	2000	5000
2	1.730E-04	6.921E-05	1.749E-05	6.996E-06	2	1.786E-04	7.085E-05	1.770E-05	7.140E-06
5	7.664E-05	2.963E-05	7.424E-06	2.882E-06	5	6.574E-05	2.592E-05	6.392E-06	2.591E-06
10	**6.329E-05**	**2.461E-05**	**6.175E-06**	**2.488E-06**	10	4.792E-05	1.852E-05	4.586E-06	1.861E-06
20	7.360E-05	2.775E-05	6.852E-06	2.753E-06	20	**4.656E-05**	**1.758E-05**	**4.303E-06**	**1.694E-06**
25	8.090E-05	3.102E-05	7.499E-06	3.012E-06	25	4.963E-05	1.836E-05	4.371E-06	1.771E-06
100	2.987E-04	8.572E-05	1.897E-05	7.456E-06	100	1.661E-04	4.169E-05	8.476E-06	3.241E-06

Acknowledgment

This work was supported by the Laboratory Directed Research and Development program at Sandia National Laboratories, a multimission laboratory managed and operated by National Technology and Engineering Solutions of Sandia LLC, a wholly owned subsidiary of Honeywell International Inc. for the U.S. Department of Energy's National Nuclear Security Administration under contract DE-NA0003525. This paper describes objective technical results and analysis. Any subjective views or opinions that might be expressed in the paper do not necessarily represent the views of the U.S. Department of Energy or the United States Government. This work was supported by the Center for Exascale Monte-Carlo Neutron Transport (CEMeNT) a PSAAP-III project funded by the Department of Energy, grant number DE-NA003967.

References

Appendix A. Some proofs

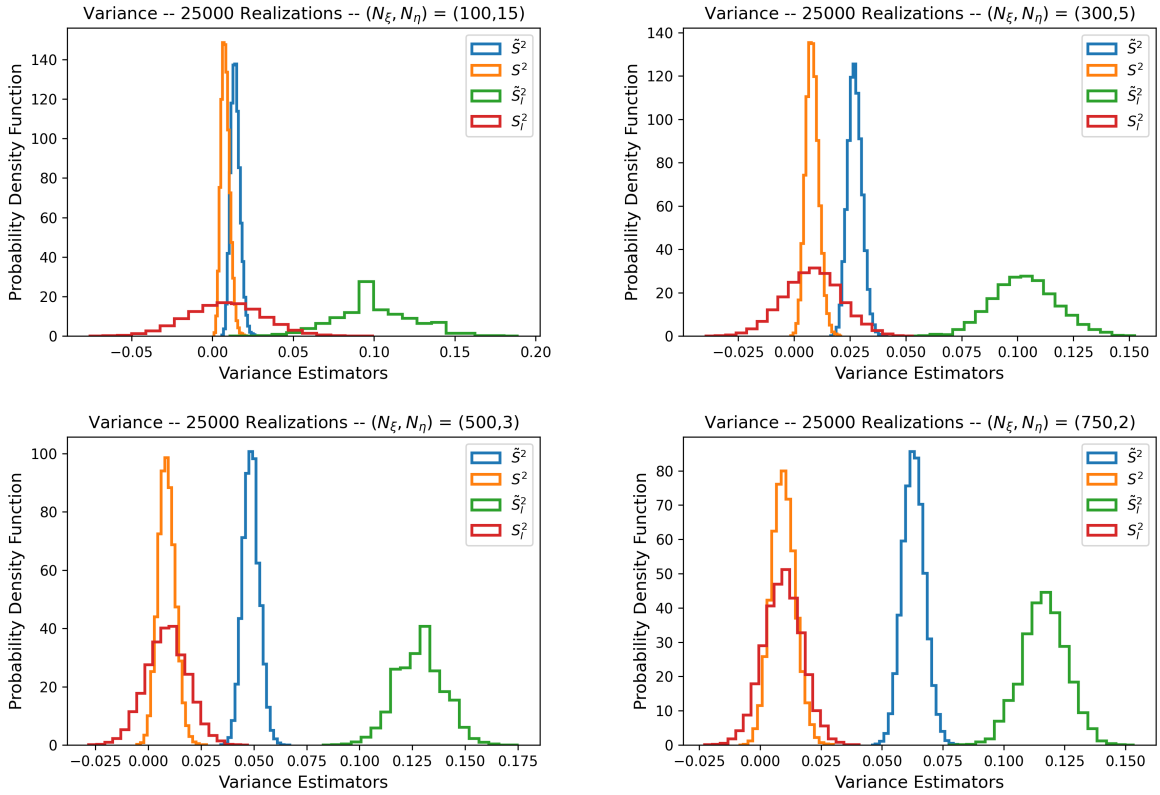

Figure 2: 1D radiation transport problem with absorption and scattering ($d = 6$). 25 000 repetitions for the estimators: the new S^2 and the previous S_I^2, [**?**], estimators are reported.

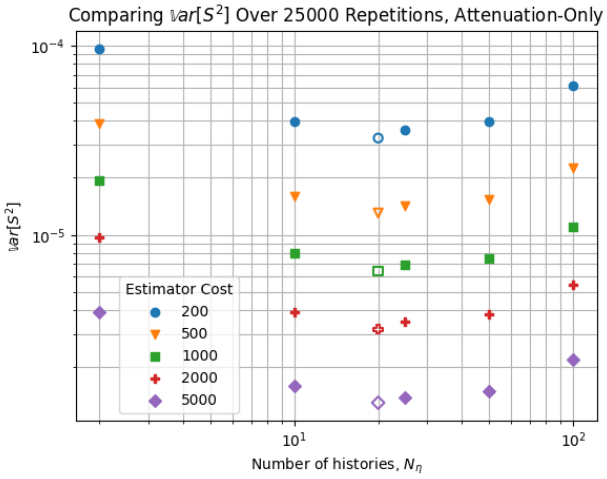

Figure 3: $\mathbb{V}ar\left[S^2\right]$ as a function of N_η for a variety of total estimator costs, log-log plot. Unfilled point is minimum $\mathbb{V}ar\left[S^2\right]$.

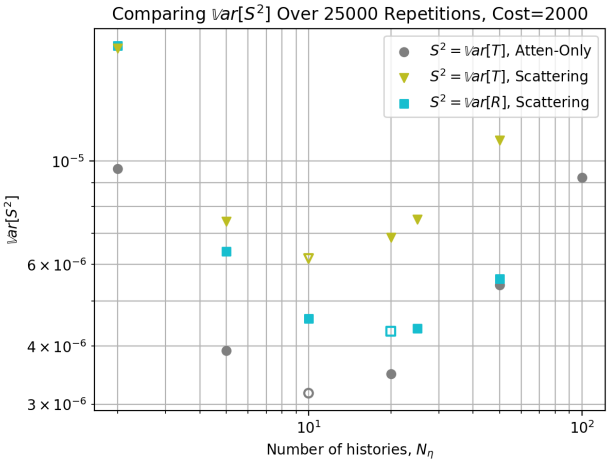

Figure 4: $\mathbb{V}ar\left[S^2\right]$ as a function of N_η for the attenuation-only and scattering cases. Log-log plot, estimator cost $N_\xi \times N_\eta = 2000$. Unfilled point is minimum $\mathbb{V}ar\left[S^2\right]$.

Bibliography

[1] A. Saltelli, S. Tarantola, F. Campolongo, and M. Ratto, *Sensitivity Analysis in Practice: A Guide to Assessing Scientific Models*, John Wiley & Sons, Inc. (2004).

[2] R. Ghanem, D. Higdon, and H. Owhadi, *Handbook of Uncertainty Quantification*, Springer International Publishing, Switzerland (2017).

[3] H. G. Matthies. *Quantifying Uncertainty: Modern Computational Representation of Probability and Applications*. In A. Ibrahimbegovic and I. Kozar, editors, *Extreme Man-Made and Natural Hazards in Dynamics of Structures*, page 105. (2007).

[4] R. C. Smith, *Uncertainty Quantification: Theory, Implementation, and Applications*, SIAM (2013).

[5] T. Wildey. *Overview of Forward and Inverse Uncertainty Quantification Methods.* Technical report, Albuquerque NM, (2018).

[6] W. H. Press, S. A. Teukolsky, W. T. Vetterling, and B. P. Flannery, *Numerical Recipes: The Art of Scientific Computing*, Cambridge University Press, New York, 3 edition (2007).

[7] A. Saltelli et al., *Global Sensitivity Analysis: The Primer*, John Wiley & Sons, Inc., United Kingdom (2008).

[8] Los Alamos National Laboratory. *MCNP - A General Monte Carlo N-Particle Transport Code, Version 5*, (2008).

[9] J. Zhang, *Modern Monte Carlo methods for efficient uncertainty quantification and propagation: a survey*, Wiley Interdisciplinary Reviews **13**, e1539 (2021).

[10] E. Cho and M. J. Cho, *Variance of Sample Variance*, Proceedings of the Survey Research Methods Section , 1291–1293 (2008).

[11] K. Clements, G. Geraci, and A. J. Olson. *A variance deconvolution approach to sampling uncertainty quantification for Monte Carlo radiation transport solvers*. In J. D. Smith and E. Galvan, editors, *Computer Science Research Institute Summer Proceedings 2021*, number Technical Report SAND2022-0653R, pages 293–307. The Computer Science Research Institute at Sandia National Laboratories, (2021). `https://cs.sandia.gov/summerproceedings/CCR2021.html`.

[12] K. Clements, G. Geraci, and A. J. Olson, *Numerical investigation on the performance of a variance deconvolution estimator*, Transactions of the American Nuclear Society **126**, 344–347 (2022).

[13] M. Saisana, A. Saltelli, and S. Tarantola, *Uncertainty and sensitivity analysis techniques as tools for the quality assessment of composite indicators*, Journal of the Royal Statistical Society **168**, 307–323 (2005).

[14] I. Sobol, *Sensitivity estimates for nonlinear mathematical models*, Mathematical Modeling and Computational Experiment **1**, 407–414 (1993).

[15] A. Saltelli and S. Tarantola, *On the relative importance of input factors in mathematical models: safety assessment for nuclear waste disposal*, Journal of the American Statistical Association **97**, 702–709 (2002).

[16] R. Larsen and M. L. Marx, *An Introduction to Mathematical Statistics and Its Applications*, Pearson Education, Boston: Prentice Hall, 5 edition (2012).

[17] A. J. Olson, *Calculation of parametric variance using variance deconvolution*, Transactions of the American Nuclear Society **120**, 461–464 (2019).

[18] A. B. Owen, *Monte Carlo theory, methods and examples* (2013).

[19] N. A. Weiss, *A Course In Probability*, Addison-Wesley (2005).

[20] E. Cho and M. J. Cho, *Variance of Sample Variance*, Proceedings of the Survey Research Methods Section , 1291–1293 (2008).

[21] B. M. Adams et al. *Dakota, A Multilevel Parallel Object-Oriented Framework for Design Optimization, Parameter Estimation, Uncertainty Quantification, and Sensitivity Analysis: Version 6.15 User's Manual.* Technical Report SAND2021-14253, Albuquerque NM, (2021).

[22] A. J. Olson, K. Clements, and J. M. Petticrew, *A sampling-based approach to solve Sobol' indices using variance deconvolution for arbitrary uncertainty distributions*, Transactions of the American Nuclear Society **127**, 450–453 (2022).

[23] G. Geraci and A. J. Olson, *Deconvolution strategies for efficient parametric variance estimation in stochastic media transport problems*, Transactions of the American Nuclear Society **126**, 279–282 (2022).

[24] G. Geraci, K. Clements, and A. Olson. *On polynomial chaos for Monte Carlo transport applications.* Extended abstract submitted for consideration to ANS M&C 2023, (2023).

[25] I. Variansyah. *MC/DC: Monte Carlo Dynamic Code.* `https://github.com/CEMeNT-PSAAP/MCDC`, (2022–ongoing).

[26] R. McClarren. *SMR Challenge Problem: Definition and progress on our demonstration problem.* CEMeNT presentation to PSAAP review team., (2022).

[27] L. L. N. L. Computing. *Quartz computing platform.*

[28] A. J. Olson, A. K. Prinja, and B. C. Franke, *Error convergence characterization for Stochastic Transport Methods*, Transactions of the International Conference on Mathematics and Computational Methods Applied to Nuclear Science and Engineering **116**, 536–539 (2017).